Eye movements used for the objective assessment of contrast sensitivity

Dissertation

der Mathematisch-Naturwissenschaftlichen Fakultät
der Eberhard Karls Universität Tübingen
zur Erlangung des Grades eines
Doktors der Naturwissenschaften
(Dr. rer. nat.)

vorgelegt von
Peter Essig
aus Prag/Tschechien

Tübingen
2023

Gedruckt mit Genehmigung der Mathematisch-Naturwissenschaftlichen Fakultät der Eberhard Karls Universität Tübingen.

Tag der mündlichen Qualifikation: 19.06.2023

Dekan:	Prof. Dr. Thilo Stehle
1. Berichterstatter:	Prof. Dr. Siegfried Wahl
2. Berichterstatter:	Prof. Dr. Frank Schaeffel

Contents

Acronyms list

AFC	Alternative forced choice
CDF	Cumulative distribution function
CI	Confidence interval
cpd	cycles per degree
CS	Contrast sensitivity
CSF	Contrast sensitivity function
Ct	Contrast threshold
D	Dioptre
DT	Dispersion threshold
fMRI	Functional magnetic resonance imaging
MAR	Minimum angular resolution
MTF	Modulation transfer function
NTF	Neural transfer function
OKN	Optokinetic nystagmus
OKN-SP	Slow phase of Optokinetic nystagmus
OKN-QP	Quick phase of Optokinetic nystagmus
OKR	Optokinetic response
REM	Rapid eye movement
VA	Visual acuity
VF	Visual field
VR	Virtual Reality
VT	Velocity threshold
SC	Superior Colliculus

1 Synopsis

1.1 Motivation

Refractive errors as well as other visual disorders affect the visual performance of an individual and hence decrease the quality of their every-day life. According to the WHO data [WHO, 2022] there are at least 2.2 billion people who suffer from a near or distance vision impairment. The leading causes of problems in vision and blindness are uncorrected refractive errors and cataracts, followed by age-related macular degeneration, glaucoma, and diabetic retinopathy [Steinmetz et al., 2021]. Furthermore, myopia, the most prevalent refractive error in humans that leads to blurred distance vision in spite of relaxed accommodation [Morgan, 2003; Wojciechowski, 2011], is also associated with an increased risk for sight-threatening pathologies [Saw et al., 2005], especially in its high or progressive forms.

Nonetheless, in the case of the majority of the eye disease, the progression can be decelerated in the early stages with an appropriate correction method or medical treatment, leading to a necessity for an early diagnosis procedure. In such a procedure or for a standard screening of an individual's visual status, a set of tests including the measurements of visual acuity, contrast sensitivity, or analysis of the visual field are commonly investigated [Drum et al., 2007].

First and the most used parameter is visual acuity, quantifying the ability to discriminate two stimuli separated in space at high contrast relative to the background at a given distance. In the clinical environment, visual acuity is evaluated by a patient's ability to discriminate letters of a known visual angle. The visual acuity is then represented as the reciprocal of the minimal angle of resolution - the size of the smallest resolved target. In such measurements, being performed in a subjective fashion, charts with optotypes or alphanumeric symbols, such as for example the Snellen optotypes or Pflüger E, are commonly used.

The limit of the angular resolution of a human eye for a given distance is given by the histological structure of the retinal tissue and the optical limits. First, the histological limits depend on the structure of the layer of photoreceptors in the human retina. Here the resolving power depends upon the density of cones in the fovea, considering two images falling on two cones, having one cone unstimulated between them [Hartridge, 1922]. Second, the optical limits of the eye's resolution are pronounced by the diffraction of the optical system [Smith and Atchison, 1997]. For the description of the eye's diffraction limit, Rayleigh's criterion could be applied, stating that two images are just resolvable when the center of the diffraction pattern of one is directly over the first minimum of the diffraction pattern of the other. This criterion is mathematically

expressed as

$$\alpha = 1.22 * \frac{\lambda}{d},$$

where α is the angular separation of the two points, λ is the light wavelength and d the pupil diameter. In connection to the diffraction limit, it is obvious that pupil size has an effect on the resolving performance of the human eye as well. On the one hand, a small pupil will lead to a reduction in optical aberrations, however, the resolution will be diffraction-limited. On the other hand, large pupils allow more light to stimulate the retina, leading to a reduction in diffraction, however affecting the vision by high-order optical aberrations. A mid-size pupil of about 3 mm to 5 mm is optimal, as it yields a compromise between the diffraction and aberration limits [Atchison et al., 1979; Smith and Atchison, 1997].

Another parameter describing an individual's visual performance is contrast sensitivity. Contrast sensitivity signifies the ability to discern between luminances of different levels in an image. It also refers to the least contrast level one needs, to be able to detect a contrast pattern of a defined spatial frequency (SF) - contrast threshold (Ct). The contrast sensitivity value is then expressed as the reciprocal value of the contrast threshold,

$$CS = \frac{1}{Ct}.$$

Contrary to visual acuity, in contrast sensitivity measurements not only the target spatial frequency is considered but also the contrast level, allowing more complex testing of the visual system. Here to mention is that contrast sensitivity indicates a potential ocular disease prior to other visual functions being affected, such as cataracts [Datta et al., 2008; Ni et al., 2015], glaucoma [Karadeniz Ugurlu et al., 2017], or age-related macular degeneration [Karadeniz Ugurlu et al., 2017; Roh et al., 2018], the parameter is considered to be one of the most relevant in the optometry and ophthalmology practice. Besides that, since contrast sensitivity is affected by refractive error [Stoimenova, 2007], or its chirurgical treatment, such as LASIK intervention [Montés-Micó et al., 2007; Oshika et al., 2006], it yields valuable information in refractive error management. Furthermore, how good the patient's visual performance at the high spatial frequency channels, which is well determined by conventional measures of visual acuity is, does not necessarily predict the visual performance at middle and lower frequencies [Richman et al., 2013]. For instance, increased higher-order aberrations, due to a LASIK intervention cause deterioration of contrast sensitivity while visual acuity might not be affected [Oshika et al., 2006]. On top of that, in glaucoma the change in contrast sensitivity has been observed, although the perimetry testing showed negative

outcomes [Ross, 1985], making the testing for contrast sensitivity a more reliable tool for early detection procedures. Moreover, in high glaucomatous patients the test-retest was shown to be high, limiting the detection of the eye disease progression [Heijl et al., 1989].

Moreover, finding the contrast sensitivity values over a range of spatial frequencies levels allows the creation of the contrast sensitivity function (CSF). As the standard CSF in healthy patients has a log-parabolic shape, the mathematical expression of such function is as follows,

$$CS(SF) = \log_{10}(\gamma_{max}) - \log_{10}(2) \left(\frac{\log_{10}(SF) - \log_{10}(SF_{max})}{\beta} \right)^2,$$

with peak sensitivity γ_{max}, peak spatial frequency SF_{max}, and the function's bandwidth β [Lesmes et al., 2010]. The CSF has its maximum around the region of 3 to 6 cpd, pronouncing that the human visual system is most sensitive to object sizes and information contained in objects around that range of spatial frequencies. However, the actual contrast sensitivity values, as well as the peak of the contrast sensitivity function depend on a wide range of influencing factors, such as the conditions of the patient's visual health [Wai et al., 2022], age [Owsley et al., 1983], as well as on the size of the target [Rovamo et al., 1994], retinal luminance [Weier et al., 2017], motion [Burr and Ross, 1982], or the frequency of flickering [Kelly, 1974]. Furthermore, contrast sensitivity of the peripheral retina is lower compared to central vision, while its value decreases with increasing distance towards the periphery in different directions in a non-uniform fashion [Rosen et al., 2014]. Besides that, contrast sensitivity is influenced not only by the properties of the stimulus or the optical and neural features of the human eye, but also by the attention of an individual, for instance [Carrasco, 2006].

In terms of the eye's limit in contrast sensitivity, the contrast sensitivity function is considered to be a product of the modulation transfer function, yielding information on how the optical system handles different spatial frequencies, and the neural transfer function, describing modulations in the perception of contrast in the retina-brain system [Campbell and Green, 1965]. In this context, the contrast sensitivity function could be expressed as follows:

$$CSF(f_x, f_y) = NTF(f_x, f_y) * MTF(f_x, f_y).$$

In contrast sensitivity examination procedures, charts with gray-scaled gratings are used, while its contrast decreases over the horizontal axis and the spatial frequency

increases in the vertical axis, as in the VISTECH chart, for instance. As the examination procedure is conducted in a strictly subjective way in clinical practice, the patient is asked to respond to the features of a stimulus, like its orientation or presence. However, such an examination procedure then leads to a lack of objectivity and hence might cause difficulties in examinations in children or non-communicative patients, or prevents an objective assessment of the patient's visual system, which could be potentially valuable in amblyopia treatment, myopia management, or any diagnosis establishment, for instance. Furthermore, as the standard contrast sensitivity test is designed only for the central visual field, a recent study disclosed an approach to assess the sensitivity for contrast across the visual field of a patient using a so-called contrast sensitivity perimetry, extending the applicability of a standard measurement to the periphery and thus being more representative of ganglion cell loss than existing clinical tests [Swanson et al., 2014].

Although the current state of art in contrast sensitivity measurements provide reliable and repeatable results in both, healthy participants and patients suffering from an eye disease, like glaucoma, cataracts or age-related macular degeneration [Kara et al., 2016], the limiting factor is the subjectivity of the performed measurements. For this reason, the already commenced research has targeted possibilities to assess this visual function in an objective way. For instance, Hemptinne et al. [2019] used visual evoked potentials detected by a 68-electrode electroencephalogram system, concluding an efficient method of assessing contrast sensitivity or visual acuity in a time-constrained clinical setting. Also Zheng et al. [2019] claimed a feasible utilization of visually evoked potentials in contrast sensitivity and visual acuity measurements, by showing comparable results from the electroencephalogram system and standard psychophysical measurements.

As the application of the electroencephalogram system might be difficult in clinical practice, other ways of detecting contrast sensitivity have been sought. In past research, the role of eye movements was found as a potential method, proposing the use of various types of eye movements in such examinations. In this context, this dissertation thesis aimed to provide optimizations in eye movement-based contrast sensitivity tests, as well as proposing novel tests for contrast sensitivity using eye movements, which might be used for objective and automated assessment of this visual function, and thus help in the future in cases of determining a diagnosis and inspections of the visual system.

1.2 Aspects of the human eye and the human visual system

1.2.1 Anatomy and physiology of the eye

The human eye is a sensory organ, which reacts to light and allows to further use the visual information in the process of vision. It has almost a spherical shape and is placed in the orbit, consisting of seven bones of the cranium. An anatomical model of the human eye is depicted in Figure 1. The outer surface of the eye consists of the sclera, giving the eye its shape and continuing as the cornea in the frontal part of the eye, bordering at the sclero-corneal limbus. The sclera is also the eye structure to which the six of extra-ocular muscles are attached enabling eye movements as well as the static position of the eye in the orbit. In the front, the eye is covered and protected by an eye lid, which structure is operated by the musculus levator palpebrae superioris, which retracts the eyelid and thus exposes the cornea enabling vision. The cornea, consisting of five layers - epithelium, Bowman's layer, stroma, Descement's membrane, and endothelium is a frontal transparent part of the eye that covers the iris, pupil, and anterior chamber. Although the cornea does not contain any blood vessels to maintain its transparency, it has unmyelinated nerve endings sensitive to touch or pressure, temperature, and chemicals, causing reflexive closure of the eye lids by any corneal disturbance. The nutrition of the cornea is supported by the tear film from the outer side and the humor aqueous from the inner side.
The optical contribution of the cornea to the total dioptric power of the human eye is the biggest among the eye's optical elements, providing approximately 43 D of the optical power, in other words approximately 2/3 of the eye's optical performance. The inner part of the human eye can be described as an organization of the anterior and posterior segments. The anterior segment consists of the visual system's main optical components, such as the cornea and the crystalline lens. The iris and pupil are located between these optical structures being responsible for aperture-like light regulation. The anterior and posterior chambers represent the aqueous-humor-filled spaces between the cornea and iris and the iris and lens, respectively. The posterior segment of the eye comprises the back two-thirds of the eye, including the vitreous body, the retina, the choroid, and the optic nerve.

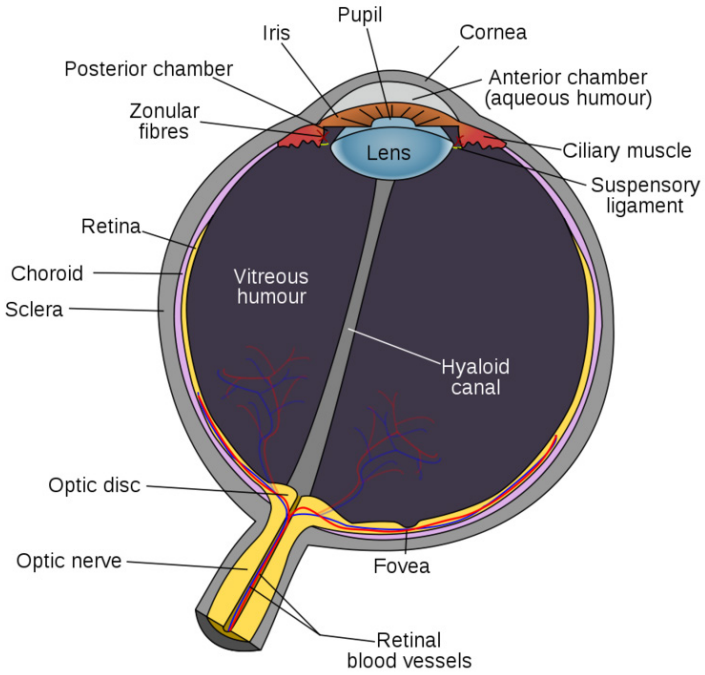

Figure 1: Anatomy of the eye. The global anatomy of the eye can be seen in this figure. This item is in the Public Domain and was reproduced from [Wilkin and Brainard, 2012].

Within the anterior eye segment, the human eye can be anatomically split into two chambers, the anterior and posterior chambers. The anterior chamber is bounded by the cornea from one side and by the iris and pupil from the other side, while the posterior chamber is bounded by the frontal surface of the lens crystalline and the back surface of the iris. The posterior chamber is an important structure involved in the production and circulation of aqueous humor, being produced by the epithelium of the ciliary body is secreted into the posterior chamber, from which it flows through the pupil to enter the anterior chamber, draining out through the trabecular meshwork and the Schlemm's canal.

The ciliary body, apart from supporting the production of the humor aqueous and being a part of the uvea of the human eye, attaches the crystalline lens by the suspensory ligaments and thus holds the active part of the lens accommodation. The crystalline lens is a transparent biconvex structure that helps, along with the cornea, to refract the light and focus it on the retina. By changing its shape, it allows to change to focal length and thus enables to focus on objects over a wide range of distances. This adjustment of the lens is known as accommodation and is actively operated by the ciliary body. Anatomically, the crystalline lens can be divided into two parts: the lens capsule, and the lens fibers. First, the lens capsule forms the outermost layer of the

lens, while the lens fibers form the interior stroma of the lens. Similarly to the cornea, the crystalline lens lacks blood vessels, however, lacks neural fibers on top of that.
The following anatomical element after the eye lens is the vitreous body, also called the vitreous humor. The vitreous body is a transparent, gelatinous mass filling the space between the lens and the retina, standing for about four-fifths of the volume of the eyeball. Furthermore, it is surrounded by a collagen layer - the vitreous membrane - separating it from the other eye structures, however attaching the vitreous body at the optic disc and the ora serrata, the anterior ending of the retina. In the human eye, the retina is the innermost and light-sensitive layer. The retinal tissue is inverted in the sense that the light-sensing cells are in the back of the retina so that the light has to pass through layers of neurons and capillaries before it reaches the photosensitive section. Anatomically is the human retina divided into ten layers: 1) Inner limiting membrane 2) Nerve fiber layer 3) Ganglion cell layer 4) Inner plexiform layer 5) Inner nuclear layer 6) Outer plexiform layer 7) Outer nuclear layer 8) External limiting membrane 9) Layer of photoreceptors 10) Retinal pigment epithelium.
Along with the cross-sectional classification, the human retina could be also described by regions of the ocular fundus in an eccentricity-dependent fashion. First, the fovea, which covers an area of approximately 1.5 mm in the center of the posterior pole, is specified by the highest cone density, hence providing a vision of the highest quality. The region surrounding the fovea, the macular region, covers approximately 6.0 mm around the foveal center. Another element, forming the posterior segment is the optic nerve head, being physiologically placed nasally, at an approximate distance of 3.4 mm from the fovea.
The cone density reduces dramatically with increasing eccentricity, reaching its minimum at approximately $\pm 10^{\circ}$ of retinal angle, remaining constant thereafter. Rods exhibit an approximate inverse distribution pattern with the peak density at 18° of retinal angle. Within the area of the optic nerve all photoreceptors are absent, and hence this area is also referred to as the blind spot. The following layer under the retina is the choroid, which is structured in five layers and is an anatomical part of the uvea. The choroid encloses the outer retina to ensure blood supply and thus supports retinal nutrition, stability, and protection. While the blood supply is the primary function of the choroid, it is also involved in the regulation of the intraocular pressure and ocular growth.

1.2.2 Visual pathway

The retina (see Figure 2) is arranged to enable an optimal light pathway to process the visual input from outer to inner retinal structures. After the light passes through the anterior segment's optical system, the photons are first absorbed by the photore-

ceptors. In this retinal layer, the process of phototransduction takes place [Mannu, 2014], subsequently forwarding the visual output as electric-potential signals through the optic nerve up to higher-level processing steps along the visual pathway and in the visual cortex [Kolb, 2009].

The neural pathway starts at the optic disc on the retina, where all the neural fibers bond to the optical nerve. The further visual pathway consists of the optical nerves (nervus opticus) of both eyes, later introducing an area of chiasma opticum (crossing of inner fibers of the optical nerves) at the base of the human brain. Anatomically, the neural bonds after the optical chiasma are referred to optical tracts, transferring the visual information to the corpus genicualtum laterale (a neural structure that serves as a processing station on the way from the retina to the occipital lobe of the cerebral cortex). Here the neurons rotate by 45° inwards and continue as the optical radiation fibers to the primary visual cortex in the occipital lobe.

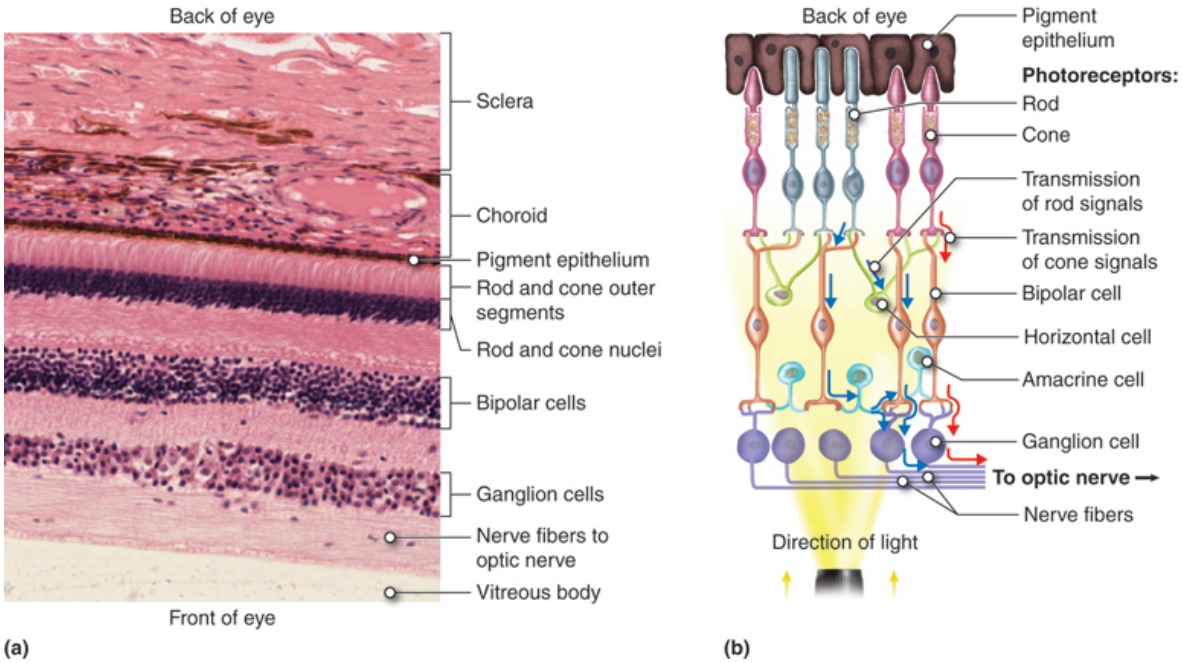

Figure 2: Layers of the retina in stained tissue (a) and as a drawing (b). The retina is composed of several layers and contains specialized cells for the initial processing of visual stimuli, with the rest of the visual processing occurring in the central nervous system. Imported from "Cenveo - Drawing Layers of the retina" at AnatomyTOOL.org, licensed by: Creative Commons Attribution.

1.2.3 Extra-ocular muscles

The human eye is equipped with six extra-ocular muscles in order to stabilize and control all of the movements of the eye. There are four rectus muscles, namely the superior, inferior, lateral and medial, being attached to the eye at the four cardinal locations, while each of the rectus muscles attaches to the eye at varying distances from

the limbus. The drawn connecting line of the insertion points is known as the Spiral of Tillaux. On top of that, there are two oblique muscles, superior and inferior attached to the eye, as depicted in Figure 3. The innervation, primary and secondary action is described in Figure 4. An additional outer muscle of the human eye is the levator palpebrae superioris, controlling the eyelid elevation.

The innervation models explaining the processes of executing eye movements have been proposed in the past by Hering, Sherington and Helmholtz. First, Hering's law of equal innervation [Hering, 1868], which is used for explanation of the conjugacy of saccadic eye, proposes innate connections in which the extra-ocular muscles responsible for each eye's movements are innervated equally. In connection to that statement, Sherrington's Law adds that any increase in innervation to an agonist muscle must also include a simultaneous decrease in innervation to the antagonist muscle. In contrast to Hering's law, Helmholtz suggested that both eyes are controlled monocularly as the binocular coordination is necessarily a learned behavior.

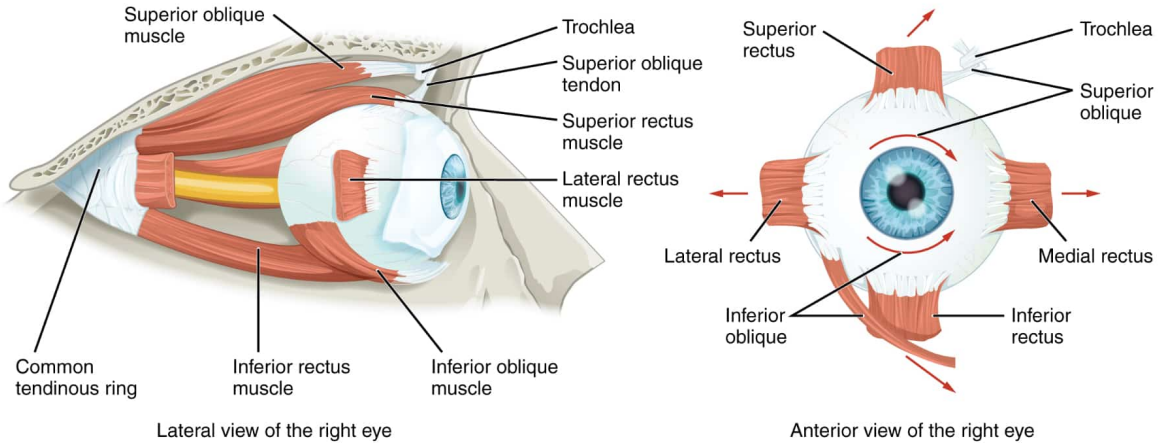

Figure 3: Extra-ocular Muscles. The extra-ocular muscles move the eye within the orbit. Imported from [Betts et al., 2013] licensed by Creative Commons Attribution.

Muscle	Innervation	Primary action	Secondary action
Medial rectus	Oculomotor nerve (inferior branch)	Adduction	
Lateral rectus	Abducens nerve	Abduction	
Superior rectus	Oculomotor nerve (superior branch)	Elevation	Incyclotorsion
Inferior rectus	Oculomotor nerve (inferior branch)	Depression	Excyclotorsion
Superior oblique	Trochlear nerve	Incyclotorsion	Depression
Inferior oblique	Oculomotor nerve (inferior branch)	Excyclotorsion	Elevation

Figure 4: Table of the six extra-ocular muscles mentioned with their innervation and functions.

1.3 Eye movements

The class of eye movements includes the voluntary and involuntary movements of the eyes, helping in acquiring, fixating, and tracking visual stimuli. These are executed with the use of the six extra-ocular muscles attached to the sclera of the eye. In this section, eye movements such as saccades, microsaccades, and optokinetic nystagmus will be introduced, as they have been used in the past in contrast sensitivity assessment or were used in the studies of this dissertation.

1.3.1 Saccades

Saccades are rapid, ballistic, conjugate movements of the eyes that allow to abruptly change the point of fixation in space and bring the image of an object of interest into the fovea. The range of their amplitude covers from small eye movements performed by reading tasks for instance, to larger movements made while scanning a scenario. Saccadic eye movements are said to be ballistic because the saccade-generating system cannot respond to subsequent changes in the position of the target during the course of the eye movement [Becker and Fuchs, 1969]. This type of eye movement is one of the fastest produced by the human eye, exceeding 500 °/sec for large saccades of 20° and more [Bieg et al., 2012], while its velocity is linearly dependent on the eye movement amplitude, resulting in a main sequence pattern, being also characteristic for fixational saccades, as elaborated below. In normal, voluntary saccades, the linear relationship in the main sequence paradigm, however, saturates for eye movements larger than approximately 10°, showing negligible differences in velocities in the high-amplitude saccades [Bieg et al., 2012].
Moreover, saccades can be triggered in a reflexive fashion as well. These reflexive, or stimulus-elicited, saccades are sort of eye movements being triggered towards a peripheral visual or auditory stimulus and were shown to be distinct from the voluntary saccadic eye movements. For instance, the latency of reflexive saccades was found to be shorter, compared to normal saccades [Walker et al., 2000] or different neural structures were thought to be involved in the respective eye movement triggering [Schall, 1995; Pierrot-Deseilligny et al., 1995; Henik et al., 1994].

1.3.2 Microsaccades

Microsaccades are a specific type of saccadic eye movement occurring while fixating a target, hence also called fixational saccades. These have a typical amplitude of $< 1°$ and occur with an approximate frequency of 1-2 Hz. In terms of the similarity of microsaccades and voluntary, large-scale, saccades, these two eye movements share a wide range of common characteristics. First, both types of eye movements are considered

to be binocular events with almost identical amplitudes and directions in both eyes [Ditchburn and Ginsborg, 1953; Krauskopf et al., 1960]. Second, both follow the main sequence pattern - the linear relationship between the peak velocity and the amplitude of the respective eye movement [Zuber et al., 1965]. Third, the execution of both eye movements is surrounded by an effect of peri-saccadic suppression [Volkmann et al., 1968; Zuber and Stark, 1966]. Next, a strong relationship between spatial attention and saccadic generation has been found as saccades are virtually always preceded by shifts of covert attention [Deubel and Schneider, 1996; Kowler et al., 1995]. Such finding has been also disclosed for microsaccades [Engbert and Kliegl, 2003b; Laubrock et al., 2005; Hafed and Clark, 2002]. These findings are consistent with the concept of microsaccades and saccades being a product of the same neural centers implementing the generation of high-velocity eye movements. A central node in that network is the superior colliculus (SC), a layered structure in the dorsal part of the mesencephalon engaged in the programming and execution of saccadic eye movements [Munoz, 2002]. The intermediate and deeper layers of the SC contain motor-related cells the activity of which is strongly correlated with the generation of saccades and visual fixation. Furthermore, the microsaccades showed a changing rate across time after stimulus onset. Shortly after the presentation of a visual stimulus, the rate of microsaccades drops abruptly, creating a minimum (microsaccadic inhibition) before showing a rate enhancement followed by final resettlement at the initial baseline level. Such temporal change in the microsaccadic rate is known as the rate signature [Rolfs et al., 2008; Scholes et al., 2015b; Bonneh et al., 2015]. Interestingly, the investigations of the microsaccadic rate signature showed that also the absence of a visual stimulus, using only an auditory cue, leads to the typical microsaccadic response [Rolfs et al., 2005].

1.3.3 Optokinetic nystagmus

Optokinetic nystagmus (OKN), also called optokinetic response (OKR) is a physiological reflexive eye movement that is activated by the eye-tracking mechanisms as a response to a drifting stimulus, thus allowing the eye to follow objects in motion when the head remains stationary [Sangi et al., 2015]. This eye movement which develops at about six months of age [Atkinson, 1984], occurs in a saw-tooth manner, which consists of two phases - the slow phase (OKN-SP) followed by a quick phase (OKN-QP). The slow phase refers to a tracking, smooth-pursuit-like eye movement in which case the eye follows the direction of the moving stimulus. The OKN-QP is a saccade-like eye movement, and although the velocity-amplitude relationship has been found to be comparable with reflexive saccades [Garbutt et al., 2001], the OKN-QP has not been assumed to be a saccade because of the different neural circuits responsible for its triggering [Hanning and Deubel, 2019]. Furthermore, based on the aim of the observer

or the request of an examiner, two types of OKN are recognized. The two types are look- and stare-OKN. Look-OKN is triggered if the subject actively tracks the drifting scenario, while the stare-OKN is elicited when trying to maintain the fixation at a single point in space. The OKN reflex remains present throughout the entire life, however, an already performed study by Valmaggia et al. [2004] found the gain (ratio of the physical velocity of a stimulus and the velocity of the respective OKN-SP) of stare OKN to be developing over a lifetime. Although considering a constant velocity of the stimulus drift, the OKN gain increases in its value till approximately five years of age, rising the value from 0.4 to 0.8, for a stimulus velocity of 15 °/sec. Thereafter, a saturation period is expected with a slightly decreasing gain after the age of 50. Furthermore, at an early stage of approximately 1 year of age, the discrepancy in the gain of nasal-to-temporal and temporal-to-nasal OKN movement diminishes and remains practically identical till the end of the life [Valmaggia et al., 2004]. Besides age, having a considerable influence on the OKN gain, also other parameters as for instance the clarity of the stimulus [Doustkouhi et al., 2020a], the stimulus spatial frequency and contrast [Rinner et al., 2005], the stimulus velocity [Valmaggia and Gottlob, 2004] or the stimulated area on the retina [Doustkouhi et al., 2020b] are factors, which play a crucial role in the responding velocity of the OKN-SP and therefore influence the OKN gain. The neural center responsible for the OKN control is the nucleus of the optic tract, dorsal terminal nucleus of the brain stem, and the middle temporal and middle superior temporal regions of the cerebral cortex. Interestingly, the OKN does not require normal functioning of higher cognitive processes when the stimulus is visible [Sakai et al., 2002].

1.3.4 Detection of eye movements

In eye movement detection procedures many different statistical methods are used to analyze the gaze data to filter the desired eye movements. Here in this chapter some of them are introduced with their advantages and disadvantages.
Velocity thresholding (VT) algorithms for saccade detection are the most commonly used ones [Komogortsev et al., 2010; Salvucci and Goldberg, 2000]. These classify events of saccades if the velocity between the consecutive points exceeds a given threshold, or as a fixation otherwise. Setting the threshold may be either fixed, resulting in a possible higher false positive detection if the threshold is set too low or missing saccades in the data set if the threshold is set too high, or methods with adaptive thresholding have been proposed to address the fixed-threshold issues [Mould et al., 2012]. For the easiness of implementation and robustness, one of the currently most used VT algorithms for saccadic detection is the Engbert's algorithm [Engbert and Kliegl, 2003c; Engbert, 2006]. Engbert set the value of the velocity threshold to be

proportional to the standard deviation of the entire velocity data, making the saccade velocity thresholding noise-adaptive. Furthermore, the Engbert's algorithm applies the velocity thresholds for the horizontal and the vertical component individually, resulting in a noise ellipsis that a potential saccade has to exceed. Such individual computing of the horizontal and vertical velocity thresholds is necessary as the noise level of the eye differs across the horizontal and vertical planes. On top of that, since a saccade is considered a binocular event, the algorithm marks events of a saccade only in sequences the velocity of both eyes exceeds the noise ellipsis. This method was then originally proposed for microsaccadic detection, by adding the limiting factor of the eye movement's least and maximum amplitude. Although the ranges of the amplitude limits are comparable the exact values differ among studies [Engbert and Kliegl, 2003c; Ciuffreda and Tannen, 1995; Scholes et al., 2015b; Bonneh et al., 2015]. However, such algorithmic detection was stated to be applicable in saccadic detection as well [Tatiyosyan et al., 2020].

Another approach used in saccadic detection is the implementation of the dispersion thresholding (DT) algorithms. Here a saccade is detected if the gaze exceeds a given area, or as a fixation, if the gaze lingers in that field. However, classifying saccades using this algorithm showed that there is no definite optimum dispersion threshold, Blignaut [2009] suggesting an acceptable range for the radius threshold between 0.7° and 1.3°. Furthermore, using this approach in saccade detection procedures, one has to consider its sensitivity to noise and ocular drift and the analysis of the start-time and the end-time of saccades is inaccurate.

Besides, other types of saccade-detection algorithms have also been proposed, however, not showing as common use as the dispersion or velocity-based approaches. Here to mention is the hidden Markov model method [Houpt et al., 2018], the identification by minimal spanning tree [Andersson et al., 2017] or acceleration-based–algorithms [Behrens and Weiss, 1992], for instance.

Furthermore, machine learning–based algorithms have also been employed for the purpose of saccade detection. For instance, König and Buffalo [2014] in their work calculated the distance, velocity, acceleration, and angular velocity of each sample with k-means clustering in order to distinguish saccades and fixations. In general, machine-learning-based algorithms have shown superior performance of saccade detection compared to hand-crafted algorithms [Zemblys et al., 2018], however using these algorithms may suffer from over-fitting problems and need for labeled data for training to detect the desired eye movement correctly.

Detection of other types of eye movements, like optokinetic nystagmus, relies either on observing of an experienced examiner, as it was performed in the past [Cetinkaya et al., 2008], using machine-learned algorithms for recognizing the saw-tooth manner

of the eye movement [Norouzifard et al., 2019], or processing of the optic flow of the eye limbus in a captured video [Turuwhenua et al., 2014].
Another approach uses the fact that although the quick-phase of OKN was not approved to be considered as a saccade [Hanning and Deubel, 2019], the velocity characteristics allow using algorithms for saccadic detection [Garbutt et al., 2001; Tatiyosyan et al., 2020]. Dakin and Turnbull [2016] used the first derivative of the eye position to compute the velocity of the eye, along with a fixed threshold the velocity had to exceed to consider the eye movement as a quick-phase (saccade), with a subsequent step of calculating the proportional eye velocity samples in agreement with the stimulus direction (slow phase moves with the stimulus and quick phase moves against the stimulus). Here the OKN was detected as the proportional velocity exceeded 0.5. In a recent work by Mooney et al. [2018], however, this method of OKN detection was stated to be affected by a high rate of false-positive detection.
A modified approach in OKN detection, recently used by Tatiyosyan et al. [2020], used Engbert's algorithm for the quick-phase detection with a subsequent search for a potential slow-phase between the two detected quick phases. This was performed by setting a threshold to the slow phase velocity, which the eye had to exceed to be successfully recognized.

1.3.5 Methods of eye movements implementation in visual performance assessment

This part covers the already performed experiments on the measurement of visual performance using several types of eye movements. Here the studies assessing the parameters such as visual acuity, contrast sensitivity, color vision, or assessment of visual field using various types of eye movements will be introduced. First, microsaccades have been shown in work by Scholes et al. [2015a] or Bonneh et al. [2015] to be feasibly used in contrast sensitivity assessment by analyzing the amplitude of the rate signature function. In this context Scholes et al. [2015a] found decreasing amplitudes of the inhibition and enhancement part of the microsaccadic rate signature depending on the contrast level, showing more profound inhibition and rebound peaks of the rate signature function in stimuli of higher contrast levels. In combination with a machine-learned vector classifier, employed for the detection of the function presence, this study concluded microsaccadic rate signature is a useful tool for contrast sensitivity assessment. Nonetheless, the microsaccadic occurrence rate has been found to be widely varying across patients, making the clinical usability of microsaccades in contrast sensitivity estimation difficult. On top of that, the study of Scholes et al. [2015a] was conducted under binocular stimulation conditions, hence not supporting the clinical fashion of such measurements, which are commonly run under monocular stimulation.

Next, optokinetic nystagmus responses have been already used in a wide range of visual performance measurements, namely visual acuity [Cetinkaya et al., 2008], contrast sensitivity [Dakin and Turnbull, 2016], color vision [Cavanagh et al., 1984; Taore et al., 2022] or assessment of patient's visual field [Doustkouhi et al., 2020b]. For stimulating the OKN response in visual performance measurements square-edge gratings, sine gratings, or noise patterns were used, drifting on a screen in a wide range of velocities, spatial frequencies, contrast levels, colours, and sizes.

First, the visual acuity obtained in OKN-based measurements was performed by changing the spatial frequency of a target, while maintaining the contrast level constant. Furthermore, two distinct approaches have been utilized in such measurement procedures - suppression and induction method, targeting either decreasing spatial frequency till a point of no OKN response, or increasing the spatial frequency till a point of the first OKN response, respectively. Both methods showed well-correlated results of OKN-based visual acuity to subjective measurements, as well as a good test reproducibility [Hyon et al., 2010].

Optokinetic nystagmus used in the context of the assessment of contrast sensitivity also showed correlated results with subjective responses to the drifting stimulus [Dakin and Turnbull, 2016], suggesting its feasibility in contrast sensitivity evaluation in a clinical way. Here the sensitivity was measured over a range of spatial frequencies, resulting in the creation of a contrast sensitivity curve. Nonetheless, the peak of the contrast sensitivity curve was found to be shifted toward smaller spatial frequencies, compared to standard measurements conducted with a stable visual stimulus, as the peak sensitivity shifts depending on the stimulus velocity [Burr and Ross, 1982].

In the assessment of the visual field, the gain of optokinetic nystagmus was analyzed showing a trend toward smaller values with increasing size of simulated scotomas, suggesting the employment of the OKN gain analysis in the evaluation of the visual field defects. Nonetheless, since the measurements were performed for scotomas of inorganic shapes, their applicability into the clinical practice remained questionable [Doustkouhi et al., 2020b].

Last, the optokinetic nystagmus responses have also been employed in color vision testing [Taore et al., 2022]. In this procedure, Taore et al. [2022] exploited the finding that first the motion of a colour-defined stimulus can be canceled by adding a low-contrast luminance-defined stimulus moving in the opposite direction and second that this equivalent luminance contrast required for such cancellation is reduced when colour vision is abnormal.

Additionally to the eye movements mentioned above, also smooth pursuit eye movements have been employed in contrast sensitivity testing in the previous works [Schütz et al., 2007; Mooney et al., 2018, 2020].

1.4 History and technical aspects of eye trackers

During the early stages of eye tracking, examiners monitored their own eye movements by observation. The eye-tracking technology was started in the late 1870s, using mirrors to observe the eye movements of subjects while reading, noting that the eyes moved in a series of jerky movements. Later, an approximate measure of the location of fixation could be obtained by inducing an afterimage in the subject's eye with a bright light, with a subsequent request to report the location of the afterimage as they read [Erdmann and Dodge, 1898]. Such procedure obviously lacked sufficient accuracy [Dodge, 1906] and thus called for an objective tool for eye-movement detection.
At the beginning of the 20^{th} century a new type of eye tracker was developed, using the principle of corneal reflections called Purkinje images. In the early eye tracking technique the reflected light from the cornea was captured by a camera and exposed to a photographic plate with later digitization of the system. Further development unveiled the Dual Purkinje Imaging eye-trackers, using two out of four Purkinje images (the first and the fourth), instead of just one. The Dual Purkinje eye tracking measures the movement of the first and fourth Purkinje images with respect to one another. Another proposed option to track the eye movements was to use the electro-oculogram, considering the eye as a dipole (the retina acts as the cathode, and the cornea acts as the anode). Using this method, the horizontal eye movements could be tracked due to the change in the electromagnetic field. The limitation of this technique was the limited accuracy and only the horizontal eye movements could be detected as the electrodes placed on the vertical plane would suffer from noise resulting from the activity of the musculus levator palpebrae superior [Holmqvist and Andersson, 2017]. Nonetheless, this procedure enables us to track the eye movements in the REM phase of sleeping [Aserinsky and Kleitman, 1953]. Another procedure previously suggested, was the utilization of the eye limbus (the sclero-corneal border) tracking, using image processing in the recorded video. The advantage of this method is the enhanced contrast at the pupil border [Holmqvist and Andersson, 2017].
The above-mentioned systems used physical effects or anatomical features of the anterior segment of the eye. Besides the anterior segment of the eye, posterior (retinal) features can also be used in eye-tracking procedures, for instance the reflectivity of the optical disc. Later approaches have used image processing to track the optic disc and its movement to determine the eye movements [Kawai et al., 1986]. Nonetheless, the latest eye trackers are video-based ones, for instance, the EyeLink (SR Research, Ottawa, Ontario, Canada) eye tracker, which was employed also in the present dissertation. At the heart of all video-based eye tracking is a camera, or cameras that take a series of images of the eye. In connection with that, the eye-tracking software uses

image processing algorithms to identify two key locations on each of the images sent by the eye-tracking camera – the center of the pupil, and the center of the corneal reflection. Here the eye movement detection relies on the relative change in the location of the center of the pupil to the location of the corneal reflection on the camera sensor.

1.5 Pending questions in eye movement-based contrast sensitivity testing

Although the findings of the previous literature targeting the objective assessment of contrast sensitivity with eye movements showed a first evidence of the usability of eye movements in such kind of examination, as well as successful replication of clinical tests, this topic critically deserves further investigation and discussion. Therefore, the following paragraph elaborates on the pending questions in eye-movement-based contrast sensitivity testing, presents a summary of the outcomes of the conducted research, and gives a further outlook.

First, as investigated by Scholes et al. [2015a] or Bonneh et al. [2015], the microsaccadic rate signature function was shown strictly for binocular stimulation, conducting the respective eye movement stimulation with only one spatial frequency of a Gabor patch. Thus this procedure gives the first evidence that contrast level affects the amplitude of the microsaccadic rate signature function, nonetheless, this phenomenon across a range of spatial frequencies has not been targeted so far. Moreover, as Scholes et al. [2015a] stimulated microsaccades binocularly, the clinical applicability of such measurement was not fulfilled. Hence it has been found necessary to extend the work of Scholes et al. [2015a], first by testing the effect of spatial frequency on the rate signature curve and most importantly finding a way to stimulate the eye movement under monocular stimulation conditions, yet being able to track both eyes, having a possibility to detect microsaccades as binocular events and thus follow their fundamentals. Only this approach using monocularly stimulated microsaccades will lead to the appropriate utilization of this kind of eye movement in the clinical measurement of contrast sensitivity.

In the context of these gaps presented above, the first project tested microsaccades under monocularly and binocularly stimulated conditions, by patching one eye with an infra-red filter in the monocular stimulation, disabling the participant to see the target with the covered eye, however enabling always binocular tracking and thus the same eye movement filtration in both stimulation conditions. This method was selected as the saccadic, hence also microsaccadic, events are considered to be purely binocular events. Furthermore, the microsaccadic stimulation was conducted over a wide range of spatial frequencies 0.5, 4.0, 11.0,22.0 cpd of a Gabor patch with a defined contrast level 50% in both stimulation conditions. In this study the rate signature curves, proposed

already before by Scholes et al. [2015a] as a tool for contrast sensitivity appraisal, were shown to be correlated for the two stimulation conditions across a wide range of spatial frequencies. Moreover, the eye-tracking quality was evaluated in both conditions, in order to answer the potential effect of the presence of the infrared filter in the one stimulation condition on the eye tracking fineness. Here the statistical testing of the data from the eye-tracker calibration and validation procedures in the two stimulation conditions showed insignificant shift in the tracking accuracy in condition of the infrared filter presence.

Discussing the major outcomes of the first project focused on extending the clinical applicability of microsaccadic-based contrast sensitivity testing into the clinical practice, the correlation of the binocularly and monocularly stimulated microsaccadic rate signatures shown in the study yields a piece of additional information to the binocularity of these fixational saccades and confirm the microsaccadic occurrence in both eyes regardless the stimulation condition, comparably to voluntary saccades [Zhou and King, 1999], and thus adds a further support to similarity of voluntary saccades and microsaccades, which are both traditionally considered to be of the same velocity-amplitude relationship [Zuber et al., 1965], being triggered by the same neural circuit [Munoz, 2002], being considered as strictly binocular events [Engbert and Kliegl, 2003a], and the execution of both types of eye movements is surrounded by an effect of peri-saccadic suppression [Volkmann et al., 1968; Zuber and Stark, 1966]. However, as the amount of the microsaccadic events has been found inconsistent among participants leading to a need for trial repetition to collect a sufficient amount of data and thus reducing the time-efficiency of such measurements, the hardware set-up demands a high-quality eye tracking system, since these fixational saccades are of small amplitude, the usability of microsaccades in contrast sensitivity measurements in the clinical practice is reduced and practically disables the use of VR headsets for its insufficient eye-tracking performance.

As shown by Cetinkaya et al. [2008]; Wester et al. [2007]; Doustkouhi et al. [2020a]; Taore et al. [2022] optokinetic nystagmus (OKN) showed strong feasibility in visual performance assessment. Most importantly, the work of Dakin and Turnbull [2016] showed a strong correlation between the OKN-based contrast sensitivity curves and subjectively measured ones. Nonetheless, as stated by Mooney et al. [2018] the detection procedure used by Dakin and Turnbull [2016] suffers from a high error rate and hence prevents from utilization a psychometric procedure which again prevents from an adaptive search of the contrast threshold and thus results in a time-consuming measurement. Furthermore, the effect of defocus in the OKN-based contrast sensitivity test remained unexamined, yielding no supportive information how the eye movement test performs in conditions of systematically worsened vision. In summary, the conducted

research performed on an objective examination of contrast sensitivity measurements using the OKN responses failed to establish a fully automated test, as well as providing information of the effect of defocus in an OKN-based contrast sensitivity test. Hence the second study targeted a customized OKN-based contrast sensitivity test with applied real-time detection and an adaptive psychometric procedure for the contrast management, as well as testing conditions without and with various levels of defocus in fine steps in emmetropes. Here the level of defocus was manages by inserting trial lenses of 1.5 D, 2.0 D and 2.5 D into a trial frame, being above an accommodational demand for a 75 cm distant target.

In results, the second study showed an expected trend of decreasing sensitivity with an increasing level of defocus, especially in the range of high spatial frequencies. This outcome was considered as a successful replication of this well-known effect of defocus on contrast sensitivity from the clinical trials, and besides the outcome of the study of Dakin and Turnbull [2016], this outcome validated the use of OKN in such kind of testing for potential clinical use. Furthermore, the combination of a newly developed live detection method of the OKN response, having comparable performance to an offline detection algorithm, and an adaptive psychometric procedure, led to an improvement in the time performance of the objective OKN-based contrast sensitivity assessment and therefore resulted in a completely new online-based contrast sensitivity test. Furthermore, as the detection rate in the current study was found to be better compared to the one proposed by Dakin and Turnbull [2016], as evaluated by Mooney et al. [2018] the novel detection method allows to implement adaptive procedures and hence extends the applicability of such a test to the clinical environment.

In discussion, although the newly proposed detection procedure was verified by an offline detection procedure and an expert judgment of the presence of the OKN response, showing the algorithmic detection to be of a similar performance in comparison to the subjective judgment a small amount of OKN has been detected false-negative. Therefore the study proposed to use a specific threshold for the least OKN-SP for each of the contrast level, as the OKN gain was shown to be changing with contrast level in zebrafish [Rinner et al., 2005]. Although such an eye-movement-based test for the objective appraisal of contrast sensitivity carried the potential to be feasibly used in the clinical practice, as well as to be implemented to the VR set-up Tatiyosyan et al. [2020] the major disadvantage of such a testing method is a need for a moving stimulus for the stimulation of the OKN responses, affecting the contrast sensitivity performance by shifting the contrast sensitivity function towards smaller spatial frequencies with increasing velocities of the moving stimulus [Burr and Ross, 1982], hence not accommodating to the standard-used tests, whose visual stimuli are stable. Furthermore, as the magnification of the inserted lenses being used to systematically worsen the

patient's vision could result in a shift of the presented spatial frequencies, this study tested only lenses above the accommodational demand respective to the testing distance and not magnify the image by more than 5% [Ohlendorf and Schaeffel, 2009].
Next, although the range of eye movements being used in contrast sensitivity testing is wide, covering for instance microsaccades [Scholes et al., 2015b; Bonneh et al., 2015], optokinetic nystagmus [Dakin and Turnbull, 2016], or smooth pursuit eye movement [Mooney et al., 2018], the patient has always fixated the visual stimulus, id est the current literature covers only the central contrast sensitivity. Such an approach has prevented testing the peripheral areas of the patient's visual field, being important, especially in the early diagnosis of various retinal diseases. As already stated by Hot et al. [2008], the subjectively performed contrast sensitivity perimetry yields extremely valuable information about the patient's visual performance across their visual field and significantly reduces the test-retest variability, in comparison to the conventional automated perimetry. As this technique has been conducted in a subjective way, there is an obvious need to translate this method to an objective fashion using eye movements. Furthermore, as Rosen et al. [2014] found different performance in contrast sensitivity across the visual field, considering various directions and eccentricity levels, the additional requirement for such a novel, objective eye movement test was to implement this knowledge and find a way to examine all the selected locations in the visual field for contrast sensitivity independently. Therefore, the last study of this thesis discloses an approach of employing reflexive saccades in such measurement across various eccentricity levels and directions in the patient's visual field. To do so, this test employed live detection of the saccadic eye movement accompanied by four individual instances of an adaptive psychometric procedure for the contrast management, respecting the individuality of the four tested cardinal directions in the patient's visual field in three different eccentricity levels. Moreover, in order to evaluate the novel approach of using reflexive saccades in contrast sensitivity assessment, two instances of subjective validation were performed, comparing the saccadic-based contrast sensitivity to a standard measurement, once in the eye movement-based test and once in a separate test. In the standard subjective measurements a keyboard-based response to the target orientation was requested. Furthermore, catch trials were added in the eye movement-based test, to validate the robustness of the testing procedure.
As supported by the results of this study, showing correlated contrast sensitivity functions for the saccadic-based and keyboard-based responses, the study concluded the use of reflexive saccades in the objective assessment of contrast sensitivity perimetry to be feasible. Furthermore, the study replicated an expected effect of decreasing contrast sensitivity in the four different directions towards the periphery in a non-uniform fashion. Discussing the obtained results of the study, the saccadic-based contrast sensitivity

systematically underperformed the two instances of the keyboard-based measurements, however yet yielded comparable and correlated results of a clinically negligible difference to the key board-based trials. As a result of the limitation of the screen size used in the study, the maximal eccentricity reached only 11°, being considered to be limiting the examination of the further periphery of the patient's visual field, which might be useful in the early diagnosis of some eye diseases, for instance, glaucoma. Furthermore, as the implemented catch trials to verify the approach of using reflexive saccades in peripheral contrast sensitivity examinations showed 4% of false positives, id est the gaze was found outside of the fixation area, although no target had been presented, the study first fulfilled a proposed criterion a false-positive rate should not exceed 20% in perimetry testing [Vingrys and Demirel, 1998] and second proposed to enlarge the fixation area as some rare instances of fixational eye movements could be of a bigger amplitude then 1°[Otero-Millan et al., 2008; Krejtz et al., 2018], and hence be possibly the source of the low false-negative rate.

Although the presented outcomes of the own studies of this thesis pushed the methodology of CS examination using eye movements forward, presenting novel approaches and procedures, further research should be conducted to answer the following and yet pending questions. First of all, in order to satisfy the need for a range of tests, objectively assessing the patient's visual performance, future research should shed more light on the examination of visual acuity, color sensitivity, or perimetry using eye movements. Furthermore, in connection to the transition of such tests to clinical practice, validation with the gold-standard methods is obviously needed, as well as the statistics focused on the repeatability of every one of the eye-movement-based tests. Moreover, stressing the importance of early detection of a potential eye disease, the translation of such eye movement-based tests to the VR environment should be investigated in order to enable home screening and thus establish the desired diagnosis as early as possible. Here the proposed utilization of VR headsets brings a significant advantage of portability, as the displaying and eye-tracking hardware are embedded in one apparatus, and affordability as a range of VR headsets is already available on the market.

From another perspective, as the stimuli used in projects of the current thesis were all artificial, proposing potential investigations using natural stimuli, which may disclose valuable information needed for the fundamental understanding of human visual performance in a real-world scenario. Also, as the eye movement-based tests critically rely on the eye movement detection procedures, the establishment and application of novel detection methods, using for instance automated algorithms based on AI, might also be a target of a future interest.

2 Objectives

Contrast sensitivity (CS), as one of the most crucial parameters in the clinical assessment of a patient's visual performance, is strictly limited to subjective testing procedures. This subjective approach may not allow examinations of children or non-communicative patients, who might have difficulties with responding to the examiner's questions, in order to perform the test appropriately. On top of that, objective testing of CS should be included to other tests of visual performance in myopia management or amblyopia treatment. For this reason, the conducted research proposed the utilization of eye movements as a possible way to test the CS objectively, with a possible translation to the clinical environment.

In this context the current thesis aimed to present three projects conducted on purpose to establish and validate novel eye movement-based CS tests, or to optimize the already established ones, using various types of eye movements.

In this context, the first study investigated the microsaccadic rate signature, which was already linked with binocular CS appraisal in the past. Nonetheless, as the performed binocular testing could not be considered clinically suitable, the aim of the first study was to disclose monocularly stimulated microsaccadic rate signatures across a range of spatial frequencies, however in conditions of binocular eye-tracking. This may yield a possibility to examine CS objectively following clinical conditions, yet keeping microsaccades as binocular events. As a control condition, the testing under binocular stimulation was performed as well. The second study aimed to use optokinetic nystagmus in CS measurements, being already used by researchers in the past. In this study, the aim was to automate the testing procedure to improve the lack of time efficiency of previously proposed methods, by establishing a novel live detection procedure of the eye movement in combination with an adaptive psychometric procedure. On top of that, this study aimed to cover measurements under several defocus conditions in fine steps, to replicate the effect of defocus on CS in an eye movement-based test.

The last experiment targeted the extension of the portfolio of eye movements used in objective testing of CS also to the peripheral vision. In this study, the measurements of CS were conducted using reflexive (reactive) saccades made towards the location of a visual stimulus appearing in various eccentricity levels and directions in the patient's visual field. In order to automate the testing procedure, four events of an adaptive psychometric procedure were utilized, to search for the contrast threshold in each location individually. On top of that, a live detection of the respective eye movement was employed. To validate the newly established approach, standard keyboard-based responses to a feature of the visual stimulus were requested once in the saccadic-based test and once in a separate measurement.

3 Microsaccadic rate signatures correlate under monocularly and binocularly stimulated conditions

Essig P., Leube A., Rifai K., & Wahl S. (2020). Microsaccadic rate signatures correlate under monocularly and binocularly stimulated conditions. Journal of Eye Movement Research, 13(5):3. doi: 10.16910/jemr.13.5.3

3.1 Abstract

Microsaccades are involuntary eye movements occurring naturally during fixation. In this study, microsaccades were investigated under monocularly and binocularly stimulated conditions with respect to their directional distribution and rate signature, which refers to a curve reporting the frequency modulation of microsaccades over time. For monocular stimulation, the left eye was covered by an infrared filter. In both stimulation conditions, participants fixated a Gabor patch presented randomly in the orientation of 45°and 135°over a wide range of spatial frequencies appearing in the center of a monitor. Considering the microsaccadic directions, this study showed microsaccades to be preferably horizontally oriented in their mean direction, regardless of the spatial characteristics of the grating. Furthermore, this outcome was found to be consistent between both stimulation conditions. Moreover, this study found that the microsaccadic rate signature curve correlates between both stimulation conditions, while the curve given for binocular stimulation was already proposed as a tool for estimation of visual performance in the past. Therefore, this study extends the applicability of microsaccades to clinical use, since parameters as contrast sensitivity, has been measured monocularly in the clinical attitude.

3.2 Introduction

Fixation on a visual target is not stable, instead such a fixation is accompanied by small involuntary eye movements – fixational eye movements (FEMs) [Martinez-Conde et al., 2004; Otero-Millan et al., 2014; Poletti and Rucci, 2016; Rolfs, 2009; Rolfs et al., 2008; Rucci and Poletti, 2015]. Among FEMs, three types of eye movements are included as tremor, drift and microsaccades [Collewijn and Kowler, 2008; Kowler, 2011], which are distinguished from each other by their amplitude and velocity (for review see [Collewijn and Kowler, 2008; Krauzlis et al., 2017; Poletti et al., 2010; Rolfs, 2009]. Microsaccades are very fast FEMs (approximate range of velocities 50 to 200 °/s) with a typical amplitude smaller than 1°[Ahissar et al., 2016] and a rate of 1–3 Hz [Collewijn and Kowler, 2008]. In the past years, microsaccades have been discussed for their potential impact

on vision. Researchers have shown that microsaccades optimize gaze position in high visual acuity tasks [Ko et al., 2010], as well as they enhance visual acuity by optimizing the image position on the retina [Intoy and Rucci, 2020]. Microsaccades have been also found to be linked with covert attention [Corbetta et al., 1998; Engbert and Kliegl, 2003b; Kustov and Robinson, 1996]. Moreover, past research showed microsaccades as an indicator for discrimination of the orientation of a contrast stimulus featured by higher spatial frequency, however not for the stimulus of lower spatial frequency [Rucci et al., 2007]. In addition, those fixational saccades indicated sensitivity in the rate signature curve for small changes in contrast using a spatially oriented pattern with fixed spatial frequency of 0.33 cpd (cycles/degree) [Scholes et al., 2015a], as well as for larger changes in contrast using a spatially oriented grating with fixed spatial frequency of 3.0 cpd [Bonneh et al., 2015]. Furthermore, it has been shown that the microsaccadic rate signature is sensitive to changes in luminance and contrast in colour of a circular visual stimulus, or to presence of an auditory stimuli [Rolfs et al., 2008]. In terms of microsaccadic orientation, it has been disclosed that microsaccades occur in the spatial direction in which the attentional cue appears [Engbert and Kliegl, 2003b; Hafed and Ignashchenkova, 2013]. Additionally to this finding, microsaccades were found to be predominantly leftwards oriented in reading tasks and thus helping to refine vision by correction of inaccuracies in saccadic landing and by moving the gaze over the nearby words [Bowers and Poletti, 2017]. The microsaccadic directional distributions have also been demonstrated to vary for binocular and monocular microsaccades, using the EyeLink II eye tracker [Hermens and Walker, 2010]. However, the search for purely monocular microsaccadic events using Dual Purkinje Image eye-tracker and magnetic induction eye- coils failed [Fang et al., 2018]. Regarding to this discrepancy, as it has been shown, the term of monocular microsaccades was understood differently across the studies (for review see Bonneh et al. [2015]; Yablonski et al. [2017]; Gautier et al. [2016]). Accordingly, as proposed by Nyström et al. [2017]; Otero-Millan et al. [2014, 2008]; Engbert and Kliegl [2003a], the current study followed the understanding of microsaccades as a strictly binocular phenomenon. Despite these findings, microsaccades have been shown to occur in both, monocularly and binocularly stimulated conditions by stimulating either under binocular viewing conditions, or randomly left and right eye, while the participant perceived blank space with the fellow eye [Kloke et al., 2009]. Previously performed experiments on monocularly stimulated microsaccades have shown some methodological limitations, as for instance performing the separation of the visual input in monocular stimulation just by presenting different visual stimuli to both eyes. Therefore, this approach may result in a not totally-separated visual stimulation and thus lead to imperfect monocular stimulation and to methodological inconsistencies between outcomes of the different literature. In this relation, the current

study protocol proposed a distinct monocular visual stimulation condition by coverage of one eye with an infrared filter. Consequently, without visual stimulation of that eye but allowing the eye tracker to capture the eye movements binocularly. According to the previous observations, the current study targeted the question, whether both, monocular and binocular stimulation of microsaccades by a spatially oriented pattern will result in a comparable rate signature curves. The expectation of the current study was that the rate signature curves will correlate under the two distinct stimulation conditions, as long as the Hering's law of equal innervation Hering [1977] was taken into account in both circumstances. In addition, recent findings of Hafed et al. [2009]; Hafed and Krauzlis [2012] indicated the same neural circuit for production of microsaccades and normal saccades. Although, it seems that microsaccades coming from both monocular and binocular fixation share the same neural origin as they are understood as a conjugate eye movements [Krauskopf et al., 1960; Møller et al., 2002], there is an unsatisfying research questioning, whether the visual performance correlation with microsaccades can provide clinically meaningful measures. On the one hand Bonneh et al. [2015] and Scholes et al. [2015a] proposed the microsaccadic rate signature as a reliable estimator of contrast sensitivity, however, measured only under binocularly stimulated conditions. On the other hand, Denniss et al. [2018] measured contrast sensitivity under monocularly stimulated conditions, however the actual comparison of the microsaccadic rate signatures under distinct stimulation conditions was not considered. As the standard clinical measurements of contrast sensitivity are performed under monocular viewing conditions [Thayaparan et al., 2007], the main aim of the current research was to establish a methodological approach of a monocularly stimulated microsaccadic rate signature in healthy subjects with appropriate comparison to classical binocular stimulation of microsaccades. This attitude could be used as a visual performance indicator in the future, following the clinical standard as already proposed by Denniss et al. [2018]. For the theoretical motivation, pushing the understanding of microsaccadic occurrence forward, this study also questioned whether the monocular and binocular stimulation will result in the same descriptive features of a microsaccadic rate signature. Thus, by showing correlated rate signature curves in both stimulation conditions, this study proposes that microsaccades, triggered by either monocular or binocular external visual input, should be rather taken as the same physiological phenomenon. Therefore, the current research provides an additional information for better future understanding the generation of those fixational eye movements. Next, the current study investigated whether the condition of monocular stimulation will have any influence on the mean direction of microsaccades. In addition, it was examined whether a low level spatial characteristics of a centrally located visual stimuli will change the distribution of microsaccadic directions and thus

will provide an information about the spatial characteristics of such a visual stimulus. This parameter could be then potentially used as an additional indicator of visual sensitivity. Accordingly, the first hypothesis assumed, that the majority of microsaccades will follow the orthogonal direction of a presented Gabor patch, since micosaccades have been shown to be potentially visual input dependent [Rucci et al., 2007; Scholes et al., 2015a]. The highest modulation of luminance, and therefore the strongest visual input, was indicated to be orthogonal to the Gabor patch orientation [Rucci et al., 2007].

3.3 Participants

Twelve participants, four males and eight females, with a mean age of 25.3±1.5 took part in the study. All participants were healthy, had normal or corrected to normal vision and were naive to the purpose of the study. The study protocol followed the Declaration of Helsinki. In addition, the study was approved by the ethics committee of the Faculty of Medicine of the University Tuebingen and the signed informed consent was obtained from all participants prior to the experiment. All participants were recruited from University Tuebingen.

3.4 Stimuli and procedure

In this study all participants were required to sit with their head rested on a chin rest and forehead bar during the experiment, while no response to the given stimulus was requested. Additionally, the head-fixation setup was equipped with a sponge on both sides of the head, to defuse any undesired head movements. Room lights were turned off, while the luminance of the LCD monitor (VIEWPixx, VPixx Technologies Inc., Saint Bruno, Quebec, Canada;) was set to default luminance L=20 cd/m^2. The monitor was featured by a pixel resolution of 1920 x 1200, temporal refresh rate of 120Hz and was placed in a distance of 70 cm from a participant. Prior to every measurement a nine- point calibration and its validation was performed, resulting in comparable quality of every measurement. For microsaccades stimulation, a spatially oriented pattern with sinusoidal change in luminance - Gabor patch [Rucci et al., 2007] and a fixed contrast level of $C = 0.5$ according to the Equation(1), was used. For testing the potential impact of spatial frequency and the spatial orientation of the Gabor patch, four different frequencies of 0.5, 4.0, 11.0 or 22.0 cycles/degree (cpd) and two orientations of 45°and 135°were included. The orientation of Gabor patch was randomized within measurement. The visual stimulus was circular in shape, of a size of 3°. Before every presentation of a Gabor patch the monitor was set to grey with a red fixation mark in the centre of a 15 arcmin size, resulting a baseline condition without any spatial visual

information. In the same fashion, the fixation mark was included in the grating stimuli as well, to assist a participant to maintain fixation in the desired area. Furthermore, for avoiding any undesired afterimages a noise mask of the same size was included in the workflow. This mask was created by pixel randomization, by changing the spatial location of every pixel of the Gabor patch and thus resulting in the same mean luminance. Additionally, all stimuli were presented through a Gaussian window, to smooth the edges in order to avoid the enhanced edge detection by the visual system [Taylor et al., 2014].The entire procedure is shown in Figure(5). The stimuli and the workflow were programmed in a matrix-based software (MATLAB R2018b, MathWorks, Natick, MA, USA) and the Psychtoolbox-3 extension [Brainard, 1997; Kleiner et al., 2007].

$$C = \frac{L_{max} - L_{min}}{L_{max} + L_{min}} \tag{1}$$

In Equation(1) L_{max} and L_{min} represents the maximal and minimal luminance of a visual stimulus. Every participant underwent 5 measurements, resulting in 200 observations of the Gabor patch observations per spatial frequency. Both types of the visual stimuli, as well as the grey-just monitor, were presented for the same time, t = 1 s. Furthermore, this workflow was performed under both monocularly and binocularly stimulated conditions, while the examining under monocularly stimulated conditions was realized by covering the left eye with an infrared (IR) filter to forestall any visual stimulation for this eye. The transmission characteristics of the IR filter (ePlastics, San Diego, CA, USA) was $T > 90\%$ for $\lambda > 800\,\text{nm}$ and thus resulting in eye tracking always in a binocular fashion, as the infrared light ($\lambda = 850 - 940\,\text{nm}$) of the eye tracker (EyeLink 1000 Plus, SR Research, Ottawa, Canada) passed the filter. The sampling frequency of the eye tracker was set to 1000 Hz in both stimulation conditions.

3.5 Analysis of the fixational eye movements

Prior to the detection of microsaccades all blinks were removed with a buffer of 50 ms before and after the blink to protect the data from semi-blinks and blink-related artefacts. Blinks were detected for pupil size equal to zero. Further filtration of microsaccades was performed using the original version of Engbert's velocity-based algorithm in the same way for both, monocularly and binocularly stimulated conditions [Engbert and Kliegl, 2003b]. This could be done because of the tracking in a binocular fashion (see Stimuli and procedure). Applying the Engbert's algorithm, the time series of a gaze position were firstly transformed to velocities as a moving average over 5 data samples, resulting in the noise suppression [Engbert and Kliegl, 2003b]. Secondly, this algorithm works with the velocity thresholds obtained by application of the median estimator to the time series separately for horizontal and vertical components. De-

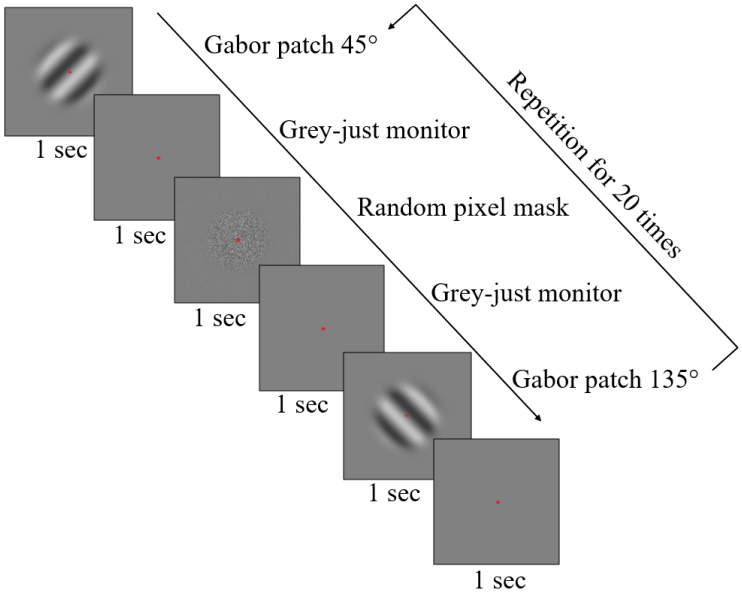

Figure 5: Workflow of the experiment. All five measurements per spatial frequency of the Gabor patch consisted of 20 presentations of the grating in both, 45°and 135°in a random order. Every Gabor patch was followed by a grey blank monitor to maintain the same baseline for both patterns. In addition, a noise mask of the same mean luminance was included resulting in cancel any retinal afterimages. A red dot was present across all patterns to help the participant to maintain the fixation in the desired area.

tection thresholds were computed separately for each trial and relatively to the noise level, as proposed by Engbert and Kliegl [2003b]. Next, the horizontal and vertical components were multiplied by a model's free parameter, that was set to a usual value, (λ=6) [Engbert and Kliegl, 2003b]. Because microsaccades are traditionally defined as a binocular occurring events [Engbert and Kliegl, 2003b; Fang et al., 2018; Kloke et al., 2009; Nyström et al., 2017; Otero-Millan et al., 2014], the Engbert's velocity-based algorithm takes this knowledge into account by including the time overlapping criterion, that could be considered in both of the stimulation conditions [Engbert and Kliegl, 2003b]. To prevent the analysis from overshoots, which may be examined as a separate eye movement events, a least time between two microsaccades was conservatively set to 50 ms [Scholes et al., 2015a]. Lastly, just microsaccades smaller than 1°and larger than 1 arcmin in their amplitude and longer than 5 ms in their duration were taken for the further analysis. For the analysis of microsaccades, MATLAB R2018b (MathWorks, Natick, USA) was used.

3.6 Data computations and statistics

If necessary, prior to the statistical assessment the particular data were tested for their normal distribution to avoid any drawbacks coming from the statistical computation. The assessment of normality was performed by Anderson-Darling test in the MATLAB

environment. All statistics was performed for the default level of significance 5%.

3.6.1 Main Sequence

Firstly, the microsaccadic peak-velocity and amplitude relationship – main sequence, as shown by Bahill et al. [1975]; Otero-Millan et al. [2008]; Zuber et al. [1965], was evaluated as a linear regression [Dumouchel et al., 1989]. This has been done separately, with respect to the two stimulation conditions. Since it has been known, that the microsaccades follow the main sequence pattern, this analysis was done to justify that the stimulation conditions did not change its typical appearance. Moreover, the statistical comparison of amplitude and peak velocity in both eyes was done as testing for potential binocular disconjugacy of microsaccades [Shaikh and Ghasia, 2017]. This testing was performed for both stimulation conditions using a non- parametric paired t-test (Wicoxson rank-sum test).

3.6.2 Directional distribution of microsaccades

The directions of microsaccades were computed for every tracking sample (1 ms). This was done by collecting the gaze position in every sample over the time length of every microsaccade and consequently treating each sample position exclusively. As originally the units were in pixels, the necessary conversion to degrees was performed by translating all gaze positions to polar coordinates. This approach resulted in a detailed description of directional distribution for all fixational saccades, as depicted on Figure (3). For the further testing, since there have been presentations of the stimulus without any microsaccadic response, the mean microsaccadic direction was calculated. Prior to the calculation, flipping of directions was performed by adding π to all direction smaller than $-\pi/2$ and subtracting a π from directions a larger then $\pi/2$. The actual microsaccadic mean direction was calculated for each measurement for all participants using the circular mean function included in circular statistics toolbox for MATLAB Berens [2009]. Testing whether the mean directions vary for the Gabor patch orientation or stimulation conditions the non-parametric two-way ANOVA (Friedman's test) was used with factors of the Gabor patch orientation and its spatial frequency. Furthermore, as the potential influence of either monocularly or binocularly stimulated conditions was tested, the non-parametric two-way ANOVA (Friedman's test) was performed with factors of spatial frequency of the Gabor patch and the two stimulation conditions, regardless the orientation of the grating.

3.6.3 Microsaccadic rate signatures

The modulation of the microsaccadic rate over time, rate signature, was calculated as proposed by Rolfs et al. [2008]. First the Dirac function was applied to all times of microsaccadic events, given the rate by temporal averaging by applying a window function. To obtain the desired rate modulation curve, the decay parameter α=1/30 was employed, comparably to Gao et al. [2015]; Rolfs et al. [2008]. Finally, the mean microsaccadic rate modulation over time was calculated by computing individual rate modulations and averaged across participants. The baseline of microsaccadic rate was calculated from the grey monitor containing just the centrally located red dot, that was taken as an irrelevant stimulus. The baseline was calculated for 300 ms before stimulus onset, that corresponds to time (t =0 ms). The curve of microsaccadic rate signature was created separately for each spatial frequency of the Gabor patch both stimulation conditions (see Results Figure (4) and Figure (5)). To analyse the shape of rate signature curve, the current study employed the derivative approach as shown by Henrich et al. [2004]. Consequently, for the correlation of the averaged rate signature curves in the two stimulation conditions, the difference between adjacent rates has been taken across the particular averaged curve. This resulted in obtaining of the actual changes in microsaccadic rate signature curve, which were directly reporting the shape [Henrich et al., 2004]. These derivatives were compared for the two stimulation conditions, separately for each of spatial frequency of the grating. Additional testing of the rate signature curves was performed for comparison of the time properties and the amplitude. For this, individual rate signature curves were calculated with respect to the spatial frequency of the grating and a stimulation condition. To test the time properties of the rate signature curve given for monocularly and binocularly stimulated conditions, the time of both peaks, the minimum in microsaccadic inhibition valley and the maximum microsaccadic enhancement, after stimulus onset were found for all subjects. The search for the times of peaks and amplitudes was performed with MATLAB finding peaks function. This resulted in a two-dimensional-coordinate outcome reporting the amplitude and time of a peak. Given times for the inhibition and enhancement have been clustered according to the spatial frequency of the grating and the two stimulation conditions and tested using the two-way ANOVA. To statistically test the effect of spatial frequency of a grating and the stimulation conditions on the rate signature amplitude, the Friedman's test was used. To test the accuracy of the eye tracker, the validation offset of the eye tracker for the left and right eye was compared in both stimulation condition. The validation offset of the eye tracker was tested over the first measurements of every spatial frequency by the paired t-test.

3.7 Results

3.7.1 Eye tracking quality

As proposed by Nyström et al. [2013] or more recently by Ehinger et al. [2019], the eye tracking data quality is here reported first considering the accuracy and precision of the calibrated eye tracking validation and data loss. The spatial accuracy of the eye tracking was analysed using the validation offset provided by the Eye Link 1000 plus as a mean value from all nine calibration points and all participants. The precision of the eye tracker was calculated as a root-means-square error of the validation offset values from the participants throughout the different measurements. Given the data loss, the proportional time in which the signal was lost, due to a blink or other disability for pupil detection, was calculated for the time of stimulus presentation. Monocularly stimulated conditions revealed a mean accuracy of 0.35±0.21°for the right eye and 0.36±0.31°for the left eye, which was covered by the infrared filter (p = 0.79, t-test). The precision was 0.41°for the right eye and 0.47°for the left eye. Binocularly stimulated conditions showed a mean accuracy value of 0.27±0.17°for the right eye and 0.31±0.24°for the left eye. The statistical comparison did not reveal significance (p = 0.35, t-test). The precision was 0.32°for the right eye and 0.39°for the left eye. The resulting proportional data loss was 3.0% (2.3%) for the right eye under monocular (binocular) stimulated conditions, while 3.5% (2.6%) for the left under monocular (binocular) stimulated conditions.

3.7.2 Main sequence

The results shown in Figure (6(a-b)) affirm that the distinct stimulation conditions did not change the typical appearance of a main sequence paradigm [Bahill et al., 1975; Otero-Millan et al., 2008; Zuber et al., 1965]. The trend of linear regression in main sequence was shown for both, monocularly and binocularly stimulated conditions for microsaccades triggered by the spatially oriented grating. Linear regression revealed R^2=0.80 for the monocularly stimulated conditions, and R^2=0.73 for the binocularly stimulated conditions covering the data obtained from all spatial frequencies of the Gabor patch.

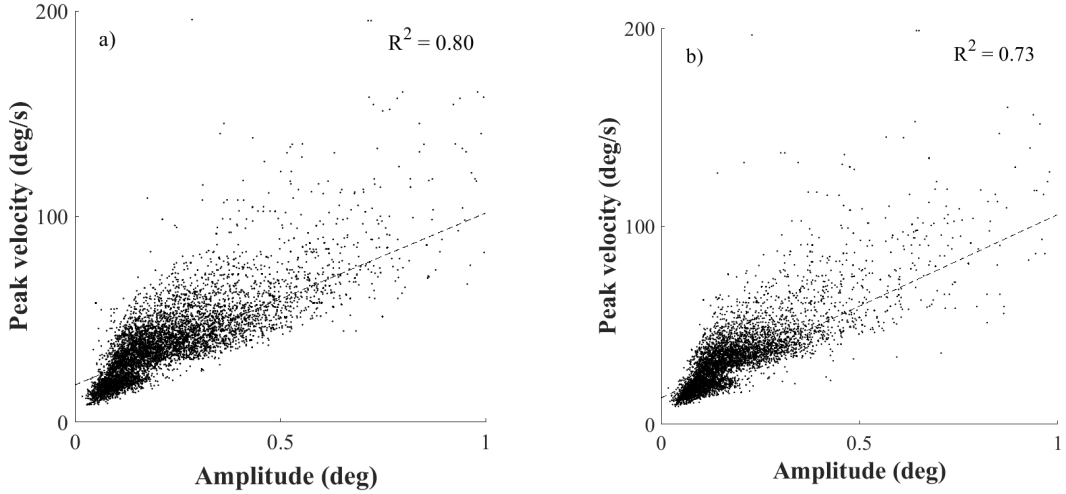

Figure 6: The row of figures shows the paradigm of the microsaccadic main sequence. Subplots a) and b) are plotted for the microsaccdes stimulated by the Gabor patch, whereas a) is for monocularly and b) for binocularly stimulated conditions. Every upper right corner of a particular plot shows the goodness of fit of the linear regression.

In the current study, the mean microsaccadic peak velocity of the right eye was 38.1±22.9 °/s (33.8±18.6 °/s) in monocularly (binocularly) stimulation. In the left eye the mean microsaccadic peak velocity was found as 38.7±19.9 °/s (33.6±17.8 °/s) in the same order. Additionally, the mean microsaccadic amplitude of the right eye was 0.21±0.14°(0.18±0.13 °) in monocularly (binocularly) stimulation condition. For the left eye the mean amplitude of microsaccades was 0.22±0.14°and 0.19±0.13°in the same order. The statistical testing revealed no significant differences for both eyes in both, amplitude (p=0.12, rank-sum test) and peak velocity of microsaccades (p=0.06, rank-sum test) in monocular stimulation. The same result was obtained for binocular stimulation for which the testing statistics revealed (p=0.55, rank-sum test) for the microsaccadic amplitude and (p=0.88, rank-sum test) for the peak velocity.

3.7.3 Directional distribution of microsaccades

According the assumption that the directions of microsaccades will be influenced by the orientation of a Gabor patch, since different visual input has been found in different directions [Rucci et al., 2007], the analysis was testing the microsaccadic directional distribution in respect of the orientation and spatial frequency of the stimulus, as shown on Figure(7). Furthermore, the comparative analysis was done for the two stimulation conditions, since a potential influence of presence of binocular vision was expected, according to the previous research. Prior to the statistical analysis the microsaccadic efficient direction was calculated, using the circular statistics [Berens, 2009] (see Data computations and statistics) and thus the mean direction of a signal was found. All

these directions and their standard deviations are shown in the Table(1) and Table(2). These calculations were performed considering visual stimulus features (orientation and spatial frequency) as well as the stimulation conditions, exclusively. Further statistical testing revealed that the spatial orientation of the Gabor patch appeared to have no significant impact on the direction of microsaccades in the monocularly stimulated conditions as the Friedman's test revealed ($q2(3) = 2.65; p = 0.45$) as a well as in the binocularly stimulated conditions ($q2(3) = 1.16; p = 0.76$) over all spatial frequencies. In testing of the potential difference in microsaccadic mean direction for the stimulation conditions, regardless the orientation of the grating, no significant influence of the stimulation conditions was found, as the Friedman's test revealed ($q2(3) = 0.71; p = 0.81$). To sum up, considering the mean microsaccadic direction, the results showed that microsaccades remained preferably horizontally oriented. This finding was shown to be consistent for all used spatial irrespective to the spatial orientation of a grating. In order to test the effect of the stimulation condition, no significant changes in the microsaccadic mean direction was observed.

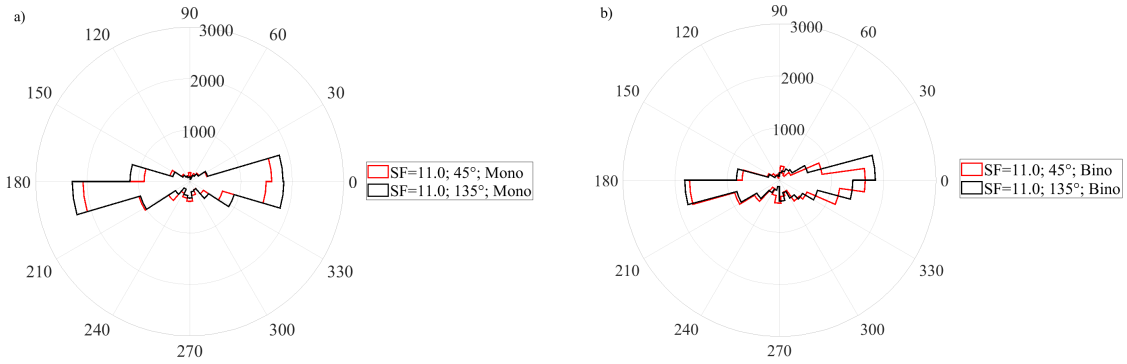

Figure 7: The two figures show the distribution of the microsaccadic orientations, which were taken over all samples in stimulation of a Gabor patch featured by $SF = 11\,\text{cpd}$ in respect to its orientation. Subfigure (a) shows the distribution for monocularly stimulated conditions, whereas subfigure (b) shows the distribution for binocularly stimulated conditions.

SF(cpd)	0.5		4.0		11.0		22.0	
GP orient. (°)	45	135	45	135	45	135	45	135
mean(°)	22	20	22	22	24	21	23	22
SD (°)	22	21	23	23	24	22	24	23

Table 1: Mean directions of microsaccades plotted for all used spatial frequencies and the orientations of Gabor patch (GP) exclusively considering monocularly stimulated conditions.

SF(cpd)	0.5		4.0		11.0		22.0	
GP orient. (°)	45	135	45	135	45	135	45	135
mean(°)	23	26	24	26	27	24	26	27
SD (°)	22	25	25	25	25	23	25	25

Table 2: Mean directions of microsaccades plotted for all used spatial frequencies and the orientations of Gabor patch (GP) exclusively considering binocularly stimulated conditions.

3.7.4 Microsaccadic rate signatures

The data analysis showed the rate signature curve for all used spatial frequencies of the Gabor patch pattern. Furthermore, this finding was obtained in both, monocularly and binocularly stimulated conditions, as shown in Figure(8a-d). To analyse the identity of microsaccadic rate signature curves triggered under monocularly and binocularly stimulated conditions (see Figure(8a-d)), first the difference between adjacent rates across the averaged microsaccadic rate signature curve was taken for all used spatial frequencies separately. The consequent Pearson correlation disclosed a linear correlation in microssaccadic rate signature changes of both stimulation conditions over a wide range of spatial frequencies of the grating ($r_{all} > 0.62$; $p_{all} < 0.0001$) as depicted on the Figure(9a-d). Furthermore, the time of microsaccadic inhibition and enhancement was compared for the given density of the grating of the two stimulation conditions across all participants. The two-way ANOVA showed no significant time shift in, microsaccadic inhibition after stimulus onset as the effect of spatial frequency was found ($F(3,88)=1.46$; $p=0.23$) and the effect of stimulation condition ($F(1,88)=1.91$; $p=0.17$), the interaction of these parameters was found as ($F(3,88)=0.42$; $p=0.74$). For microsaccadic enhancement the two-way ANOVA showed no significant time shift as well, as the effect of spatial frequency was found ($F(3,88)=1.98$; $p=0.12$) and the effect of stimulation condition ($F(1,88)=0.99$; $p=0.32$), the interaction of these parameters was found as ($F(3,88)=0.29$; $p=0.83$). Thus the matching timing of those rate signature parameters is expected in both stimulation conditions. In testing the effect of stimulation conditions and spatial frequency of a Gabor patch on the rate signature amplitudes, Friedman's test revealed no significant change over all spatial frequencies in the two used stimulation conditions for both, amplitude of microsaccadic inhibition ($\chi 2(3)=1.0$; $p=0.80$) and microsaccadic enhancement ($\chi 2(3)=1.62$; $p=0.66$).

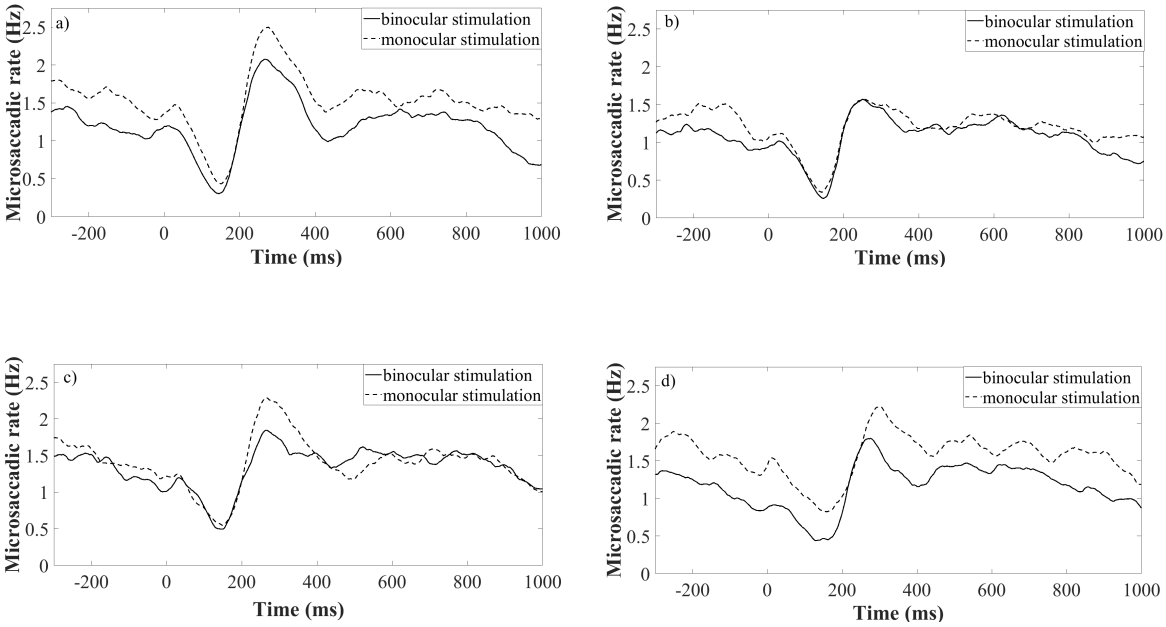

Figure 8: Rate signatures triggered by various density of a grating under monocularly (dotted lines) and binocularly (continuous lines) stimulated conditions. Each of the subfigures represent one spatial frequency of a grating. Subfigure a) is plotted for sf=0.5 cpd, b) 4.0 cpd c) 11.0 cpd, d) 22.0 cpd. Time = 0 corresponds to the stimulus onset.

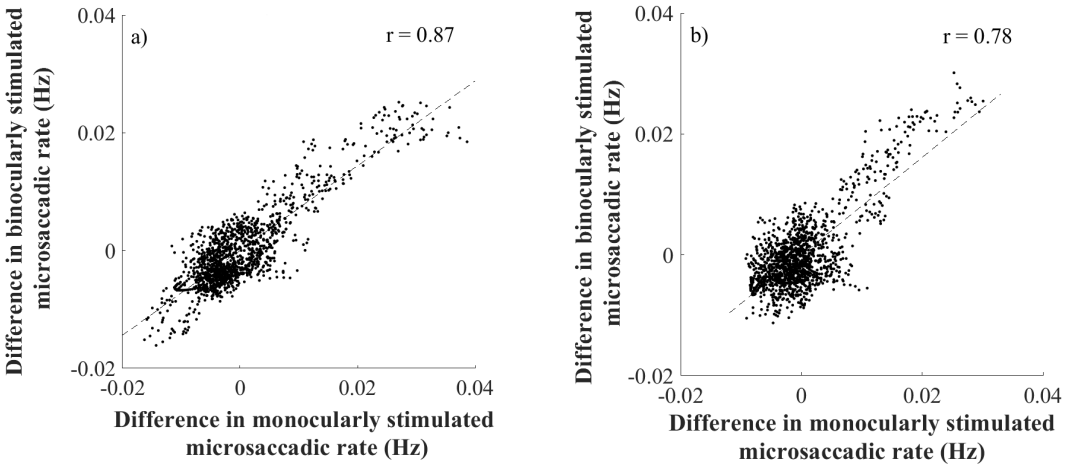

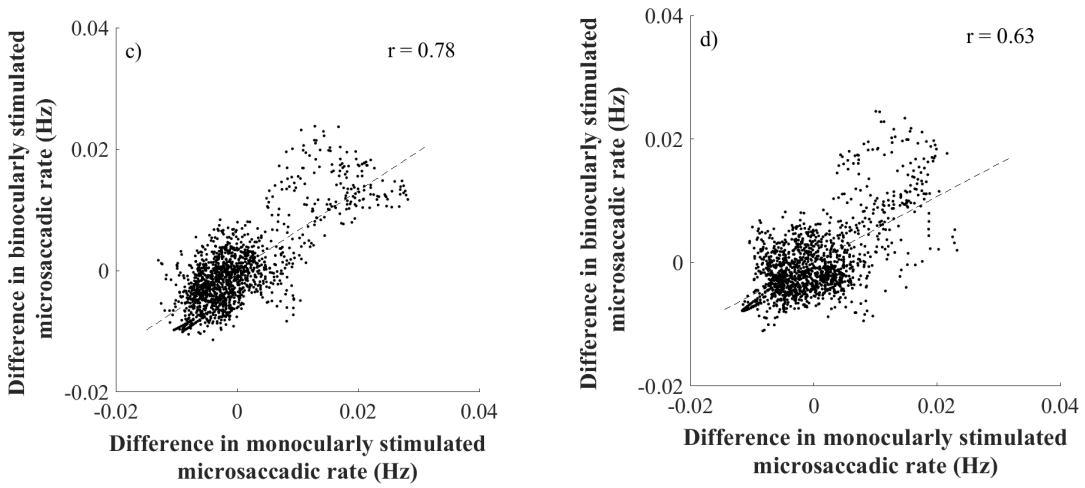

Figure 9: The figure a) represents the correlation for SF=0.5cpd, b) represents the correlation for SF=4.0cpd, c) represents the correlation for SF=11.0cpd and figure d) represents the correlation for SF=22.0cpd. Every upper right corner shows the index of correlation.

3.8 Discussion

In the current study, the analysis of the directional distribution and the rate signatures of microsaccades was performed under monocularly and binocularly stimulated conditions, while under monocular stimulation the left eye was covered by an IR filter. The evaluation of the microsaccadic metrics was done in respect of spatial characteristics of a spatially oriented grating - Gabor patch. As these metrics, the orientation and spatial frequency were taken into consideration. In both stimulation conditions, microsaccades followed the typical pattern for peak velocity and amplitude relationship – main sequence [Martinez-Conde et al., 2009; Otero-Millan et al., 2008; Zuber et al., 1965]. Additionally, the current study compared the microsaccadic amplitude and peak velocity in both eyes in both stimulation conditions. The slight inequality in the microsaccadic amplitude and peak velocity of the left and right eye in both stimulation conditions may come from a potential binocular disconjugacy of microsaccades as found by Shaikh and Ghasia [2017]. Nonetheless, such a difference was not considered as a reason for claiming microsaccades as not conjugate and thus the protocol of the current study followed the approach to see microsaccades as a conjugate eye movement events respecting the Hering's law of equal innervation [Hering, 1977].

3.8.1 Directions of microsaccades

The hypothesis of the current study covered an assumption that microsaccades will follow the orthogonal direction to the orientation of the centrally located spatially oriented pattern preferably. As it was already shown, the orthogonal direction to the

orientation of such a grating is characterized by the highest modulation of luminance, which could be described by a sine function, and therefore is this direction expected to provide the maximum of visual input [Rucci et al., 2007]. Nonetheless, in the current study, microsaccades were found as mainly horizontally oriented with a small vertical component. As it was found by Engbert and Kliegl [2003b]; Hermens and Walker [2010]; Meyberg et al. [2015] microsaccades occur as preferably horizontally oriented and towards a peripheral cue. This finding was explained as a relationship between the location of an attentional cue and microsaccadic orientation. As the visual stimuli appeared always in the center of a screen, the attention of all participants was expected to be at that area as well [Engbert, 2006]. Furthermore, for centrally located visual stimuli is the outcome of mainly horizontally oriented microsaccades in accordance with Kloke et al. [2009]. As it was already speculated, mainly horizontally oriented microsaccades are assumed to occur for their potential purpose of binocular correction of the disparity [Engbert, 2006]. Moreover, the current study found matching directional distribution by taking into comparison the mean microsaccadic directions for monocularly and binocularly stimulated conditions. On the one hand, this finding is again assumed to be explained by the attentional location, that was always in the centre of the screen in both stimulation conditions [Engbert and Kliegl, 2003b; Hafed and Ignashchenkova, 2013; Hermens and Walker, 2010]. On the other hand, as shown by Hermens and Walker [2010]; Kloke et al. [2009] the microsaccadic directional distribution may vary with the implementation of the term of monocular microsaccades into the analysis, as the larger number of vertically oriented microsaccades was found considering fixational saccades as monocular events. As the current study protocol took microsaccades strictly as a binocular phenomenon with a respective microsaccadic time overlapping on both eyes in both stimulation conditions, coming from the original version of Engbert's algorithm [Engbert and Kliegl, 2003b] the finding of preferably horizontally oriented microsaccades is then in correlation with both mentioned studies of Hermens and Walker [2010]; Kloke et al. [2009] when considering matching microsaccadic events in both eyes. Furthermore, the outcome of preferably horizontally oriented microsaccades could be explained by assumption that these fixational saccades share common oculomotor generator with normal saccades [Martinez-Conde et al., 2013; Otero-Millan et al., 2011; Zuber et al., 1965]. Recently it was shown, that people perform normal saccades as mainly horizontally oriented when observing natural images Foulsham et al. [2011]. Additionally, it has been shown by Foulsham et al. [2011] willing saccades to be oblique, following a tilt of an image and thus to be mainly horizontally oriented relatively to the image orientation. In addition Wismeijer and Gegenfurtner [2012] showed saccades to mainly follow the direction of a spatially oriented grating. However, since micosaccades have been understood as involuntary fixational eye movements

it is expected, that their preferably horizontal orientation comes from their involuntary character, as controlling of involuntary oblique movements has been shown as questionable [Engbert, 2006].

3.8.2 Microsaccadic rate signatures

The current study found a significantly correlated behaviour of the well-known microsaccadic rate signature curve for both monocularly and binocularly stimulated conditions by taking into comparison the rate differences over the entire rate signature curve, that reported the actual change of the rate in time. This finding was expected, as it was assumed that the microsaccades share common neural mechanism with normal saccades for their creation [Martinez-Conde et al., 2013; Otero-Millan et al., 2011; Zuber et al., 1965]. Hence, microsaccades can be understood as conjugate eye movements, following the Hering's law of equal innervation [Hering, 1977], resulting in synchronized microsaccadic events in both eyes in both stimulation conditions. This assumption was affirmed by comparable amplitudes of microsaccades in both eyes in the current study. Recently, the microsaccadic rate signatures have been found to be sensitive to small changes in contrast of visual stimuli ranging from 1.3% to 4%. In detail, the change in contrast for a Gabor patch of spatial frequency of 0.33 cpd caused a distinct change in the amplitude of the microsaccadic rate signature curve [Scholes et al., 2015a]. Additionally, the similar outcomes were shown by Bonneh et al. [2015], where the microsaccadic rate signature curve revealed decreasing amplitude with decreasing contrast level of a Gabor patch featured by 3.0 cpd with varying contrast level from 0.8% to 25%. On top of that, the past research disclosed that the rate signature varies over different contrast levels for a visual stimuli of circular shape, not defined by any preferred direction of luminance modulation [Rolfs et al., 2008]. In the current study, distinctly to Scholes et al. [2015a], one single contrast level of the visual stimuli was taken; $C = 0.5$, however the spatially oriented pattern was featured by a wider range of spatial frequencies (0.5; 4.0; 11.0; 22.0) cpd, compared to Bonneh et al. [2015]. In respect to the previous research the microsaccadic inhibitions shown by Scholes et al. [2015a] for spatially oriented patterns are about 30 ms delayed in comparison to those ones obtained for the Gabor patch in the current study. It is assumed that this could be explained by much higher contrast level in the current study, thus the visual input is expected to be more vivid. This assumption is confirmed by Bonneh et al. [2015], as the comparable time of microsaccadic inhibition was found for the visual stimuli of 25% in the level of contrast. Additionally, to this finding, it was already proposed, that microsaccadic rate modulation is highly dependent on the visibility of presented visual stimulus Cui et al. [2009]; Martinez-Conde et al. [2006]. Hence, the connection to the distinction in rate signature curves over different contrast levels of a visual stim-

ulus. Furthermore, in accordance to the previous research, no significant differences in timing and amplitude of microsaccadic rate signature inhibition and enhancement among the used spatial frequencies of the Gabor patch was found. This finding is notably comparable with Bonneh et al. [2015], for smaller range of spatial frequencies of a spatially oriented patterns, however. In connection to the previous research, that proposed to use the shape of a microsaccadic rate signature for an objective estimation of visual performance, like contrast sensitivity [Bonneh et al., 2015; Scholes et al., 2015a], the current study extended the applicability of microsaccadic rate signature into the clinical practise. The current study showed the evidence of correlated rate signature curves under distinct stimulation conditions in healthy subjects and thus proposes to use monocularly stimulated microsaccadic rate signature as a tool for estimation of visual sensitivity following the clinical attitude, since such a metric of visual performance as contrast sensitivity has been measured under monocular conditions in the clinical environment.

3.9 Limitations

To keep the comparable quality of every measurement a nine-point calibration was performed. Despite this fact, it should be still considered that microsaccades are tiny in the amplitude, thus even a usual inaccuracy in the calibration may result in a potential error. This may result in eye tracking artefacts, wrongly labelled as eye movements. Another considerable limitation is setting a threshold of amplitude of microsaccades, setting a minimum of microsaccadic length, or decay parameter for the rate signature analysis (α), or the parameter for the velocity based algorithm (λ) Engbert and Kliegl [2003b] as it is a non-objective method. These parameters have been chosen in regards to the previous research, however they may vary across researches and therefore the outcomes may not be exactly comparable. According to this problem, another approach like machine learning software for detecting microsaccades may be considered, in which case this disadvantage is solved [Scholes et al., 2015a; Zemblys et al., 2018]. At the last point all measurements were conducted under a head-fixed position, by adding sponges on both sides of the head-rest. This condition is far from the natural viewing the scenario, and therefore the potential influence on the revealed data is expected.

3.10 Conclusion

In conclusion, the current study has found the direction of microsaccades as preferably horizontally oriented independently to the orientation of the Gabor patch, as well as for the spatial frequency of that grating. Furthermore, the results presented in this study suggest, that the mean direction of microsaccaedes does not change under either mon-

ocularly or binocularly stimulated conditions. Therefore, this study could not report a finding of microsaccades to be sensitive to distinct spatial orientation of a grating or distinct stimulation condition and thus could not fulfil the hypothesis to possibly employ the microsaccadic directions in future contrast sensitivity testing. However, for the curves of microsaccadic rate signature a significant correlation was found for monocularly and binocularly stimulated microsaccades across a wide range of spatial frequencies of a Gabor patch. In connection to the previous studies, proposing to use the microsaccadic rate signature curve as a useful metric for estimating visual performance, as for instance contrast sensitivity by varying the contrast of a grating stimuli, the current study shows a methodological correction to the previous research resulting in a possible usage of monocularly stimulated microsaccadic rate signatures. These have been shown to behave in a similar way in healthy subjects, in two distinct stimulation conditions, while in both following the fundamental understanding of microsaccades as a binocular phenomenon. To conclude, this study proposes to analyse microsaccades under monocularly stimulated conditions, since clinical metrics of visual performance have been usually estimated under monocular viewing conditions as well. In such a way the estimation of visual performance from microsaccades could follow the clinical standard.

3.11 Ethics and Conflict of Interest

The authors declare that the contents of the article are in agreement with the ethics described in http://bib-lio.unibe.ch/portale/elibrary/BOP/jemr/ethics.html. This work was done in an industry-on-campus- cooperation between the University of Tuebingen and Carl Zeiss Vision International GmbH. Author P.E. declares no potential conflict of interest. A.L., K.R. and S.W. are employed by Carl Zeiss Vision International GmbH and are scientists at the University Tuebingen.

3.12 Acknowledgements

Funding was received from Eberhard-Karls-University Tuebingen (ZUK 63) as part of the German Excellence initiative from the Federal Ministry of Education and Research (BMBF). Further funding received from Deutsche Forschungsgemeinschaft and Open Access Publishing Fund of University of Tuebingen.

4 Contrast Sensitivity Testing in Healthy and Blurred Vision Conditions Using a Novel Optokinetic Nystagmus Live-Detection Method

Essig P., Sauer Y., & Wahl S. (2021). Contrast Sensitivity Testing in Healthy and Blurred Vision Conditions Using a Novel Optokinetic Nystagmus Live-Detection Method. Translational Vision Science & Technology, 10(12):12. doi:10.1167/tvst.10.12.12

4.1 Abstract

Purpose: The aim of the current study was to develop and validate an automated contrast sensitivity (CS) test using a live- detection of optokinetic nystagmus (OKN) and an adaptive psychometric procedure. In addition, the study sought to replicate the known effect of defocus on CS for the OKN-based measurements in emmetropic participants.

Methods: Fifteen participants viewed a horizontally moving grating while their eyes were tracked with an infra-red (IR) eye-tracker. To simulate the clinical conditions of the CS measurements, the participants were stimulated monocularly as the left eye was occluded by an IR filter. The horizontal eye position was continuously analyzed for OKN responses, and the stimulus contrast was changed by an adaptive psychometric method depending on the outcome. Furthermore, the newly proposed OKN live-detection was verified against an offline analysis and an expert-observer judgement. The OKN-based CS was measured for six spatial frequencies at normal vision and three levels of defocus using spherical convex lenses.

Results: The newly proposed OKN live-detection method showed a sufficient detection performance for implementation of adaptive procedures, and the detection rate is similar or better compared to offline detection methods. Spatial frequency and defocus had a significant effect on the OKN-based CS (P ¡ 0.0001 for both).

Conclusions: The current study presents a novel method to measure motion CS in an automated way, combining the real-time detection of OKN and an adaptive psychometric procedure. Furthermore, the known effect of defocus on CS was successfully replicated with the newly developed tool.

Translational Relevance: OKN-based CS is a novel approach to assess spatial vision, which is sensitive to subtle effects of defocus, allowing use with nonverbal patients and infants. Furthermore, the newly developed tool may improve the performance of such measurements.

4.2 Introduction

Assessment of contrast sensitivity (CS) from eye movements has already been proposed as a possible method to gain objective information. Moreover, these measurements may help examine noncommunicative participants [Mooney et al., 2018]. Previous research has shown that in objective testing of CS, several types of eye movements can be implemented, namely microsaccades [Scholes et al., 2015a; Bonneh et al., 2015; Denniss et al., 2018] or smooth pursuit eye movements [Mooney et al., 2018]. In addition, the eye movement occurring in response to a moving scenario, optokinetic nystagmus (OKN), has been linked to the appraisal of CS (motion CS) [Dakin and Turnbull, 2016; Wester et al., 2007; Leguire et al., 1991]. Canonically, OKN is a saw-tooth displacement of the eye, denoting the two phases of the OKN. The slow phase (OKN-SP) identifies a motion-tracking eye movement occurring in the direction of the visual stimulus drift. This phase is similar in nature to smooth pursuit eye movements, because largely overlapping neural circuitry was found in fMRI measurements [Konen et al., 2005]. Furthermore, the velocity of the OKN-SP appears to be lower, but nonetheless comparable to the velocity of the moving pattern, because the OKN gain (the ratio of the OKN-SP velocity to the stimulus velocity) was found to be 0.76 ± 0.15 using EOG [Wester et al., 2007]. In contrast, the quick phase of OKN (OKN-QP) occurs in the direction against the stimulus drift in a saccade-like fashion, moving the eye into the original position. It has been previously believed that the OKN-QPs are similar to normal saccades, because the main sequence parameters have not revealed any statistical difference between saccades and OKN-QPs, although the velocity of an OKN-QP was found to be slightly lower [Garbutt et al., 2001]. However, recent research revealed that the OKN-QPs are not triggered by an attentional input, and therefore the OKN-QP should not be considered as a classical saccade [Hanning and Deubel, 2019]. Despite this, the detection of an OKN-QP is possible using the velocity-based algorithms initially proposed for saccadic (microsaccadic) detection [Tatiyosyan et al., 2020]. Furthermore, two types of OKN can be differentiated based on the initial instructions provided to an observer: stare-OKN, in which case the participant is required to attempt to fixate a limited area on a screen, and look-OKN, where the participant tries to follow the stimulus and, hence, pays attention. Although the execution of stare-OKN failed to activate cortical oculomotor centers significantly, it was suggested that the look-OKN demands more higher-level neural processing [Konen et al., 2005]. In agreement with the study by Dakin and Turnbull [2016] we used the stare-OKN paradigm in the current study. With regard to OKN and visual performance appraisal, OKN appeared to be a reliable eye movement in assessment of visual functions in participants suffering from several visual impairments [Wester et al., 2007]. Although previous research focused

on detecting visual acuity from OKN returned results that correlated with subjective measurements in both youth and adults, [Schwob and Palmowski-Wolfe, 2019; Millodot et al., 1973] the estimation of visual acuity in children using OKN reflexes did not show sufficient performance [Cetinkaya et al., 2008]. Regarding the testing of contrast sensitivity, Sangi et al. [2015] showed an efficient assessment of CS in children, as did Leguire et al. [1991] in emmetropic adults. In addition, Dakin and Turnbull [2016] showed highly correlated CS curves obtained by OKN responses and actual responses of the participants to moving noise patterns, implicating OKN responses as a potentially useful tool in CS measurements. Nonetheless, OKN has been identified either by subjective judgements or using offline detection algorithms after the measurement was conducted. The approach of searching for the OKN contrast threshold offline suffers from poor time efficiency, because it prevents the implementation of adaptive procedures that adjust stimulus parameters while performing the experiment. Some of the current algorithmic OKN-detection methods could be adapted to OKN live detection, as suggested by Mooney et al. [2018] however, they deemed the existing methods of OKN detection to be insufficient. Therefore we aimed to develop a real-time OKN detection method with sufficient detection performance that allows the application of adaptive procedures for time-efficient and automated OKN-based measurements of CS. In this method, the contrast level was sought over a selected range of spatial frequencies at which the OKN response just occurs and therefore extends the applicability of OKN into clinical domain. Here, for performing the search of the contrast thresholds, we used the QUEST+ adaptive psychometric procedure [Watson, 2017]. The used psychometric function used was the Weibull function, which is used in both clinical [Wallis et al., 2013] and OKN-based [Dakin and Turnbull, 2016] CS measurements. Furthermore, replication of the known effect of defocus on CS has not been tested in OKN-based CS measurements. Hence, the new tool was used to measure OKN CS under normal vision, as well as in three conditions of defocused vision using convex spherical lenses. Because contrast thresholds have been shown to shift toward higher contrast levels with increasing defocus mainly for visual stimuli of higher spatial frequencies in clinical measurements of CS using various stimuli, [Marmor and Gawande, 1988; Green and Campbell, 1965; Jansonius and Kooijman, 1997] the current study was targeted to obtain a similar effect in the OKN-based CS measurements. The results of the OKN-based CS being influenced by defocus serves as an additional verification of OKN as a tool for CS measurements. After the clinical measure of CS, testing was performed under monocular stimulation. The left eye was covered by an IR filter that still allowed binocular eye tracking. This method did not show any significant change in accuracy of the video-based eye tracking [Essig et al., 2020].

4.3 Methods

4.3.1 Participants

Fifteen participants in a mean age of 24.7±3 (four male and 11 female), participated in the current study. All participants were emmetropic. The current study considered emmetropia as a refractive error of smaller than ±0.5 D in spherical equivalent obtained by the wavefront-based autorefraction (ZEISS i.Profiler plus; Carl Zeiss Vision, Aalen, Germany) in their tested (right) eye. Furthermore, all participants had a negative history of ocular, systemic, or neurological disease, amblyopia, or trauma. The study protocol followed the Declaration of Helsinki. In addition, the study was approved by the ethics committee of the Faculty of Medicine of the University Tuebingen, and signed informed consent was obtained from all participants before the experiment. All participants were recruited from the University of Tuebingen.

4.3.2 Visual Stimulus and Eye Tracking

For triggering OKN, we used a vertically oriented square-wave grating drifting over the horizontal plane with a constant velocity of $v = 2.3°/s$, as used in the previous studies [Wester et al., 2007; Tatiyosyan et al., 2020; Schober and Hilz, 1965; Nachmias, 1967] in OKN-based visual performance measurements. Because no clear effect of OKN gain has been found between the two horizontal directions, [Van den Berg and Collewijn, 1988] the grating was moved either nasally or temporally in an equal number of trials, in a random order. The stimuli were created in MATLAB (MATLAB2018b; MathWorks, Natick, MA, USA) using Psychtoolbox-3 [Brainard, 1997; Kleiner et al., 2007] and were covering the entire Viewpixx screen (VIEWPixx; VPixx Technologies Inc., Saint Bruno, Quebec, Canada). Because the screen provided a resolution of 1920 x 1200 pixels with a pixel pitch of 0.252 mm, the covered visual field from the viewing distance 75 cm was 36°and 23°in the horizontal and vertical planes, respectively. Furthermore, the screen provided a gray-scale bit depth of 12 bits, whereas the luminance nonlinearity was corrected via gamma correction. Here the mean luminance of the screen was 130 cd/m^2. The refresh rate was 120 Hz. The selected spatial frequencies (SFs), calculated for the observing distance of 75 cm, were SF = 0.7, 1.5, 2.6, 3.7, 5.2, 6.5 cycles per degree (cpd). The order of measured SFs was randomized for every defocus condition. The contrast of the stimulus for each trial was selected from 39 available contrast levels ranging from 0.03% to 66%. The motion of the stimulus of a given contrast level was aborted at t = 4 s after stimulus onset or immediately after a robust OKN response was detected by the live analysis, making the testing as time-efficient as possible. The number of trials per SF was set to a constant value of 64, giving a comparable amount of data for all tested conditions. After every presentation of the stimulus, a gray cross

of 1.25°in size appeared for t = 1.3 s. Participants were asked to blink during the presentation of this irrelevant stimulus, whereas the contrast level for the next trial was defined by QUEST+, running in the background. Eye tracking was performed using the EyeLink 1000 Plus eye tracker (SR Research, Ontario, Canada) with a fixed sampling rate of 1000 Hz. To measure CS under monocular condition, the left eye was covered by an IR filter (ePlastics, San Diego, CA, USA) with a transmission of $T > 90\%$ for $\lambda > 800\,\text{nm}$, allowing tracking of both eyes while presenting the stimulus only to the right eye. Before every measurement, a nine-point calibration procedure of the eye tracker was performed.

4.3.3 Live OKN Detection

In the current study, we propose a new method for OKN live detection during stimulus presentation. This approach in combination with an adaptive psychometric procedure allows the searching for a contrast thresh- old in an automated and time-efficient way. Here, the sampling and consequent analysis of gaze data was coupled to the refresh rate of the of the screen (120 Hz). For the OKN-QP detection, we used a modified version of Engbert's velocity-based algorithm [Engbert and Kliegl, 2003b] with the model's free parameter $\Lambda = 7$. Noise-level calculation of both eyes was performed just over the horizontal plane from the gaze data over the first 34 frames (283 ms) of every presentation of the grating. This time period was used only for the noise assessment. To reduce the computational demand, only horizontal gaze data was evaluated and Engbert's algorithm was applied to data samples from the last detected saccade. The binocular overlap criterion for saccadic detection was used, as originally proposed by Engbert and Kliegl [2003b] as the gaze position was captured for both eyes. For the detection of OKN-SP, the time frame between the end of any first saccade and the start of a subsequent saccade was identified, as an OKN-SP appears between two OKN-QPs, as shown in the Figure10. Whenever the start of a second saccade was detected, the horizontal gaze data samples were analyzed considering a potential OKN-SP. In the next step, the direction and the mean velocity of the OKN-SP were calculated, with a prior smoothing over five data samples using a moving average filter in MATLAB. Moreover, the analyzed data was shortened by adding (subtracting) 17 ms (two refreshments of the screen) to the start (end) of a saccade, to avoid saccadic overshoot influencing the OKN-SP velocity calculation. Last, the sign of the velocity was compared with the direction of the moving stimulus, as only OKN events that occurred in the direction of the moving stimulus were taken into consideration. Furthermore, we required a robust OKN response to a given stimulus. Therefore, similarly to Turuwhenua et al. [2014] at least two OKN events must have been detected to consider the stimulus as seen, as depicted in Figure10. The performance of the newly developed OKN detection al-

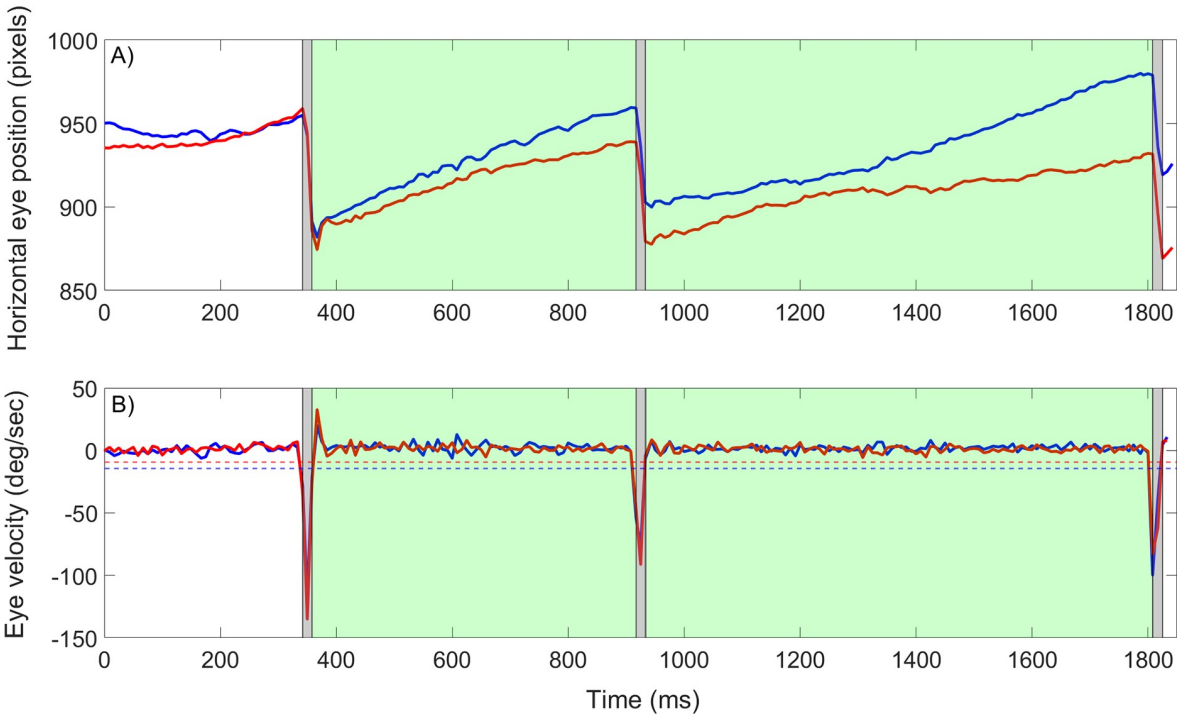

Figure 10: Horizontal eye position for both eyes (A) and derived velocity (B) during one trial with OKN. In both figures the gray areas denote the limits of detected saccades (OKN-QP), followed by a green area for a successfully detected OKN-SP. In panel B, the noise threshold for saccade detection is depicted in blue for the left eye and red for the right eye. Note that with the maximum time for grating presentation set to 4 s, this trial was aborted after ≈1.8 s, because a robust OKN was detected with the live detection method.

gorithm, coupled to the screen refresh rate (120 Hz), was compared to offline analysis of the same measurements with the full sampling frequency of 1000 Hz. Both the online and offline OKN detection procedures were compared with the judgement of an experienced observer. In the expert rating, the first author (P.E.) affirmed whether a correctly oriented robust OKN response (two OKN events) could be seen in the gaze data. For the offline OKN detection, we used the original version of Engbert's velocity-based algorithm Engbert and Kliegl [2003b] for OKN-QP detection, with the model's free parameter λ set to 7 and the minimum time difference between two saccades set to 50 ms to prevent overshoots from being detected as separate eye movements. In contrast to the live detection method, the offline analysis included blink detection. Here the blinks were detected as missing pupil events. These events were removed with a buffer of t=50 ms to protect the data from blink-related artefacts. The OKN detection in both live and offline method relied on the OKN-SP velocity thresholding.

4.3.4 Experimental Procedure

The current study considered the implementation of an adaptive psychometric algorithm as an efficient method to estimate CS from OKN in real time. Hence, we used the QUEST+ algorithm [Watson, 2017] to change the contrast level depending on whether an OKN response was detected, to return the threshold contrast for OKN. As a psychometric function, the Weibull function was used with the parameters threshold and slope. Upper asymptote (lapse rate) and lower asymptote (guess rate) were set to zero. The parameter space for threshold had 39 contrast levels. Because Dakin and Turnbull [2016] showed that the slope can vary across subjects and parameters of the visual stimulus, the slope also had a predefined parameter space of 0.5 to 5.5 in steps of 0.5. Furthermore, because the duration for convergence was expected to vary among subjects, the number of the grating presentations was fixed, resulting in comparable amounts of data for every participant. Moreover, although Dakin and Turnbull [2016] showed that OKN can be used to objectively assess CS, there is limited evidence that decreased CS can be reliably measured as corresponding OKN decrements if defocus is present. Hence, we systematically evaluated the effects of defocus, which decrease VA and CS, on the OKN-based CS. To study this effect, we introduced three convex lenses of different optical power in fine steps, 1.5 D, 2.0 D, and 2.5 D. These lenses were inserted in a trial frame in a random order with a fixed vertex distance of 12 mm. We considered the defocus-induced magnification to be negligible, given its low values below 5% [Ohlendorf and Schaeffel, 2009]. The viewing distance of the screen was d=75 cm, leading to an accommodational demand of 1.33 D. The lenses were selected to have the optical power above this demand.

4.3.5 Data Analysis

To find the OKN contrast threshold, OKN occurrence rate dependent on stimulus contrast level was fitted with a psychometric function using Psignifit [Schütt et al., 2015] in MATLAB. Here, the cumulative Weibull distribution function was used as the fitting function with the following parametrization

$$\Psi(x; m, w, \gamma, \lambda) = \gamma + (1 - \lambda - \gamma)\left(1 - e^{\log(0.5)e^{c\frac{\log(x)-m}{w}}}\right) \tag{2}$$

with $c = \log\left(-\log(0.05)\right) - \log\left(-\log(0.95)\right)$. Guess rate γ and lapse rate λ, representing the lower and upper asymptote, were both set to zero. The threshold m and the width w, defining the zone between the 0.05 and 0.95 points, are in log space of the stimulus parameter x. The relationship between the width w and the slope s of the Weibull function is $s = \frac{c}{w}$. The contrast threshold CT was calculated from m as

$C = e^m$, at which the OKN occurs with a probability of 50 %. This threshold was taken for every measured spatial frequency of the grating and was later converted to a CS value as $CS = \frac{1}{CT}$.

The contrast sensitivity function (CSF) was created as a fit of the CS values depending on spatial frequency SF with a log-parabola, considering the ascending and descending part of the CSF as already suggested by Lesmes et al. [2010], or more recently by Dakin and Turnbull [2016] using the following fitting function:

$$CS(SF) = \log_{10}(\gamma_{max}) - \log_{10}(2) \left(\frac{\log_{10}(SF) - \log_{10}(SF_{max})}{\beta} \right)^2, \tag{3}$$

with fitting parameters γ_{max}, SF_{max}, β. These denote the peak sensitivity, the peak spatial frequency and the function's bandwidth, respectivelyLesmes et al. [2010]. The statistical analysis tested the effect of spatial frequency and defocus level on contrast sensitivity using a repeated measures two-way analysis of variance. Data have been tested for their normality on a default level of significance 5% in MATLAB. We evaluated the goodness of fit of the proposed log-parabola CSF with the coefficient of determination for the various conditions of defocus.

4.4 Results

4.4.1 Evaluation of the OKN Detection Performance

The newly proposed OKN live detection algorithm was designed to abort the trial after two valid OKN events, as shown in Figure(10). Here, the performance of the live detection was evaluated against a subjective judgement of an experienced observer and the offline post-analysis of the data with original sampling rate of the eye tracker, as shown in Figure(11). For this analysis, 1600 trials were randomly selected from the whole study data set, covering trials of all subjects, defocus conditions and spatial frequencies. Both approaches showed decent performance in OKN detection in trials of actual presence of robust OKN response by correctly identifying 83.3% and 85.5%, using the offline and live detection method, respectively. Furthermore, these algorithms showed nearly excellent classification of trials of no actual OKN response, because a correct judgement was found in 94.0% and 97.4% for the respective approaches. These results show a successful application of the live tracking in OKN detection procedure.

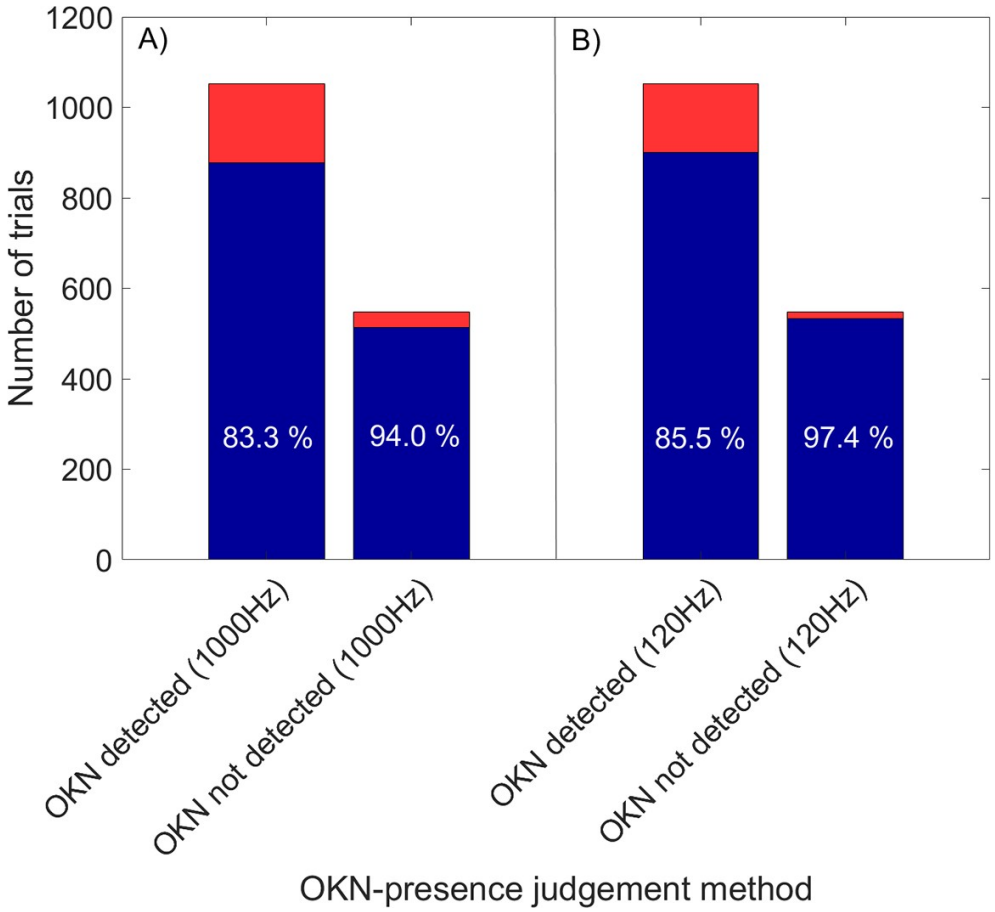

Figure 11: Two approaches of OKN analysis are compared to the subjective judgment of OKN presence across 1600 tested trials. These approaches were the offline post-measurement analysis using the original sampling rate of the eye tracker—1000 Hz, and the newly proposed live OKN analysis limited by the screen refresh rate of 120 Hz. The amount of trials (not) containing the robust OKN response are given by the first (second) of the two groups (A and B). The first bar in both groups shows the true-positive (blue) and the false-negative (red) proportion similarly to the second bar showing the true-negative (blue) and false-positive (red) OKN detection, respectively.

4.4.2 Contrast Sensitivity Revealed by OKN With and Without Induced Defocus

The CS values were obtained from the Weibull psychometric fits of the OKN proportion detected across a range of tested contrast levels. These were acquired for each of the six tested spatial frequencies, as shown in Figure(12A) for one typical subject. As depicted in panel (A) of Figure(12), the smallest contrast thresh- old (the best CS), is given for the green fit, obtained for a grating of 1.5 cpd, later resulting in the peak of the CSF, followed by the blue and red fit for gratings of 2.6 cpd and 0.7 cpd, respectively, giving the CSF the log-parabolic shape. Last, the brown, orange, and cyan fits show the results for the gratings of 3.7 cpd, 5.2 cpd, and 6.5 cpd in spatial frequency, showing the already observed trend of decreasing CS with increasing SF. In panel (B), the four

Weibull fits are provided from measurements of healthy vision and the three defocus steps for the highest used spatial frequency, 6.5 cpd in one selected subject. Finally, the CSFs were fitted for each defocus condition and clustered for every subject, as shown in Figure(13). The time needed to perform a single measurement of CS for one given spatial frequency, considering the number of trials, the set cross-presentation time, and the velocity of the stimulus, ranged between four and five minutes, depending on the defocus condition.

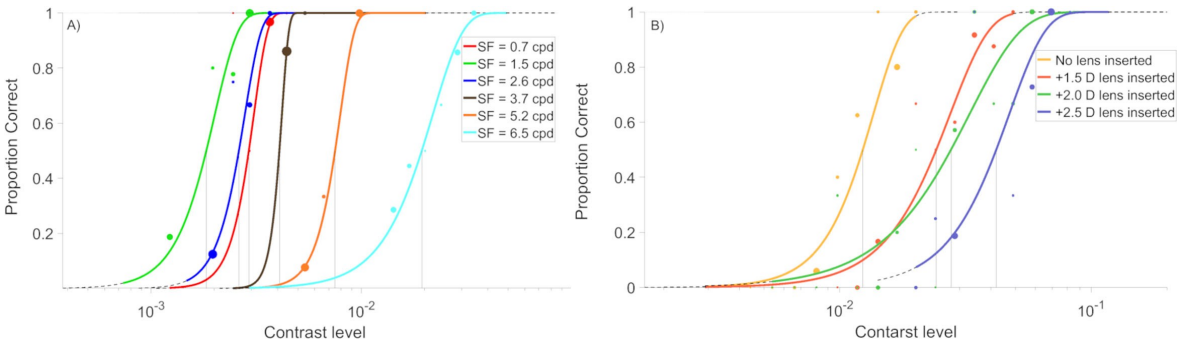

Figure 12: (A) The six Weibull fits correspond to the measurements of the six spatial frequencies within one defocus condition (here the fits shown were obtained for the highest defocus level in one selected participant). (B) The four Weibull fits represent the measurements of the four conditions of defocus within one spatial frequency (here the fits shown were obtained for the SF 3.7 cpd in one selected participant). The black lines always target the contrast level, at which the OKN response is estimated to occur with the probability of 50%. Dot size scales with the testing frequency of the particular contrast level, as selected by the adaptive psychometric procedure.

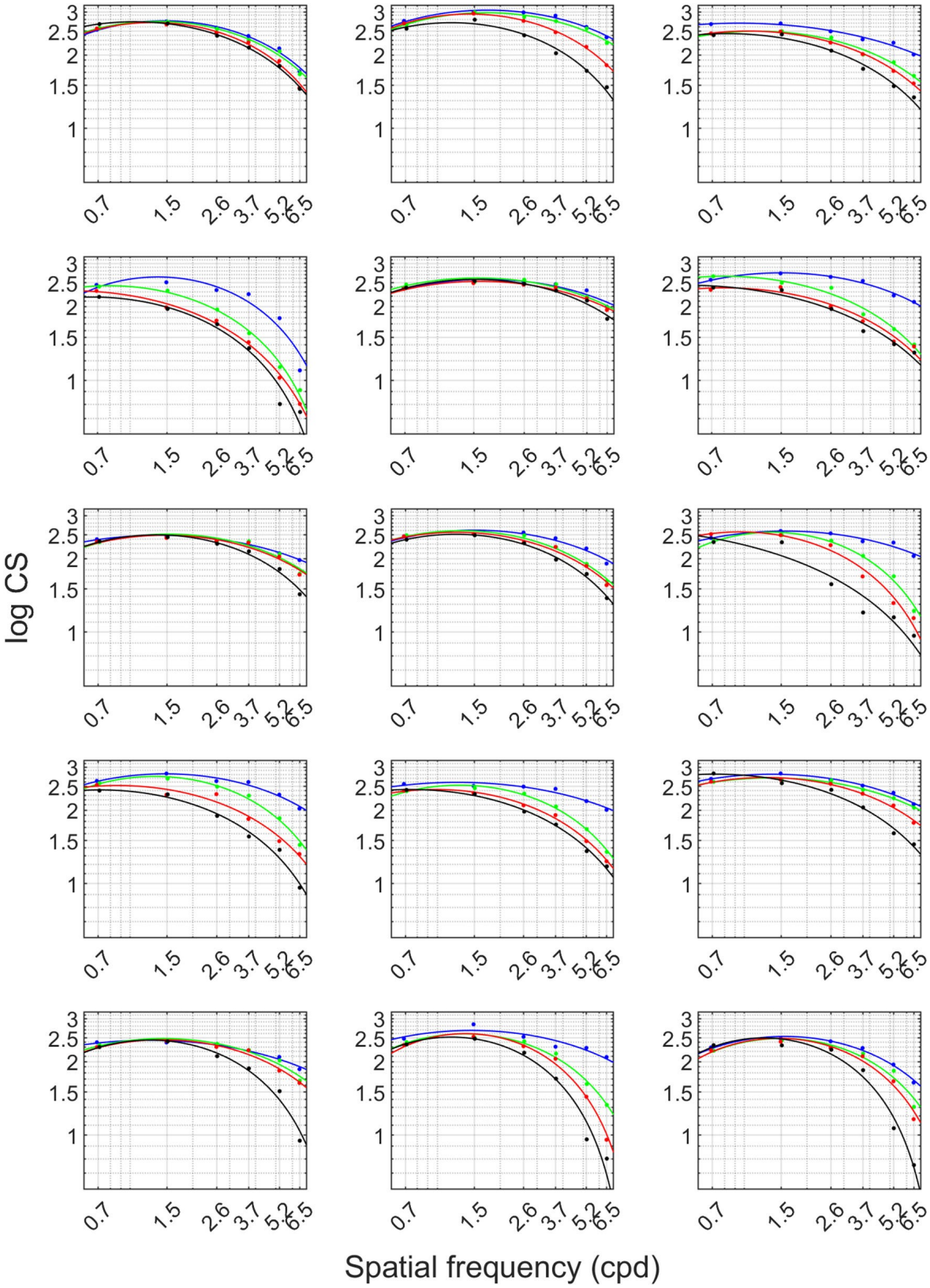

Figure 13: The figure contains fifteen panels, each representing data for an individual participant. The four curves in every panel show the estimated CSF for every measurement condition. The blue curve always represents natural viewing condition of the tested emmetropes, the following green line represents the first step in defocus (+1.5 D lens inserted in the trial frame), continuing with the red (black) curve obtained for the viewing conditions through the +2.0 D (+2.5 D) lens, respectively.

The proposed log-parabola curve used for fitting the CS values over a range of spatial frequencies showed a goodness of fit of $R^2 > 0.84$ in every condition. Further statistical testing, using repeated measures two-way analysis of variance, showed a significant effect of both spatial frequency (F(5,340) 188.98; $P < 0.0001$) and defocus level (F(3,342) 52.98; $P < 0.0001$). Further- more, the interaction of the two independent variables effect showed a strong significance (F(15,330) 19.16; $P < 0.0001$). Thus the known effect of defocus decreasing the ability to detect a contrast pattern, as well as a disclosure of CSF created for a wide range of spatial frequencies, was successfully replicated with the newly developed tool.

4.5 Discussion

Obtaining information about patient's visual performance in an objective way using eye movements has become an area of interest for many researchers [Mooney et al., 2018; Scholes et al., 2015a; Bonneh et al., 2015; Denniss et al., 2018; Dakin and Turnbull, 2016; Cetinkaya et al., 2008; Essig et al., 2020; Doustkouhi et al., 2020a]. The current study followed the finding that OKN responses may serve as a reliable tool for assessment of CS [Dakin and Turnbull, 2016] and extended the applicability by using an automated search method for the contrast threshold, based on a live evaluation of eye-tracking data. Moreover, the replication of the clinically-known effect of defocus on CS, already shown by Marmor and Gawande [1988], Green and Campbell [1965] or similarly by Jansonius and Kooijman [1997] in edge-CS measurements, were not sufficiently tested in OKN-based CS measurements. Hence, we aimed to replicate the consequence of defocus with the newly developed tool in emmetropic subjects. We used a live OKN detection and an adaptive psychometric method to measure CS by searching for the contrast threshold at which the OKN just occurs for a given spatial frequency. As an adaptive psychometric method, we used the QUEST+ algorithm, because this procedure was advised to be used in CS testing [Watson, 2017]. We implemented the algorithm in its one-dimensional form for the contrast level management; however, the implementation could be extended by using a multidimensional psychometric function on spatial or temporal frequency to increase the speed of the assessment of the spatiotemporal CSF. The OKN detection performance of the newly proposed method showed sufficient accuracy compared to the subjective judgment and very similar performance to the offline algorithmic-based analysis, therefore allowing the implementation of an adaptive psychometric procedure. However, not all trials were detected correctly. Some trials were found to contain a robust OKN response in the correct direction but have not been detected by the proposed algorithm, or vice versa. A possible reason for this is the limitation of not having a blink identification in the live OKN detection procedure. A second limitation is that the noise level has been

estimated across a quite short time period, because the time performance of the measurements was privileged over an extended detection time. Third, some trails, especially those in which a low-contrast-grating was presented, may have contained OKN-SPs of a velocity below the defined threshold, whereas the experienced observer recognized it still as a valid OKN-SP. Such algorithmic misjudgment may have happened because the detection algorithms used a fixed threshold value for the OKN- SP velocity. As already shown in the zebrafish experiment by Rinner et al. [2005] the gain of OKN (ratio of the OKN-SP velocity to the physical velocity of the stimulus) varies across contrast levels and is lower for low- contrast stimuli. Hence, we suggest instead thresholding the OKN-SP according to the contrast level, which could be implemented in the future. Nonetheless, the method of OKN detection we used in the current study was found to be superior to previous works, because the false-positive rate of existing detection algorithms was judged as too high for the implementation of adaptive methods [Mooney et al., 2018]. The CS value was obtained from the Weibull fit, already used in the previous research, [Dakin and Turnbull, 2016] because the inverted value of the contrast level at which the OKN response was expected to occur with a probability of 50%. Furthermore, the assessment of the log-parabolic fit, which was already proposed in the previous work by Lesmes et al. [2010] showed robust goodness of fit in the trend of CS values over selected spatial frequencies. Here, the CSF's peak is shifted toward smaller spatial frequencies, compared to the CS curves obtained in clinical practice in which nonmov- ing stimuli are used. However, this effect has already been observed in the previous study [Burr and Ross, 1982]. Moreover, the current study results show an agreement of the CSF-peak placement with the previous study by Burr and Ross [1982] considering the stimulus velocity used in each experiment. As a next point, the current study aimed to measure CS under healthy and blurred vision conditions in several steps, and thus replicate the known effect of decreasing CS with increasing defocus, [Marmor and Gawande, 1988; Green and Campbell, 1965; Jansonius and Kooijman, 1997] mainly having an impact on gratings of higher spatial frequencies. Such testing is possibly done in two ways, once by decreasing vision to a certain value of visual performance, as done by Marmor and Gawande [1988] or by using an optical power of a lens resulting in comparable refractive error (defocus) across subjects [Doustkouhi et al., 2020a]. Since the current study tested emmetropes, lenses of constant values have been used over all participants to artificially worsen their vision. Here, the defocus levels have been chosen to induce the desired blur, although with negligible simultaneous magnification-induced effects on the presented spatial frequencies [Ohlendorf and Schaeffel, 2009]. Hence, lenses in the range from 1.5 D to 2.5 D in 0.5 D steps were used. Because the current study targeted clinical testing, similar to previous work, [Doustkouhi et al., 2020a] we did not use cycloplegic agents to suppress accommod-

ation. Furthermore, we avoided cycloplegia because these substances result in pupil dilation, leading to increasing high-order aberrations and decreasing the CS. As the results show decreasing CS to increasing defocus, mainly for higher spatial frequencies, the current study successfully replicated the effect of defocus on CS in OKN-based measurements. Possible reasons for the variation in the impact of defocus are the residual refractive error of the emmetropic participants, their status of high-order aberrations, or differences in lags of accommodations, because these factors are highly individual [Seidemann and Schaeffel, 2003; Atchison and Markwell, 2008]. At the last point, since the current study used a square-wave grating to enable displaying also gratings of high spatial frequencies, the effect of higher harmonics might be comprised in the data. As shown by Campbell and Robson [1968] and Graham and Nachmias [1971] based on Fourier theory the detection threshold for a mixture of sine-waves is the determined by the component that reaches its contrast threshold first. In our case, for a square-wave of a base frequency SF 1.5 cpd or higher, the first-order harmonic (three times the base frequency) is SF 4.5 cpd or higher. Given that the detection thresholds for this spatial frequencies are beyond the peak of the CSF, only the higher harmonics of low-spatial-frequency square-wave gratings might be considered as relevant. Nonetheless, because no subject showed a peak CS that was three times higher than the one at about SF 0.7 cpd in the previous study using a sine-wave grating,[Burr and Ross, 1982] it appears that the participants detected the square wave gratings by its fundamental SF and not by one of the higher harmonics. In summary we consider the effect of higher harmonics on our OKN-based CS in our selected range of spatial frequencies to be negligible.

4.6 Conclusion

In conclusion, the current study successfully tested CS with the newly developed tool in a clinical environment over various conditions of healthy and blurred vision. We found that the proposed OKN live detection method is accurate enough for the usage with an adaptive psychometric procedure, estimating the participant's CS in an automated and time-efficient way. Furthermore, this study showed a successful replication of the blur effect on CS measured with the newly developed tool. Hence, the current study indicates the possibility to use OKN to assess visual performance for non-communicative patients, not only considering CS but also visual acuity or visual field loss, as recently suggested.

4.7 Acknowledgements

Supported by Eberhard-Karls-University Tuebingen (ZUK 63) as part of the German Excellence initiative from the Federal Ministry of Education and Research (BMBF). Further funding received from Deutsche Forschungsgemeinschaft and Open Access Publishing Fund of University of Tuebingen. Disclosure: P. Essig, None; Y. Sauer, None; S. Wahl, Carl Zeiss Vision International GmbH (E, F)

5 Reflexive Saccades Used for Objective and Automated Measurements of Contrast Sensitivity in Selected Areas of Visual Field

Essig P., Sauer Y., & Wahl S. (2022). Reflexive Saccades Used for Objective and Automated Measurements of Contrast Sensitivity in Selected Areas of Visual Field. Translational Vision Science & Technology, 11(5):29. doi:10.1167/tvst.11.5.29

5.1 Abstract

Purpose: This study proposes a novel approach for objective and automated peripheral contrast sensitivity (CS) testing using reflexive saccades. Here the CS was examined in various areas the of visual field (VF) using a live analysis of gaze data. For validation of the new test, we examined CS with an established procedure of identifying the orientation of a contrast stimulus.

Methods: To perform and validate the saccade-based testing, two separate measurement events were performed. In the first, participants were asked to execute a saccade toward a newly-appeared stimulus in their VF. After the saccade execution or stimulus expiry, reporting the target orientation was required in a four-alternatives forced choice (4AFC). Therefore the first measurement yields two outcomes (objective and subjective). In the second measurement, only the identification of the stimulus orientation was requested, while fixating a central mark. Stimulus contrast was controlled by an adaptive psychometric procedure in both measurements.

Results: The study found strong correlations (all $r \geq 0.79$) of CS values for all three possible testing methods (saccade-based responding in saccadic measurements, keyboard- based responding in saccadic measurements, keyboard-based responding in non- saccadic measurements), showing the feasibility of employment of reflexive saccades in such testing. Second, this study shows a significant influence of eccentricity and direction of the stimulus on the CS function.

Conclusions: CS measured with reflexive saccades is comparable to other testing methods over several areas of the participant's VF. Hence, we propose it as a novel and objective testing procedure for CS measurements.

Translational Relevance: Assessment of CS using reflexive saccades extends the portfolio of suggested eye movement-based tests, allowing objective examination across the VF, which might be helpful especially in the early detection of various eye diseases.

5.2 Introduction

Objective assessment of visual performance is possible using several types of eye movements. Previous research showed a successful implementation of microsaccades, [Scholes et al., 2015a] smooth pursuit eye movements, [Mooney et al., 2018] or the optokinetic nystagmus [Dakin and Turnbull, 2016; Essig et al., 2021a; Tatiyosyan et al., 2020] in contrast sensitivity (CS) measurements. It has been already stated that eye movement-based measurements may help to examine non-communicative participants, [Mooney et al., 2018] and make the measurements more time-efficient when using a live gaze data analysis. [Essig et al., 2021a] Their utilization is considered an objective approach for visual performance testing [Scholes et al., 2015a; Mooney et al., 2018; Dakin and Turnbull, 2016; Essig et al., 2021a; Doustkouhi et al., 2020a; Essig et al., 2020]. However, by now, these methods measure only the central CS, whereas an eye movement-based test for peripheral CS has not been developed yet. Peripheral vision is extensively used in patients with central visual field loss resulting from macular diseases [Crossland et al., 2005]. Moreover, a reduction in peripheral vision may be the first indication of serious eye diseases, such as glaucoma. Next, the optical quality on the peripheral retina might contribute to the enigmatic myopia development process [Smith III, 2011]. Last, good peripheral vision is important for many daily tasks, such as scene recognition, [Larson and Loschky, 2009] driving [Owsley and McGwin Jr, 2010] or performing sports activities [Lemmink et al., 2005]. In light of these facts, we aimed to transfer the advantages of an eye movement-based visual performance test to the examination of peripheral CS. To reach this goal, we use live detection (live gaze data analysis) of reflexive saccades (visually-guided eye movements), which are performed in the direction of a newly appeared visual stimulus, as an objective eye movement-based response [Walker et al., 2000]. Searching for the contrast level at which a reflexive saccade just occurs could be therefore used as an objective measure of peripheral CS. To effectively change the contrast level of the visual stimulus while searching for the contrast threshold, an adaptive psychometric procedure was applied. As shown by Murray et al. [2013] or more recently by Perperidis et al. [2021] reflexive saccades were successfully used for perimetry testing (SVOP technique). The motivation of the current study was to extend the portfolio of eye movement-based visual field tests to examinations of peripheral CS. The already established eye movement-based procedures, along with our newly proposed one, could serve as a set of tests for objective assessment of visual performance across the visual field of a patient. Reflexive saccades are controlled by different neural structures than voluntary saccades [Pierrot-Deseilligny et al., 1995]. Moreover, the latency of the reflexive saccades was found to be lower (the eye movement was performed faster) compared to voluntary saccades [Walker et al., 2000]. Similar to

optokinetic nystagmus, [Essig et al., 2021b] the onset time of reflexive saccades is influenced by the contrast level of a stimulus [Ludwig et al., 2004]. Therefore we used the visual stimulus presentation time limit of 500 ms, which was shown to cover all the onsets across a wide range of contrast levels [Ludwig et al., 2004]. Reflexive saccades are often also referred to as reactive saccades. Throughout the article we use the term reflexive saccade to keep this work uniform [Walker et al., 2000; Briand et al., 1999; Gremmler and Lappe, 2017]. Because previous subjective examinations of peripheral CS showed varying values of CS depending on the eccentricity and direction (nasal, temporal, inferior, and superior), [Rosen et al., 2014] we aimed to replicate this VF location-specific contrast sensitivity function (CSF) for the objective measurements. Location dependent variations of CS have been explained by variations in peripheral refraction, higher-order aberrations, and asymmetrically decreasing sampling of the ganglion cells toward the periphery [Curcio et al., 1990]. To validate our proposed objective test, we also executed the subjective measurements. In the subjective measurements, participants were asked to respond to the perceived orientation of a Gabor patch with a keyboard. This subjective procedure was performed twice: once in the saccade-based measurements directly after performing a saccade (or after stimulus expiration), and once in a separate measurement, while maintaining the fixation in the center of the screen (non-saccadic measurements). To keep uniform references to the measurement instances we performed, we address them as saccade-based responding in saccadic measurements, keyboard-based responding in saccadic measurements and keyboard- based responding in non-saccadic measurements. CS is clinically tested under monocular viewing conditions. Hence, we followed this approach by patching the left eye. Moreover, we used one fixed stimulus size as the potential effect of cortical magnification varies substantially among subjects and visual field [Benson et al., 2021] and one stimulus size for all tested eccentricity levels was used in a previous study [Rosen et al., 2014]. Furthermore, as the current study aimed to test CS in different visual field areas, namely the central, macular and near peripheral, the target was presented accordingly displaced relative to the center of the screen. The estimated ranges of the respective visual field areas are $< 5°$, $\approx 5°$to $\approx 9°$and $\approx 9°$to $\approx 17°$, as reviewed by Strasburger et al. [2011]. In our study, the contrast thresholds were measured independently over a selected range of spatial frequencies at four cardinal directions in three eccentricity levels. These measurements were conducted using saccade-based and keyboard-based procedures.

5.3 Methods

5.3.1 Participants

Twelve participants (eight male and four female) with a mean age of 24.5±2.6 took part in the current study. All participants were emmetropic and had normal vision. The current study considered emmetropia as a refractive error smaller than ±0.5 D in spherical equivalent measured by the wavefront-based autorefraction (ZEISS i.Profiler plus, Carl Zeiss Vision, Aalen, Germany). The study protocol followed the Declaration of Helsinki. In addition, the study was approved by the ethics committee of the Faculty of Medicine of the University Tuebingen. Signed informed consent was obtained from all participants before the experiment. All participants were recruited from the University Tuebingen.

5.3.2 Visual Stimulus and Eye Tracking

For the presentation of the visual stimulus, the Viewpixx screen (VIEWPixx; VPixx Technologies Inc., Saint Bruno, Quebec, Canada) was used, providing 12 bits of bit depth in gray-scale resolution and refresh rate of 120 Hz. The screen was gamma-corrected to compensate for the nonlinearity in the pixel value and luminance. For eye tracking, the EyeLink 1000 Plus infra-red (IR) eye-tracker (SR Research, Ottawa, Ontario, Canada) was used with monocular tracking of the right eye with a sampling frequency of 1000 Hz. For the visual stimulus creation and data analysis MATLAB2018b (MATLAB2018b; MathWorks, Natick, MA, USA) and Psychtoolbox-3 [Brainard, 1997; Kleiner et al., 2007] were used. The reflexive saccade-evoking stimulus was a Gabor patch with a diameter of 1.4°, presented on a screen at a distance of 62 cm to the participant's right eye (left eye was patched for monocular testing). The stimulus size was chosen to be large enough to not influence the detection performance across a wide range of eccentricities [Khuu and Kalloniatis, 2015]. Also, the size was fixed for all eccentricity levels because the cortical magnification, and thus the related retinal cone density, [Curcio et al., 1990] was expected to vary among subjects and to be different in the four tested directions. One constant stimulus size for different eccentricities was used in a previous study on peripheral CS as well [Rosen et al., 2014]. During one measurement, the target was presented in a random order in one of the four possible directions respecting the nasal, temporal, inferior, and superior visual field; hence, always displayed at the 0°, 90°, 180°, or 270°meridian. The orientation of the target was also randomly selected for every target presentation from four available orientations 45°, 90°, 135°, or 180°. Each measurement was performed separately for three predefined eccentricity levels, matching the central, macular, and near-peripheral visual field. Here the corresponding displacements of the target relatively to the center

of the screen were 2.0°, 6.5°, and 11.0°. The selection of tested spatial frequencies was dependent on the eccentricity level. We aimed to test the relevant range around the peak of the CSF for each eccentricity level, also considering the hardware limitations of our setup. We tested spatial frequencies 0.8, 1.4, 2.2, and 4.3 cycles per degree (cpd) for all three eccentricity levels, with one additional (7.2 cpd) for the macular eccentricity level and two additional (7.2 and 10.7 cpd) for the central eccentricity level, because the detection of high spatial frequencies is too low in the near peripheral eccentricity level [Rosen et al., 2014]. To ensure stimulation at the desired visual field location, the participants' gaze was controlled to be on the central fixation mark before the visual stimulus was presented. This fixation check was implemented using live analysis of gaze data and continuous calculations of the gaze position running with the sampling rate of the eye-tracker. A gray dot, displayed at the center of the screen in size of 0.3°, served as the fixation mark. The radius of the fixation area was set to 1°so that potential fixational eye movements would not be accidentally detected as false-positive responses in the saccade-based measurements [Essig et al., 2020; Zuber et al., 1965]. Furthermore, the fixation phase varied in duration because the time was randomly selected from a range between 500 to 650 ms in every trial. Live gaze analysis allowed us to switch to an irrelevant stimulus (empty circle) as soon as the gaze position had exceeded the fixation area and, second, to let a particular trial be repeated if a blink was detected or if inappropriate fixation was detected in the keyboard-based measurements. In case of a blink, the order of the remaining trials was randomized again. In the saccade-based measurements, as soon as the gaze was found to be out of the fixation area, the direction of the performed saccade (bg) was calculated as follows:

$$\beta_g = \text{atan2}(y_{\text{eye}} - y_{\text{center}}\ ,\ x_{\text{eye}} - x_{\text{center}}). \tag{4}$$

In Equation4 x_{eye} and y_{eye} stand for the Cartesian coordinates of the gaze position in pixels captured after exceeding the fixation area, and the variables x_{center} and y_{center} are the coordinates of the center of the screen. The calculated angular difference between target location and saccade direction βg had to be in a range of ±22.5°to be accepted as a correct response.

5.3.3 Task for the Participants

The participants' task was slightly different between the two types of measurement. All subjects performed both measurements in a randomized order. In the saccade-based measurement, participants were instructed to move their gaze toward the location where the target was identified (to try to catch the target with their gaze). After the eye movement or target expiration, subjects had to answer the orientation of the Gabor

patch in a 4AFC (four-alternatives forced choice) paradigm, using a keyboard as depicted on Figure(14). For controlling the location-specific QUEST+ algorithm, correctly oriented saccades were taken as correct responses, or otherwise, if no or wrongly oriented saccade was detected. The keyboard-based responses to the grating orientation within this method were collected as additional data and did not influence the adaptive psychometric procedure. This data was only collected to better compare the CSFs of the saccade- and keyboard-based measurements, because there was a discrepancy in the fixational mark presence (in the keyboard-based measurement events, the fixation mark was present in the stimulus presentation phase to avoid reflexive saccades). The second measurement method covered a purely subjective approach in which only the orientation of the target was asked in a 4AFC paradigm. Fixation had to be maintained on the central fixation mark, which was present also during the stimulus presentation phase. Equally to the first method, the initial fixation phase varied in time. Participants had to respond to the four available visual stimulus orientations with the keys 1 or 9, 2 or 8, 3 or 7, and 4 or 6, respectively. The correct answer to the spatial orientation of the stimulus was considered as "seen" or "not seen" otherwise. This response was used as input for QUEST+. Each eccentricity and spatial frequency combination was tested with both measurement methods with 120 target presentations each. There were always 30 target presentations per direction, and every orientation of the grating was presented 30 times. The total number of trials in the saccade-based measurements was 132, from which 12 were catch-trials at which no target was present. However, they followed the same workflow to hide them among other trials.

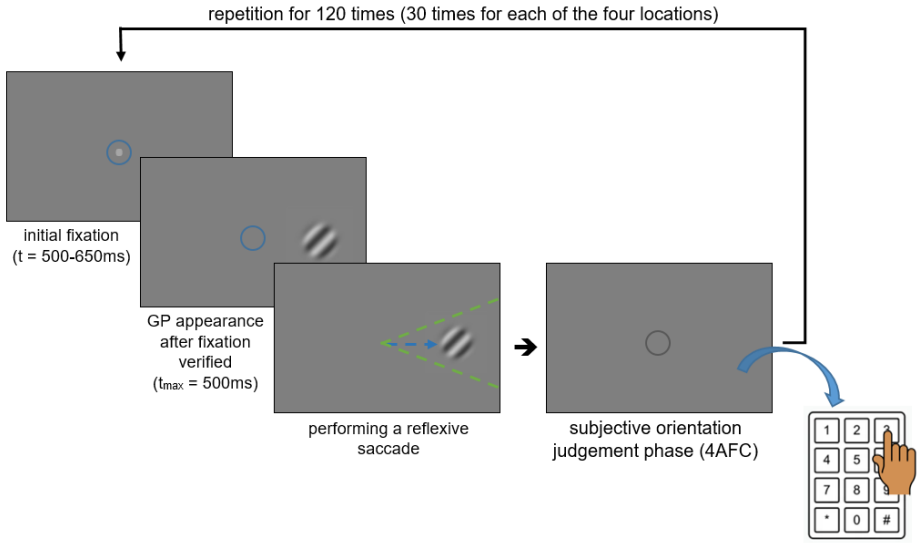

Figure 14: Procedure for the saccade-based measurements. The blue circles represent the area of fixation. The blue arrow illustrates the expected direction of a reflexive saccade. The green dashed lines show the cone within which the saccade was considered correctly oriented. When the gray circle was shown, the test required answering the grating orientation (in this example, the correct response was pressing 3 or 7 on the number pad).

5.3.4 Application of the Adaptive Psychometric Procedures

The QUEST+ adaptive psychometric procedure [Watson, 2017] was used to control the contrast level of the stimuli at each of the four VF directions (nasal, temporal, inferior, and superior) independently (four instances of the psychometric procedure were used) because CS varies between different visual field locations [Rosen et al., 2014]. As the psychometric function of the entropy-based adaptive psychometric algorithm, the cumulative Weibull distribution function was used with the parameters threshold, slope, upper and lower asymptote. The parameter space for threshold had 15 contrast levels ranging from ≈0.024% to ≈66.0%. The slope had a predefined parameter space of 0.5 to 5.5 in steps of 0.5 since it could differ among subjects and tested locations. Since the convergence of the entropy function could vary among subjects and tested locations, the number of grating presentations was fixed, resulting in the same amount of data for every participant.

5.3.5 Analysis of the Acquired Data

To find the contrast threshold for the calculation of CS, the occurrence rate of reflexive saccades depending on the stimulus contrast level was fitted with a psychometric function using Psignifit [Schütt et al., 2015] in MATLAB. The cumulative Weibull dis-

tribution function was used as the fitting function with the following parametrization

$$\Psi(x; m, w, \gamma, \lambda) = \gamma + (1 - \lambda - \gamma)\left(1 - e^{\log(0.5)e^{c\frac{\log(x)-m}{w}}}\right) \tag{5}$$

with $c = \log(-\log(0.05)) - \log(-\log(0.95))$. The fitting parameters were guess rate γ and lapse rate λ, representing the lower and upper asymptote, as well as the threshold m and the width w between the 0.05 and 0.95 points. Both m and w are in log space of the stimulus parameter x. The relation between the width w and the slope s of the cumulative Weibull distribution function, as also used by QUEST+, is $s = \frac{c}{w}$. The contrast threshold CT was calculated from m as $C = e^m$. Furthermore, the threshold was taken for every measured spatial frequency of the grating and was later converted to the CS value as $CS = \frac{1}{CT}$. For plotting of the data and statistics, the $\log_{10}(CS)$ was used. At last, the contrast sensitivity function (CSF) was created as a fit of the CS values depending on spatial frequency SF with a log-parabola, considering the ascending and descending part of the CSF as already suggested by Lesmes et al. [2010], using the following fitting function:

$$CS(SF) = \log_{10}(\gamma_{max}) - \log_{10}(2)\left(\frac{\log_{10}(SF) - \log_{10}(SF_{max})}{\beta}\right)^2, \tag{6}$$

with peak sensitivity γ_{max}, peak spatial frequency SF_{max}, and the function's bandwidth β [Lesmes et al., 2010]. The CSFs were fitted individually for each subject and all tested retinal locations in the three eccentricity levels. Additionally, the mean CSFs were fitted, calculated across all participants for all tested locations, eccentricities and testing methods.

5.4 Results

5.4.1 Psychometric Fits

The psychometric function fits for all three testing procedures (saccade-based responding in saccadic measurements, keyboard-based responding in saccadic measurements and keyboard-based responding in non- saccadic measurements) are shown in Figure(15) for one example subject.

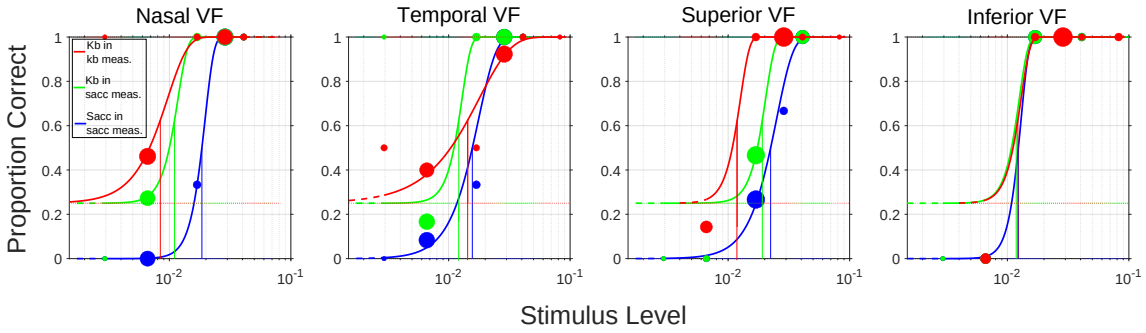

Figure 15: Four subplots are shown for the four tested visual field directions. Each subplot contains three psychometric functions for the three testing procedures. The red fits represent the keyboard-based responses in non-saccadic measurements, the green fits represent the keyboard-based responses in saccadic measurements, and the blue fits represent saccade-based responses in saccadic measurements. Please note that for the keyboard-based measurements, the lower asymptote (guess rate) is shifted to 25% because of the 4AFC paradigm. The dot size (area) scales with the testing frequency of the particular contrast level, as selected by the adaptive psychometric procedure. The shown data are one example measurement of one subject at spatial frequency 2.2 cpd) and eccentricity 2°.

5.4.2 Correlation of the CS Values

We created three correlation (Figure(16)(and Bland-Altman (Figure(17)) plots of the obtained CS values to compare the three measurement methods to have a first insight into the comparability of our data. Correlation of CS values is strong for all combinations of the three measurement procedures with correlation coefficients of $r = 0.79$ or higher. However, the Bland-Altman plots show an offset between the saccade-based responses in saccadic measurements and keyboard-based responses in non-saccadic measurements (0.1379) as well as between the saccade- based responses and keyboard-based responses in saccadic measurements (0.1645). The smallest offset was found between the two keyboard-based responses in saccadic and non-saccadic measurements (-0.0266). Friedman's test shows a significant effect of the testing procedure ($\chi^2(2159) = 482$; $P < 0.0001$) with significant group-wise differences between all three approaches ($P_{all} < 0.0001$). The median CS for the three testing procedures was 1.39, 1.54, and 1.52 in the saccade-based measurements, in the keyboard-based responses in saccadic trials, and the non-saccadic keyboard-based measurements, respectively.

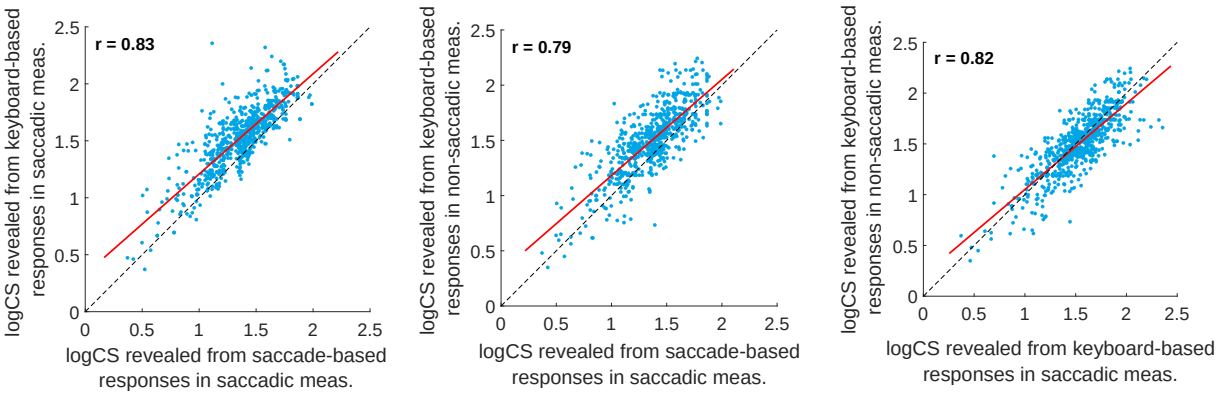

Figure 16: The three possible combinations of correlations are shown for the three testing methods. The blue points represent the logCS values for all tested subjects, directions, eccentricities and spatial frequencies. Please note the correlation coefficients are provided in each subfigure.

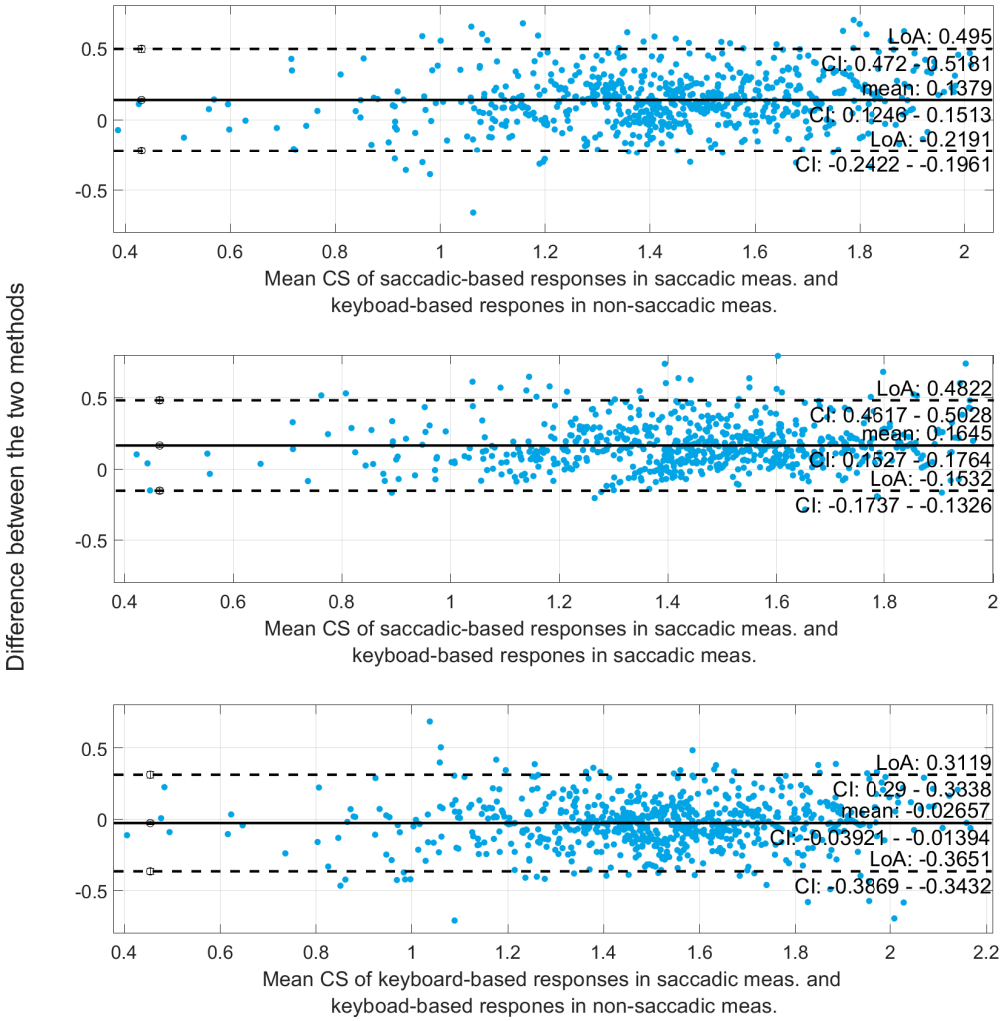

Figure 17: The blue points represent the logCS values for all tested subjects, directions, eccentricities and spatial frequencies. Please note that the confidence intervals (CI), mean value, and the lower and upper bounds are provided in the figure. These plots along with the correlation plots above were considered to yield a first insight about the possibility to use reflexive saccades as another type of eye movement for CS testing.

5.4.3 Mean CFSs

Mean CSFs (Figure(18)) were calculated over all participants for the three testing procedures and the three tested eccentricity levels, considering them as another way of comparing the three testing approaches besides the correlation plots described in the previous section. The results in the saccade-based measurements show slightly worse values of CS than the two other approaches, supporting the median outcomes presented in the previous section. Nonetheless, the trend of all the CSFs remained comparable

across all testing procedures. Second, CS was better in the nasal and temporal visual field compared to the superior and inferior direction, with more profound differences for higher eccentricity levels and higher spatial frequencies. Furthermore, we statistically tested the effects of the method, eccentricity and direction on the fitting parameters of the mean CSFs (peak sensitivity, peak spatial frequency and the function's bandwidth). The three-way analysis of variance showed significant effect of the direction of the visual stimulus ($F(3,32) = 16.97$; $P < 0.0001$) eccentricity ($F(3,33) = 256.78$; $P < 0.0001$) and method ($F(3,33) = 60.01$; $P < 0.0001$) on the peak sensitivity. The peak spatial frequency is significantly influenced by the direction of the visual stimulus ($F(3,32) = 20.45$; $P < 0.0001$) and eccentricity ($F(3,33) = 187.00$; $P < 0.0001$) but not by the method ($F(3,32) = 0.01$; $P = 0.99$). Finally, our data show a significant effect of the direction of the visual stimulus ($F(3,32) = 7.26$; $P = 0.0009$) and eccentricity ($F(3,33) = 3.69$; $P = 0.038$), yet the method continued to have an insignificant effect ($F(3,33) = 1.63$; $P = 0.21$) on the function's bandwidth.

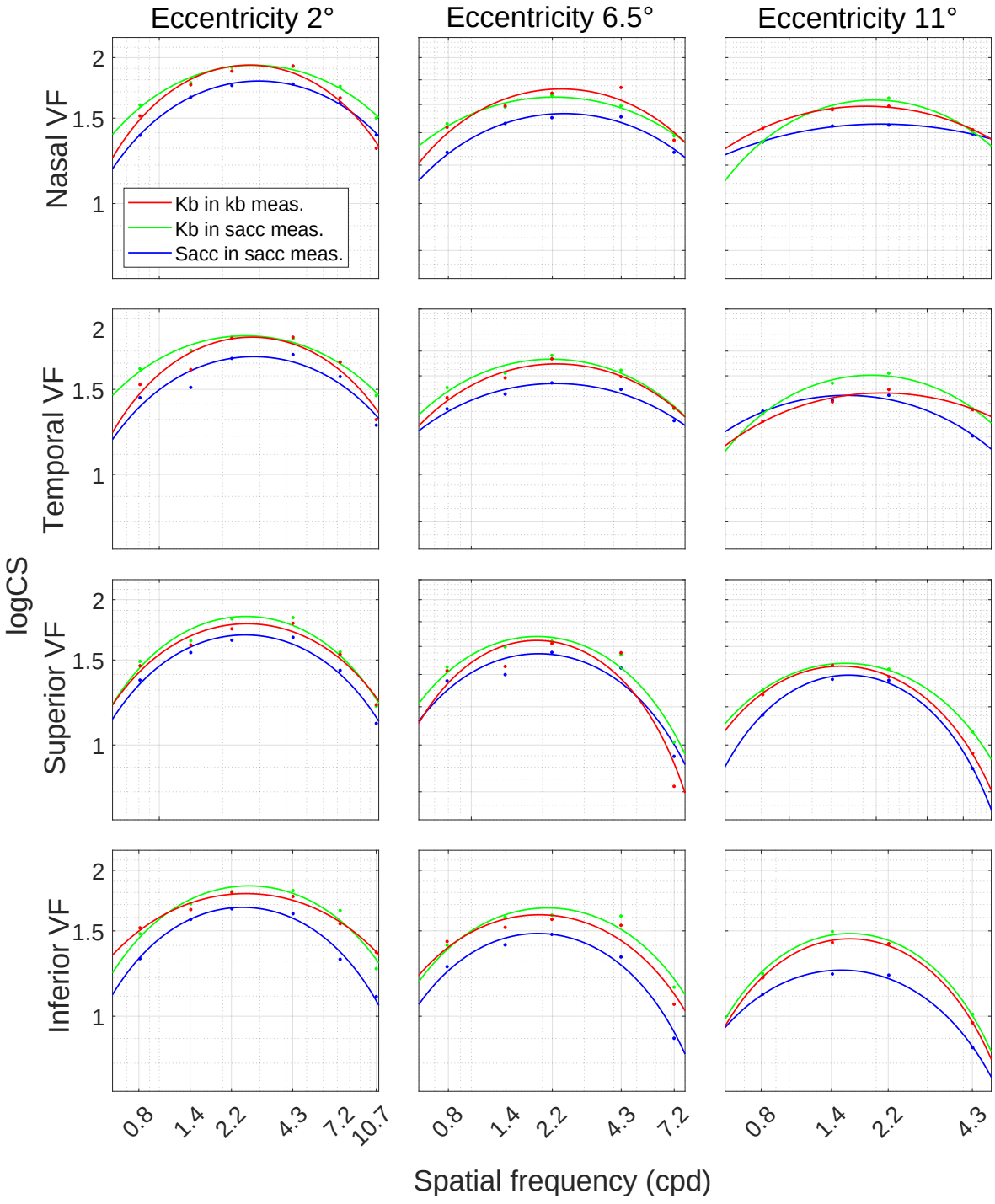

Figure 18: The mean CSFs of all subjects were fitted for every eccentricity level (column) and every visual field direction (row). The first column corresponds to the first eccentricity level (2°), second column to the second eccentricity level (6.5°) and the third column to the third eccentricity level (11°). Each subplot contains a blue CSF representing the saccade-based responses in saccadic measurements, green CSF representing the keyboard-based responses in saccadic measurements, and a red CSF representing the keyboard-based responses in non-saccadic measurements. Note that the ranges of spatial frequencies vary for every eccentricity level

5.4.4 Individual Visual Field Location-Specific CSFs Measured With Reflexive Saccades

Figure(19) shows the CSFs of saccade-based measurements for all participants for the four directions and the three eccentricity levels. We also present median and mean CS values with standard deviation in the Table(3), calculated for every combination of direction and eccentricity. Furthermore, we tested the effect of the spatial frequency and the direction on CS for the three eccentricity levels individually. The two-way analysis of variance revealed a significant effect of the spatial frequency and the direction on CS for the first ($F(5,282) = 41.58$; $P < 0.0001$, $F(3,284) = 4.93$; $P = 0.0024$), second ($F(4,235) = 55.69$; $P < 0.0001$, $F(3,236) = 10.18$; $P < 0.0001$) and third ($F(3,188) = 40.39$;$P < 0.0001$, $F(3,188) = 30.11$; $P < 0.0001$) eccentricity level. The interaction of the two variables was not significant on the first eccentricity level ($F(15,272) = 0.49$; $P = 0.94$); however, the significance was shown for the second ($F(12,227) = 2.56$; $P = 0.0034$) and third ($F(9,182) = 3.03$; $P = 0.0022$) eccentricity. On top of that, the 2160 catch-trials had a false-positive rate of 4.3%, with 93 catch-trials in which the gaze exceeded the fixation area although no target was present.

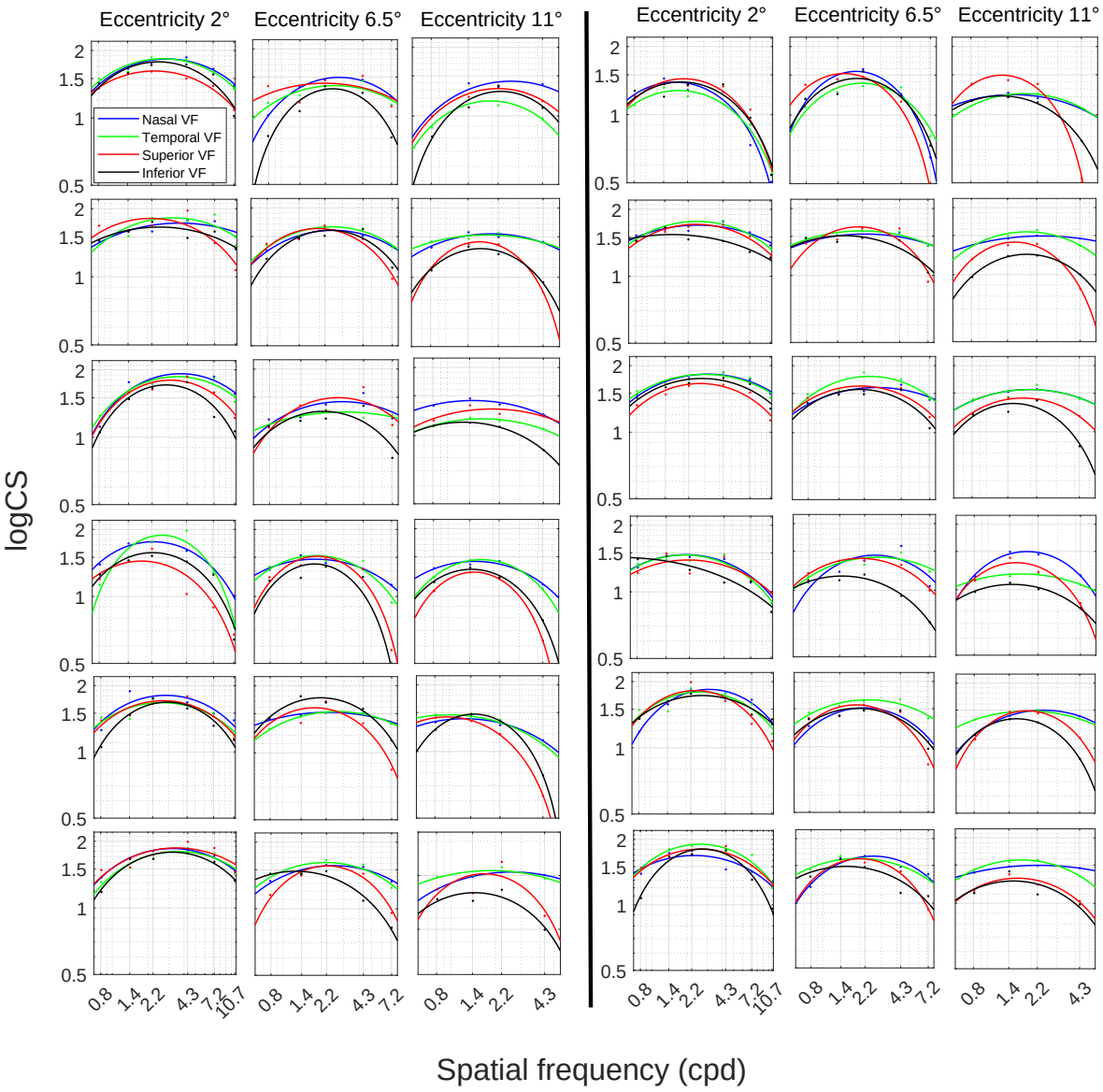

Figure 19: The location-specific CSF for the saccade-based measurement is presented for each participant (row) and eccentricity level (column). Similar to the previous figure, each subplot shows a blue CSF representing the nasal VF, green CSF for the temporal VF, red CSF representing the superior VF, and a black CSF for the inferior VF.

–	Eccentricity 2°	Eccentricity 6.5°	Eccentricity 11°
Nasal VF	1.57 (1.52 ± 0.27)	1.41 (1.38 ±0.18)	1.38 (1.36 ± 0.14)
Temporal VF	1.51 (1.51 ± 0.29)	1.42 (1.40 ± 0.19)	1.36 (1.31 ± 0.18)
Superior VF	1.47 (1.44 ± 0.29)	1.38 (1.32 ± 0.26)	1.21 (1.19 ± 0.23)
Inferior VF	1.44 (1.40 ± 0.27)	1.26 (1.25 ± 0.27)	1.11 (1.11 ± 0.19)

Table 3: Median (mean ± SD) of CS values were calculated over all subjects and spatial frequencies, individually for the three eccentricity levels and the four visual field directions.

5.5 Discussion

The current study aimed to establish and validate a novel approach of objective assessment of peripheral CS based on eye movements, extending already conducted research on eye movement-based central CS testing [Scholes et al., 2015a; Dakin and Turnbull, 2016; Essig et al., 2021a; Doustkouhi et al., 2020a]. For our testing, we used reflexive saccades, a visually-guided eye movement occurring toward a novel stimulus in the visual field of an observer [Walker et al., 2000]. Our test also extends the portfolio of saccade-based tests, containing for instance the SVOP technique, [Murray et al., 2013; Perperidis et al., 2021] for peripheral visual performance examinations. Such a set of tests may help to examine noncommunicative participants [Scholes et al., 2015a] or children [Perperidis et al., 2021]. In our study we presented a visual stimulus (Gabor patch) defined by a spatial frequency and eccentricity level in four possible directions in a random order. In our novel test, the task for the participant was to perform a saccade toward the stimulus (to catch the target with their gaze). To validate our newly proposed peripheral CS test, saccade-based measurements were compared to an established subjective test based on a response to the orientation of the stimulus. In this non- saccadic subjective measurement, a stable centrally-located fixation mark was present, leading to possible differences in attention between the two measurement events. To study this possible influence, the subjective judgement was also performed directly in the saccade-based measurement by identifying the orientation after each trial. A significant difference was found between the two keyboard-based procedures (CS measured by the keyboard-based responding in the saccadic measurements performed better). However, this difference is small (mean difference 0.027), and therefore we consider it irrelevant for clinical testing. On top of that, the Bland-Altman plots showed the highest agreement between the two keyboard-based procedures. In contrast to a previous study by Rosen et al. [2014] we randomized the target directions and orientations within one eccentricity level and spatial frequency in every measurement to minimize the potential influence of attention [Carrasco et al., 2004]. Moreover, we implemented catch-trials, containing no visual stimulus. In 4.3% of catch-trials a saccade was detected. A previous study on accuracy and precision of saccades showed at least 9% of catch-trials containing a saccade [Kowler and Blaser, 1995]. Vingrys and Demirel [1998] stated that a false-response rate should be lower than 20% to consider a visual field test as reliable. Therefore we consider our false-response rate low and our test to be solid. Nonetheless, we cannot report on the reason for our false-response rate because our saccadic detection did not consider the landing point (the amplitude). A potential explanation could be the occurrence of large fixational eye movements exceeding the central fixation area (1°). As found by Krejtz et al. [2018]

or Martinez-Conde and Macknik [2015] events of fixational eye movements larger than 1°are rare; hence, only a small amount of our catch-trials was found as false-positive. In future clinical testing, catch-trials might be used as a verification of the test reliability in individual subjects, as already suggested before [Vingrys and Demirel, 1998]. The results of the current study show first a strong correlation of CS values obtained from the saccade-based measurements and both types of keyboard-based responses, whereas all correlations calculated indicate that the different response types are highly comparable. However, the saccade-based measurements generally show slightly worse performance in CS testing than both keyboard-based measurements. This offset is shown by the Bland-Altman plots comparing the CS of saccade-based responding to both keyboard-based procedures. One reason for this finding could be the difference in the psychometric testing method (4AFC vs. yes-no-task), leading to different guess rates in the fitting procedure (guess rate set to 25% in both keyboard-based responses, while set to zero in the saccade-based responses) [Wichmann and Hill, 2001]. Furthermore, it might be the case that sometimes, in low-contrast testing (high CS), the contrast of the visual stimulus was too low to trigger a reflexive saccade, even if the target was judged correctly for its orientation. Another possible reason for the saccade-based responses to underperform the other two measurement procedures could be that the latency of the saccadic onset was longer than the stimulus presentation time, because the onset time was found to be contrast-dependent [Ludwig et al., 2004]. Moreover, the current study found a systematic decrease of CS with increasing eccentricity, as was hypothesized already after the outcomes of a previous study testing other eccentricity levels [Rosen et al., 2014]. Our study confirmed better CS in the horizontal visual field over the vertical one in both eye movement-based and keyboard-based trials. However, our test's eccentricity levels were smaller than in other studies [Rosen et al., 2014; Mackeben, 1999; Daitch and Green, 1969]. Here we also consider the maximum eccentricity we reached in our study (11°) as a limitation of our set-up, because the further eccentricities would have provided relevant information of patient's peripheral visual performance, particularly in early-detection procedures of various eye diseases. For testing larger eccentricity levels, our test would require a larger screen or performing the examination using a projector for instance. From previous research, better CS is expected in the inferior VF compared to the superior VF. Our study could confirm this only in keyboard-based measurements, whereas saccadic trials show an opposite trend. This finding could be explained by nonuniformity in triggering vertical saccades. For example, Abegg et al. [2015] found shorter latencies for upward oriented saccades than downward oriented ones. On top of that, Tzelepi et al. [2010] suggested that stimuli in the upper and lower visual field may have different impacts on areas of the visual system related to visual attention and motor preparation, concluding behavioral

asymmetries in ocular motor performance. Nonetheless, the previous research showed a successful assessment of the patient's VF using reflexive saccades [Perperidis et al., 2021]. We suggest that such testing procedures are also suitable for remote screening using, for instance, a VR headset, as already done by Tatiyosyan et al. [2020] for optokinetic nystagmus-based CS examinations. Although there are some considerable technical limitations, as for instance the eye-tracking latency [Stein et al., 2021] or its quality, [Pastel et al., 2021] the VR headsets provide a bigger field of view for possible testing of larger eccentricities, [Sauer et al., 2022] compared to our setup. Testing further eccentricities would be useful in the early detection of several eye diseases such as glaucoma. Our test design should support such testing because the direction of a saccade has been calculated right after exceeding the fixation area (no need for high accuracy of the eye tracker in the periphery).

5.6 Conclusion

The current study shows a possible approach of objective and fully automated estimation of CS in selected areas of the visual field. We found a strong correlation of the CS values between the newly developed method and an established procedure. On top of that, the current study showed a successful replication of the CSF across various visual field locations. Hence, this study indicates the possibility of using reflexive (visually-guided) saccades to assess visual performance over the whole visual field objectively, not only considering CS but also visual acuity or the actual size of the visual field.

5.7 Acknowledgements

Supported by Eberhard-Karls-University Tuebin- gen (ZUK 63) as part of the German Excellence initiative from the Federal Ministry of Education and Research (BMBF). Further funding was received from Deutsche Forschungsgemeinschaft and the Open Access Publishing Fund of the University of Tuebingen. Disclosure: P. Essig, None; Y. Sauer, None; S. Wahl, Carl Zeiss Vision International GmbH (E, F)

6 Summary

The primary purpose of this dissertation was to improve existing or establish new contrast sensitivity assessment methods based on eye movements, in order to provide solutions to objectively assess this visual function. The individual studies provide insights into the question of contrast sensitivity appraisal with eye movements using several types of eye movements, namely microsaccades, optokinetic nystagmus and reflexive saccades. The results of the presented work lead to the following summary:
(1) The previous research showed that the amplitude of the rate signature curve - modulation of microsaccadic count after stimulus onset - is contrast dependent and thus proposed it as a tool for the contrast sensitivity assessment, however, measured under binocular conditions and thus not following the clinical approach. The first own study of this thesis showed evidence that also under monocular simulation, the microsaccadic rate follows the known signature behavior, while still taking the eye movement as a binocular event. Therefore this study improves such procedure by extending its applicability to the clinical environment.
(2) Because microsaccadic eye movements are rare and occur inconsistently among subjects, the next study used optokinetic nystagmus for contrast sensitivity measurements. Here the second study successfully implemented a live detection procedure - detecting the optokinetic nystagmus response in real time - and a one-dimensional adaptive psychometric procedure for contrast management, in order to develop a fully automated eye movement-based contrast sensitivity test. In this study, the measurements were conducted for a range of spatial frequencies of a target, presented without and with various defocus conditions. In this study, the replication of a contrast sensitivity curve was performed with an optokinetic nystagmus-based test, and on top of that, this study found the first evidence of defocus having a similar impact on contrast sensitivity compared to classical measurements.
(3) The third study aimed to extend the eye movement based contrast sensitivity measurements also to the peripheral vision as some of the serious eye diseases and retinal detachments affect the peripheral vision first. In this study the implementation of live detection of reflexive saccades along with an adaptive psychometric procedure controlling the stimulus level at four locations independently was successfully performed. In this study the contrast sensitivity was measured in four cardinal directions and three eccentricity levels. On top of that the current study verified the newly established procedure with a subjective one performed with keyboard-based responses. First this study replicated the trend of decreasing sensitivity with increasing eccentricity as well as showing better sensitivity over the horizontal visual field compared to the vertical visual field. Moreover, this study showed highly comparable results for the eye

movement-based and subjective measurement procedure suggesting a possible implementation of this sort of eye movement into contrast sensitivity testing.
In conclusion, microsaccades, although showing binocular occurrence in monocular stimulation and thus feasible implementation in clinical measurements of contrast sensitivity, rather fragile algorithmic detection and inconsistency of their occurrence among subjects does not show sufficient performance for clinical use and thus leaves such testing only for scientific purposes for now. In connection with that, optokinetic nystagmus shows better performance in contrast sensitivity testing with correlated outcomes to subjective measurements, being only disregarded by the moving visual stimulus. Nonetheless, such a test using the newly established live detection method along with an adaptive psychometric procedure might be possibly used for screening purposes. Besides the foveal contrast sensitivity being tested with the above-mentioned eye movement-based tests, this thesis shows also an approach to test the peripheral contrast sensitivity using reflexive saccades, independently in various locations in the patient's visual field. This test then shows a novel transformation of a standard contrast sensitivity perimetry test to an eye movement-based test, having the potential to be used in the clinical practice in the future.
Despite the range of findings in the current thesis, this field requires further research prior to its application into clinical practice. Future developments of algorithms for eye movement detection as well as psychometric procedures could further improve the quality and time-efficiency of such measurements. On top of that, the rounded validation of the currently established eye movement-based contrast sensitivity tests against the clinically measured ones has to be performed to directly compare the efficiency of such measurements, their repeatability, and the viability prior to the implementation in the clinical practice. Furthermore, as contrast sensitivity is not the only parameter to be tested in the visual performance assessment of a patient, the current work could be extended to other examinations, as for instance visual acuity, size of the visual field, detection of colors, or reading speed. With the improved algorithms for eye movement detection as mentioned above, combined with an embedded frontal camera and display of sufficient parameters, such measurements could be feasibly transferred to portable devices as a tablet, smart phone, or VR head-set.

7 Zusammenfassung

Das Hauptziel dieser Dissertation war die Verbesserung bestehender oder die Etablierung neuer Methoden zur Bewertung der Kontrastempfindlichkeit auf der Grundlage von Augenbewegungen, um Lösungen für die objektive Bewertung dieser visuellen Funktion zu finden. Die einzelnen Studien geben Einblicke in die Frage der Kontrastempfindlichkeitsbeurteilung mit Augenbewegungen unter Verwendung verschiedener Arten von Augenbewegungen, nämlich Mikrosakkaden, optokinetischer Nystagmus und reflexive Sakkaden. Die Ergebnisse der vorgestellten Arbeiten lassen sich wie folgt zusammenfassen:

(1) Die bisherige Forschung hat gezeigt, dass die Amplitude der Häufigkeits-Signatur-Kurve - Modulation der Mikrosakkadenzahl nach Stimulusbeginn - kontrastabhängig ist und schlug sie daher als Instrument zur Beurteilung der Kontrastsensitivität vor, allerdings unter binokularen Bedingungen gemessen und damit nicht dem klinischen Ansatz folgend. Die erste Studie dieser Dissertation hat gezeigt, dass die Häufigkeit der Mikrosakkaden auch unter monokularer Stimulation dem bekannten Verhalten folgt, wobei die Augenbewegungen weiterhin als binokulare Ereignisse betrachtet werden. Diese Studie verbessert daher dieses Verfahren, indem sie seine Anwendbarkeit auf die klinische Umgebung ausweitet.

(2) Da mikrosakkadische Augenbewegungen selten sind und bei den Probanden uneinheitlich auftreten, wurde in der nächsten Studie der optokinetische Nystagmus für Messungen der Kontrastempfindlichkeit verwendet. In dieser zweiten Studie wurde erfolgreich ein Live-Detektionsverfahren - die Erkennung der optokinetischen Nystagmusreaktion in Echtzeit - und ein eindimensionales adaptives psychometrisches Verfahren für das Kontrastmanagement implementiert, um einen vollautomatischen Test für Kontrastempfindlichkeit basierend auf Augenbewegungen zu entwickeln. In dieser Studie wurden die Messungen für eine Reihe von Ortsfrequenzen eines Stimulus durchgeführt, der ohne und mit verschiedenen Defokusbedingungen präsentiert wurde. In dieser Studie wurde die Replikation einer Kontrastempfindlichkeitskurve mit einem auf optokinetischem Nystagmus basierenden Test durchgeführt. Darüber hinaus wurde in dieser Studie der erste Nachweis erbracht, dass Defokus bei OKN einen ähnlichen Einfluss auf die Kontrastempfindlichkeit hat wie bei den klassischen Messungen.

(3) Die dritte Studie zielte darauf ab, die augenbewegungsbasierte Kontrastempfindlichkeitsmessung auch auf das periphere Sehen auszudehnen, da einige der schwerwiegenden Augenerkrankungen und Netzhautablösungen zuerst das periphere Sehen betreffen. In dieser Studie wurde die Live-Erkennung von reflexiven Sakkaden zusammen mit einem adaptiven psychometrischen Verfahren, das den Stimuluskontrast an vier Stellen unabhängig voneinander kontrolliert, erfolgreich durchgeführt. In dieser Studie

wurde die Kontrastempfindlichkeit entlang der horizontalen und vertikalen Achse bei drei Exzentrizitätsstufen gemessen. Darüber hinaus verifizierte die aktuelle Studie das neu etablierte Verfahren mit einem subjektiven Verfahren, das mit tastaturbasierten Antworten durchgeführt wurde. Zunächst wurde in dieser Studie der Trend einer abnehmenden Empfindlichkeit mit zunehmender Exzentrizität bestätigt, und es zeigte sich eine bessere Empfindlichkeit im horizontalen Gesichtsfeld im Vergleich zum vertikalen Gesichtsfeld. Darüber hinaus zeigte diese Studie sehr vergleichbare Ergebnisse für das augenbewegungsbasierte und das subjektive Messverfahren, was eine mögliche Verwendung dieser Art von Augenbewegung für die klinische Kontrastempfindlichkeitsmessung nahelegt.

Zusammenfassend lässt sich sagen, dass Mikrosakkaden bei monokularer Stimulation zwar binokular auftreten und daher bei klinischen Messungen der Kontrastsensitivität eingesetzt werden können, dass ihre algorithmische Erkennung und die Inkonsistenz ihres Auftretens bei den Probanden jedoch nicht ausreichend für den klinischen Einsatz sind, so dass derartige Tests vorerst nur für wissenschaftliche Zwecke in Frage kommen. In diesem Zusammenhang zeigt der optokinetische Nystagmus eine bessere Leistung bei der Prüfung der Kontrastempfindlichkeit mit korrelierten Ergebnissen zu den subjektiven Messungen, da er nur durch einen sich bewegenden visuellen Stimulus ausgelöst wird. Dennoch könnte ein solcher Test mit der neu etablierten Live-Erkennung in Verbindung mit einem adaptiven psychometrischen Verfahren möglicherweise für Untersuchungs-Zwecke eingesetzt werden. Neben der fovealen Kontrastsensitivität, die mit den oben erwähnten augenbewegungsbasierten Tests geprüft wird, wird in dieser Arbeit auch ein Ansatz zur Prüfung der peripheren Kontrastsensitivität mit Hilfe von reflexiven Sakkaden gezeigt, die unabhängig voneinander an verschiedenen Stellen im Gesichtsfeld des Patienten stimuliert werden. Dieser Test stellt eine neuartige Anpassung eines Standard-Kontrastsensitivitätstests in einen augenbewegungsbasierten Test dar, der das Potenzial hat, in Zukunft in der klinischen Praxis eingesetzt zu werden.

Trotz der Bandbreite der in der vorliegenden Arbeit gewonnenen Erkenntnisse besteht auf diesem Gebiet vor der Anwendung in der klinischen Praxis weiterer Forschungsbedarf. Zukünftige Entwicklungen von Algorithmen zur Augenbewegungsdetektion sowie von psychometrischen Verfahren könnten die Qualität und Zeiteffizienz solcher Messungen weiter verbessern. Darüber hinaus muss die Validierung der derzeit etablierten auf Augenbewegungen basierenden Kontrastsensitivitätstests mit den klinisch gemessenen Tests durchgeführt werden, um die Effizienz solcher Messungen, ihre Wiederholbarkeit und die Durchführbarkeit vor der Implementierung in der klinischen Praxis direkt zu vergleichen. Da die Kontrastempfindlichkeit nicht der einzige Parameter ist, der bei der Beurteilung der Sehleistung eines Patienten getestet werden muss, könnte die aktuelle Forschung auf andere Untersuchungen ausgedehnt werden, wie zum Beispiel

auf die Sehschärfe, die Größe des Gesichtsfelds, die Farbwahrnehmung oder die Lesegeschwindigkeit. Mit den oben erwähnten verbesserten Algorithmen zur Erkennung von Augenbewegungen in Verbindung mit einer integrierten Frontalkamera und einem Display mit ausreichender Spezifikation könnten solche Messungen auf tragbare Geräte wie Tablets, Smartphones oder VR-Headsets ausgeweitet werden. Dieser Schritt könnte dazu führen, dass das Screening einer größeren Bevölkerungsgruppe vereinfacht wird und sogar in der häuslichen Umgebung möglich ist.

8 References

Abegg, M., Pianezzi, D., and Barton, J. J. (2015). A vertical asymmetry in saccades. *Journal of Eye Movement Research*, 8(5).

Ahissar, E., Arieli, A., Fried, M., and Bonneh, Y. (2016). On the possible roles of microsaccades and drifts in visual perception. *Vision Research*, 118:25–30.

Andersson, R., Larsson, L., Holmqvist, K., Stridh, M., and Nyström, M. (2017). One algorithm to rule them all? an evaluation and discussion of ten eye movement event-detection algorithms. *Behavior research methods*, 49:616–637.

Aserinsky, E. and Kleitman, N. (1953). Regularly occurring periods of eye motility, and concomitant phenomena, during sleep. *Science*, 118(3062):273–274.

Atchison, D. A. and Markwell, E. L. (2008). Aberrations of emmetropic subjects at different ages. *Vision research*, 48(21):2224–2231.

Atchison, D. A., Smith, G., and Efron, N. (1979). The effect of pupil size on visual acuity in uncorrected and corrected myopia. *American journal of optometry and physiological optics*, 56(5):315–323.

Atkinson, J. (1984). Human visual development over the first 6 months of life. a review and a hypothesis. *Human neurobiology*, 3(2):61–74.

Bahill, A. T., Clark, M. R., and Stark, L. (1975). The main sequence, a tool for studying human eye movements. *Mathematical Biosciences*, 24(3-4):191–204.

Becker, W. and Fuchs, A. F. (1969). Further properties of the human saccadic system: eye movements and correction saccades with and without visual fixation points. *Vision research*, 9(10):1247–1258.

Behrens, F. and Weiss, L. (1992). An algorithm separating saccadic from nonsaccadic eye movements automatically by use of the acceleration signal. *Vision Res*, 32(5):889–893.

Benson, N. C., Kupers, E. R., Barbot, A., Carrasco, M., and Winawer, J. (2021). Cortical magnification in human visual cortex parallels task performance around the visual field. *Elife*, 10:e67685.

Berens, P. (2009). Circstat: a matlab toolbox for circular statistics. *Journal of statistical software*, 31:1–21.

Betts, J. G., Young, K. A., Wise, J. A., Johnson, E., Poe, B., Kruse, D. H., Korol, O., Johnson, J. E., Womble, M., and DeSaix, P. (2013). *Anatomy and physiology*.

Bieg, H.-J., Bresciani, J.-P., Bülthoff, H. H., and Chuang, L. L. (2012). Looking for discriminating is different from looking for looking's sake.

Blignaut, P. (2009). Fixation identification: The optimum threshold for a dispersion algorithm. *Attention, Perception, & Psychophysics*, 71(4):881–895.

Bonneh, Y. S., Adini, Y., and Polat, U. (2015). Contrast sensitivity revealed by microsaccades. *Journal of Vision*, 15(9):11–11.

Bowers, N. R. and Poletti, M. (2017). Microsaccades during reading. *PloS one*, 12(9):e0185180.

Brainard, D. H. (1997). The psychophysics toolbox. *Spatial vision*, 10:433–436.

Briand, K. A., Strallow, D., Hening, W., Poizner, H., and Sereno, A. B. (1999). Control of voluntary and reflexive saccades in parkinson's disease. *Experimental brain research*, 129(1):38–48.

Burr, D. C. and Ross, J. (1982). Contrast sensitivity at high velocities. *Vision research*, 22(4):479–484.

Campbell, F. and Green, D. (1965). Optical and retinal factors affecting visual resolution. *The Journal of physiology*, 181(3):576.

Campbell, F. W. and Robson, J. G. (1968). Application of fourier analysis to the visibility of gratings. *The Journal of physiology*, 197(3):551.

Carrasco, M. (2006). Covert attention increases contrast sensitivity: Psychophysical, neurophysiological and neuroimaging studies. *Progress in brain research*, 154:33–70.

Carrasco, M., Ling, S., and Read, S. (2004). Attention alters appearance. *Nature neuroscience*, 7(3):308–313.

Cavanagh, P., Anstis, S., and Mather, G. (1984). Screening for color blindness using optokinetic nystagmus. *Investigative ophthalmology & visual science*, 25(4):463–466.

Cetinkaya, A., Oto, S., Akman, A., and Akova, Y. (2008). Relationship between optokinetic nystagmus response and recognition visual acuity. *Eye*, 22(1):77–81.

Ciuffreda, K. J. and Tannen, B. (1995). *Eye movement basics for the clinician*. Mosby Incorporated.

Collewijn, H. and Kowler, E. (2008). The significance of microsaccades for vision and oculomotor control. *Journal of Vision*, 8(14):20–20.

Corbetta, M., Akbudak, E., Conturo, T. E., Snyder, A. Z., Ollinger, J. M., Drury, H. A., Linenweber, M. R., Petersen, S. E., Raichle, M. E., Van Essen, D. C., et al. (1998). A common network of functional areas for attention and eye movements. *Neuron*, 21(4):761–773.

Crossland, M. D., Culham, L. E., Kabanarou, S. A., and Rubin, G. S. (2005). Preferred retinal locus development in patients with macular disease. *Ophthalmology*, 112(9):1579–1585.

Cui, J., Wilke, M., Logothetis, N. K., Leopold, D. A., and Liang, H. (2009). Visibility states modulate microsaccade rate and direction. *Vision research*, 49(2):228–236.

Curcio, C. A., Sloan, K. R., Kalina, R. E., and Hendrickson, A. E. (1990). Human photoreceptor topography. *Journal of comparative neurology*, 292(4):497–523.

Daitch, J. and Green, D. (1969). Contrast sensitivity of the human peripheral retina. *Vision Research*, 9(8):947–952.

Dakin, S. C. and Turnbull, P. R. (2016). Similar contrast sensitivity functions measured using psychophysics and optokinetic nystagmus. *Scientific reports*, 6:34514.

Datta, S., Foss, A. J., Grainge, M. J., Gregson, R. M., Zaman, A., Masud, T., Osborn, F., and Harwood, R. H. (2008). The importance of acuity, stereopsis, and contrast sensitivity for health-related quality of life in elderly women with cataracts. *Investigative ophthalmology & visual science*, 49(1):1–6.

Denniss, J., Scholes, C., McGraw, P. V., Nam, S.-H., and Roach, N. W. (2018). Estimation of contrast sensitivity from fixational eye movements. *Investigative ophthalmology & visual science*, 59(13):5408–5416.

Deubel, H. and Schneider, W. X. (1996). Saccade target selection and object recognition: Evidence for a common attentional mechanism. *Vision research*, 36(12):1827–1837.

Ditchburn, R. W. and Ginsborg, B. L. (1953). Involuntary eye movements during fixation. *The Journal of physiology*, 119(1):1.

Dodge, R. (1906). Recent studies in the correlation of eye movement and visual perception. *Psychological Bulletin*, 3(3):85.

Doustkouhi, S. M., Turnbull, P. R., and Dakin, S. C. (2020a). The effect of refractive error on optokinetic nystagmus. *Scientific Reports*, 10(1):1–14.

Doustkouhi, S. M., Turnbull, P. R., and Dakin, S. C. (2020b). The effect of simulated visual field loss on optokinetic nystagmus. *Translational Vision Science & Technology*, 9(3):25–25.

Drum, B., Calogero, D., and Rorer, E. (2007). Assessment of visual performance in the evaluation of new medical products. *Drug Discovery Today: Technologies*, 4(2):55–61.

Dumouchel, W., O'Brien, F., et al. (1989). Integrating a robust option into a multiple regression computing environment. In *Computer science and statistics: Proceedings of the 21st symposium on the interface*, pages 297–302. American Statistical Association Alexandria, VA.

Ehinger, B. V., Groß, K., Ibs, I., and König, P. (2019). A new comprehensive eye-tracking test battery concurrently evaluating the pupil labs glasses and the eyelink 1000. *PeerJ*, 7:e7086.

Engbert, R. (2006). Microsaccades: A microcosm for research on oculomotor control, attention, and visual perception. *Progress in brain research*, 154:177–192.

Engbert, R. and Kliegl, R. (2003a). Binocular coordination in microsaccades. In *The Mind's Eye*, pages 103–117. Elsevier.

Engbert, R. and Kliegl, R. (2003b). Microsaccades uncover the orientation of covert attention. *Vision research*, 43(9):1035–1045.

Engbert, R. and Kliegl, R. (2003c). Microsaccades uncover the orientation of covert attention. *Vision research*, 43(9):1035–1045.

Erdmann, B. and Dodge, R. (1898). *Psychologische Untersuchungen über das Lesen auf experimenteller Grundlage*. Niemeyer.

Essig, P., Leube, A., Rifai, K., and Wahl, S. (2020). Microsaccadic rate signatures correlate under monocular and binocular stimulation conditions. *Journal of Eye Movement Research*, 11(4).

Essig, P., Sauer, Y., and Wahl, S. (2021a). Contrast sensitivity testing in healthy and blurred vision conditions using a novel optokinetic nystagmus live-detection method. *Translational Vision Science & Technology*, 10(12):12–12.

Essig, P., Sauer, Y., and Wahl, S. (2021b). Okn-onset is influenced by the contrast level of a visual stimulus. *Investigative Ophthalmology & Visual Science*, 62(8):3330–3330.

Fang, Y., Gill, C., Poletti, M., and Rucci, M. (2018). Monocular microsaccades: Do they really occur? *Journal of vision*, 18(3):18–18.

Foulsham, T., Teszka, R., and Kingstone, A. (2011). Saccade control in natural images is shaped by the information visible at fixation: Evidence from asymmetric gaze-contingent windows. *Attention, Perception, & Psychophysics*, 73(1):266–283.

Gao, X., Yan, H., and Sun, H.-j. (2015). Modulation of microsaccade rate by task difficulty revealed through between-and within-trial comparisons. *Journal of vision*, 15(3):3–3.

Garbutt, S., Harwood, M. R., and Harris, C. M. (2001). Comparison of the main sequence of reflexive saccades and the quick phases of optokinetic nystagmus. *British Journal of Ophthalmology*, 85(12):1477–1483.

Gautier, J., Bedell, H. E., Siderov, J., and Waugh, S. J. (2016). Monocular microsaccades are visual-task related. *Journal of vision*, 16(3):37–37.

Graham, N. and Nachmias, J. (1971). Detection of grating patterns containing two spatial frequencies: A comparison of single-channel and multiple-channels models. *Vision research*, 11(3):251–IN4.

Green, D. and Campbell, F. (1965). Effect of focus on the visual response to a sinusoidally modulated spatial stimulus. *JOSA*, 55(9):1154–1157.

Gremmler, S. and Lappe, M. (2017). Saccadic suppression during voluntary versus reactive saccades. *Journal of vision*, 17(8):8–8.

Hafed, Z. M. and Clark, J. J. (2002). Microsaccades as an overt measure of covert attention shifts. *Vision research*, 42(22):2533–2545.

Hafed, Z. M., Goffart, L., and Krauzlis, R. J. (2009). A neural mechanism for microsaccade generation in the primate superior colliculus. *science*, 323(5916):940–943.

Hafed, Z. M. and Ignashchenkova, A. (2013). On the dissociation between microsaccade rate and direction after peripheral cues: microsaccadic inhibition revisited. *Journal of Neuroscience*, 33(41):16220–16235.

Hafed, Z. M. and Krauzlis, R. J. (2012). Similarity of superior colliculus involvement in microsaccade and saccade generation. *Journal of neurophysiology*, 107(7):1904–1916.

Hanning, N. M. and Deubel, H. (2019). Unlike saccades, quick phases of optokinetic nystagmus (okn) are not preceded by shifts of attention. *Journal of Vision*, 19(10):53c–53c.

Hartridge, H. (1922). Visual acuity and the resolving power of the eye. *The Journal of Physiology*, 57(1-2):52.

Heijl, A., Lindgren, A., and Lindgren, G. (1989). Test-retest variability in glaucomatous visual fields. *American journal of ophthalmology*, 108(2):130–135.

Hemptinne, C., Liu-Shuang, J., Yuksel, D., and Rossion, B. (2019). Rapid objective assessment of contrast sensitivity and visual acuity with sweep visual evoked potentials and an extended electrode array. *Journal of Vision*, 19(8):87–87.

Henik, A., Rafal, R., and Rhodes, D. (1994). Endogenously generated and visually guided saccades after lesions of the human frontal eye fields. *Journal of Cognitive Neuroscience*, 6(4):400–411.

Henrich, N., d'Alessandro, C., Doval, B., and Castellengo, M. (2004). On the use of the derivative of electroglottographic signals for characterization of nonpathological phonation. *The Journal of the Acoustical Society of America*, 115(3):1321–1332.

Hering, E. (1868). *Die lehre vom binocularen sehen*. Engelmann.

Hering, E. (1977). *The Theory of Binocular Vision: Ewald Hering (1868)*. Springer.

Hermens, F. and Walker, R. (2010). What determines the direction of microsaccades? *Journal of Eye Movement Research*, 3(4).

Holmqvist, K. and Andersson, R. (2017). Eye tracking: A comprehensive guide to methods. *paradigms and measures*.

Hot, A., Dul, M. W., and Swanson, W. H. (2008). Development and evaluation of a contrast sensitivity perimetry test for patients with glaucoma. *Investigative ophthalmology & visual science*, 49(7):3049–3057.

Houpt, J. W., Frame, M. E., and Blaha, L. M. (2018). Unsupervised parsing of gaze data with a beta-process vector auto-regressive hidden markov model. *Behavior research methods*, 50(5):2074–2096.

Hyon, J. Y., Yeo, H. E., Seo, J.-M., Lee, I. B., Lee, J. H., and Hwang, J.-M. (2010). Objective measurement of distance visual acuity determined by computerized optokinetic nystagmus test. *Investigative ophthalmology & visual science*, 51(2):752–757.

Intoy, J. and Rucci, M. (2020). Finely tuned eye movements enhance visual acuity. *Nature communications*, 11(1):1–11.

Jansonius, N. and Kooijman, A. (1997). The effect of defocus on edge contrast sensitivity. *Ophthalmic and Physiological Optics*, 17(2):128–132.

Kara, S., Gencer, B., Ersan, I., Arikan, S., Kocabiyik, O., Tufan, H. A., and Comez, A. (2016). Repeatability of contrast sensitivity testing in patients with age-related macular degeneration, glaucoma, and cataract. *Arquivos Brasileiros de Oftalmologia*, 79:323–327.

Karadeniz Ugurlu, S., Kocakaya Altundal, A., and Altin Ekin, M. (2017). Comparison of vision-related quality of life in primary open-angle glaucoma and dry-type age-related macular degeneration. *Eye*, 31(3):395–405.

Kawai, H., Tamura, S., Kani, K., and Kariya, K. (1986). Eye movement analysis system using fundus images. *pattern Recognition*, 19(1):77–84.

Kelly, D. (1974). Spatio-temporal frequency characteristics of color-vision mechanisms. *JOSA*, 64(7):983–990.

Khuu, S. K. and Kalloniatis, M. (2015). Standard automated perimetry: determining spatial summation and its effect on contrast sensitivity across the visual field. *Investigative ophthalmology & visual science*, 56(6):3565–3576.

Kleiner, M., Brainard, D., and Pelli, D. (2007). What's new in psychtoolbox-3? *Perception*, 14.

Kloke, W. B., Jaschinski, W., and Jainta, S. (2009). Microsaccades under monocular viewing conditions. *Journal of Eye Movement Research*, 3(1).

Ko, H.-k., Poletti, M., and Rucci, M. (2010). Microsaccades precisely relocate gaze in a high visual acuity task. *Nature neuroscience*, 13(12):1549.

Kolb, H. (2009). Cone pathways through the retina. *Webvision: The Organization of the Retina and Visual System [Internet]*.

Komogortsev, O. V., Gobert, D. V., Jayarathna, S., Gowda, S. M., et al. (2010). Standardization of automated analyses of oculomotor fixation and saccadic behaviors. *IEEE Transactions on biomedical engineering*, 57(11):2635–2645.

Konen, C. S., Kleiser, R., Seitz, R. J., and Bremmer, F. (2005). An fmri study of optokinetic nystagmus and smooth-pursuit eye movements in humans. *Experimental Brain Research*, 165(2):203–216.

König, S. D. and Buffalo, E. A. (2014). A nonparametric method for detecting fixations and saccades using cluster analysis: Removing the need for arbitrary thresholds. *Journal of neuroscience methods*, 227:121–131.

Kowler, E. (2011). Eye movements: the past 25 years. *Vision research*, 51(13):1457–1483.

Kowler, E., Anderson, E., Dosher, B., and Blaser, E. (1995). The role of attention in the programming of saccades. *Vision research*, 35(13):1897–1916.

Kowler, E. and Blaser, E. (1995). The accuracy and precision of saccades to small and large targets. *Vision research*, 35(12):1741–1754.

Krauskopf, J., Cornsweet, T., and Riggs, L. (1960). Analysis of eye movements during monocular and binocular fixation. *JOSA*, 50(6):572–578.

Krauzlis, R. J., Goffart, L., and Hafed, Z. M. (2017). Neuronal control of fixation and fixational eye movements. *Philosophical Transactions of the Royal Society B: Biological Sciences*, 372(1718):20160205.

Krejtz, K., Duchowski, A. T., Niedzielska, A., Biele, C., and Krejtz, I. (2018). Eye tracking cognitive load using pupil diameter and microsaccades with fixed gaze. *PloS one*, 13(9):e0203629.

Kustov, A. A. and Robinson, D. L. (1996). Shared neural control of attentional shifts and eye movements. *Nature*, 384(6604):74.

Larson, A. M. and Loschky, L. C. (2009). The contributions of central versus peripheral vision to scene gist recognition. *Journal of Vision*, 9(10):6–6.

Laubrock, J., Engbert, R., and Kliegl, R. (2005). Microsaccade dynamics during covert attention. *Vision research*, 45(6):721–730.

Leguire, L., Zaff, B., Freeman, S., Rogers, G., Bremer, D., and Wali, N. (1991). Contrast sensitivity of optokinetic nystagmus. *Vision research*, 31(1):89–97.

Lemmink, K. A., Dijkstra, B., and Visscher, C. (2005). Effects of limited peripheral vision on shuttle sprint performance of soccer players. *Perceptual and motor skills*, 100(1):167–175.

Lesmes, L. A., Lu, Z.-L., Baek, J., and Albright, T. D. (2010). Bayesian adaptive estimation of the contrast sensitivity function: The quick csf method. *Journal of vision*, 10(3):17–17.

Ludwig, C. J., Gilchrist, I. D., and McSorley, E. (2004). The influence of spatial frequency and contrast on saccade latencies. *Vision research*, 44(22):2597–2604.

Mackeben, M. (1999). Sustained focal attention and peripheral letter recognition. *Spatial Vision*.

Mannu, G. S. (2014). Retinal phototransduction. *Neurosciences Journal*, 19(4):275–280.

Marmor, M. F. and Gawande, A. (1988). Effect of visual blur on contrast sensitivity: clinical implications. *Ophthalmology*, 95(1):139–143.

Martinez-Conde, S. and Macknik, S. L. (2015). From exploration to fixation: An integrative view of yarbus's vision. *Perception*, 44(8-9):884–899.

Martinez-Conde, S., Macknik, S. L., and Hubel, D. H. (2004). The role of fixational eye movements in visual perception. *Nature reviews neuroscience*, 5(3):229.

Martinez-Conde, S., Macknik, S. L., Troncoso, X. G., and Dyar, T. A. (2006). Microsaccades counteract visual fading during fixation. *Neuron*, 49(2):297–305.

Martinez-Conde, S., Macknik, S. L., Troncoso, X. G., and Hubel, D. H. (2009). Microsaccades: a neurophysiological analysis. *Trends in neurosciences*, 32(9):463–475.

Martinez-Conde, S., Otero-Millan, J., and Macknik, S. L. (2013). The impact of microsaccades on vision: towards a unified theory of saccadic function. *Nature Reviews Neuroscience*, 14(2):83–96.

Meyberg, S., Werkle-Bergner, M., Sommer, W., and Dimigen, O. (2015). Microsaccade-related brain potentials signal the focus of visuospatial attention. *NeuroImage*, 104:79–88.

Millodot, M., Miller, D., and Jernigan, M. E. (1973). Evaluation of an objective acuity device. *Archives of Ophthalmology*, 90(6):449–452.

Møller, F., Laursen, M., Tygesen, J., and Sjølie, A. (2002). Binocular quantification and characterization of microsaccades. *Graefe's archive for clinical and experimental ophthalmology*, 240(9):765–770.

Montés-Micó, R., Rodríguez-Galietero, A., Alió, J. L., and Cerviño, A. (2007). Contrast sensitivity after lasik flap creation with a femtosecond laser and a mechanical microkeratome.

Mooney, S. W., Alam, N. M., Hill, N. J., and Prusky, G. T. (2020). Gradiate: a radial sweep approach to measuring detailed contrast sensitivity functions from eye movements. *Journal of Vision*, 20(13):17–17.

Mooney, S. W., Hill, N. J., Tuzun, M. S., Alam, N. M., Carmel, J. B., and Prusky, G. T. (2018). Curveball: A tool for rapid measurement of contrast sensitivity based on smooth eye movements. *Journal of vision*, 18(12):7–7.

Morgan, I. G. (2003). The biological basis of myopic refractive error. *Clinical and Experimental Optometry*, 86(5):276–288.

Mould, M. S., Foster, D. H., Amano, K., and Oakley, J. P. (2012). A simple nonparametric method for classifying eye fixations. *Vision Research*, 57:18–25.

Munoz, D. P. (2002). Commentary: saccadic eye movements: overview of neural circuitry. *Progress in brain research*, 140:89–96.

Murray, I., Perperidis, A., Brash, H., Cameron, L., McTrusty, A., Fleck, B., and Minns, R. (2013). Saccadic vector optokinetic perimetry (svop): a novel technique for automated static perimetry in children using eye tracking. In *2013 35th Annual International Conference of the IEEE Engineering in Medicine and Biology Society (EMBC)*, pages 3186–3189. IEEE.

Nachmias, J. (1967). Effect of exposure duration on visual contrast sensitivity with square-wave gratings. *Josa*, 57(3):421–427.

Ni, W., Li, X., Hou, Z., Zhang, H., Qiu, W., and Wang, W. (2015). Impact of cataract surgery on vision-related life performances: the usefulness of real-life vision test for cataract surgery outcomes evaluation. *Eye*, 29(12):1545–1554.

Norouzifard, M., Black, J., Thompson, B., Klette, R., and Turuwhenua, J. (2019). A real-time eye tracking method for detecting optokinetic nystagmus. In *Asian Conference on Pattern Recognition*, pages 143–155. Springer.

Nyström, M., Andersson, R., Holmqvist, K., and Van De Weijer, J. (2013). The influence of calibration method and eye physiology on eyetracking data quality. *Behavior research methods*, 45(1):272–288.

Nyström, M., Andersson, R., Niehorster, D. C., and Hooge, I. (2017). Searching for monocular microsaccades–a red hering of modern eye trackers? *Vision research*, 140:44–54.

Ohlendorf, A. and Schaeffel, F. (2009). Contrast adaptation induced by defocus–a possible error signal for emmetropization? *Vision Research*, 49(2):249–256.

Oshika, T., Tokunaga, T., Samejima, T., Miyata, K., Kawana, K., and Kaji, Y. (2006). Influence of pupil diameter on the relation between ocular higher-order aberration and contrast sensitivity after laser in situ keratomileusis. *Investigative ophthalmology & visual science*, 47(4):1334–1338.

Otero-Millan, J., Macknik, S. L., and Martinez-Conde, S. (2014). Fixational eye movements and binocular vision. *Frontiers in integrative neuroscience*, 8:52.

Otero-Millan, J., Macknik, S. L., Serra, A., Leigh, R. J., and Martinez-Conde, S. (2011). Triggering mechanisms in microsaccade and saccade generation: a novel proposal. *Annals of the New York Academy of Sciences*, 1233(1):107–116.

Otero-Millan, J., Troncoso, X. G., Macknik, S. L., Serrano-Pedraza, I., and Martinez-Conde, S. (2008). Saccades and microsaccades during visual fixation, exploration, and search: foundations for a common saccadic generator. *Journal of vision*, 8(14):21–21.

Owsley, C. and McGwin Jr, G. (2010). Vision and driving. *Vision research*, 50(23):2348–2361.

Owsley, C., Sekuler, R., and Siemsen, D. (1983). Contrast sensitivity throughout adulthood. *Vision research*, 23(7):689–699.

Pastel, S., Chen, C.-H., Martin, L., Naujoks, M., Petri, K., and Witte, K. (2021). Comparison of gaze accuracy and precision in real-world and virtual reality. *Virtual Reality*, 25(1):175–189.

Perperidis, A., McTrusty, A. D., Cameron, L. A., Murray, I. C., Brash, H. M., Fleck, B. W., Minns, R. A., and Tatham, A. J. (2021). The assessment of visual fields in infants using saccadic vector optokinetic perimetry (svop): A feasibility study. *Translational Vision Science & Technology*, 10(3):14–14.

Pierrot-Deseilligny, C., Rivaud, S., Gaymard, B., Müri, R., and Vermersch, A.-I. (1995). Cortical control of saccades. *Annals of Neurology: Official Journal of the American Neurological Association and the Child Neurology Society*, 37(5):557–567.

Poletti, M., Listorti, C., and Rucci, M. (2010). Stability of the visual world during eye drift. *Journal of Neuroscience*, 30(33):11143–11150.

Poletti, M. and Rucci, M. (2016). A compact field guide to the study of microsaccades: Challenges and functions. *Vision research*, 118:83–97.

Richman, J., Spaeth, G. L., and Wirostko, B. (2013). Contrast sensitivity basics and a critique of currently available tests. *Journal of Cataract & Refractive Surgery*, 39(7):1100–1106.

Rinner, O., Rick, J. M., and Neuhauss, S. C. (2005). Contrast sensitivity, spatial and temporal tuning of the larval zebrafish optokinetic response. *Investigative ophthalmology & visual science*, 46(1):137–142.

Roh, M., Selivanova, A., Shin, H. J., Miller, J. W., and Jackson, M. L. (2018). Visual acuity and contrast sensitivity are two important factors affecting vision-related quality of life in advanced age-related macular degeneration. *PloS one*, 13(5):e0196481.

Rolfs, M. (2009). Microsaccades: small steps on a long way. *Vision research*, 49(20):2415–2441.

Rolfs, M., Engbert, R., and Kliegl, R. (2005). Crossmodal coupling of oculomotor control and spatial attention in vision and audition. *Experimental Brain Research*, 166(3):427–439.

Rolfs, M., Kliegl, R., and Engbert, R. (2008). Toward a model of microsaccade generation: The case of microsaccadic inhibition. *Journal of vision*, 8(11):5–5.

Rosen, R., Lundström, L., Venkataraman, A. P., Winter, S., and Unsbo, P. (2014). Quick contrast sensitivity measurements in the periphery. *Journal of Vision*, 14(8):3–3.

Ross, J. (1985). Clinical detection of abnormalities in central vision in chronic simple glaucoma using contrast sensitivity. *International ophthalmology*, 8(3):167–177.

Rovamo, J., Mustonen, J., and Näsänen, R. (1994). Modelling contrast sensitivity as a function of retinal illuminance and grating area. *Vision research*, 34(10):1301–1314.

Rucci, M., Iovin, R., Poletti, M., and Santini, F. (2007). Miniature eye movements enhance fine spatial detail. *Nature*, 447(7146):852.

Rucci, M. and Poletti, M. (2015). Control and functions of fixational eye movements. *Annual review of vision science*, 1:499.

Sakai, S., Hirayama, K., Iwasaki, S., Yamadori, A., Sato, N., Ito, A., Kato, M., Sudo, M., and Tsuburaya, K. (2002). Contrast sensitivity of patients with severe motor and intellectual disabilities and cerebral visual impairment. *Journal of Child Neurology*, 17(10):731–737.

Salvucci, D. D. and Goldberg, J. H. (2000). Identifying fixations and saccades in eye-tracking protocols. In *Proceedings of the 2000 symposium on Eye tracking research & applications*, pages 71–78.

Sangi, M., Thompson, B., and Turuwhenua, J. (2015). An optokinetic nystagmus detection method for use with young children. *IEEE journal of translational engineering in health and medicine*, 3:1–10.

Sauer, Y., Sipatchin, A., Wahl, S., and García García, M. (2022). Assessment of consumer vr-headsets' objective and subjective field of view (fov) and its feasibility for visual field testing. *Virtual Reality*, pages 1–13.

Saw, S.-M., Gazzard, G., Shih-Yen, E. C., and Chua, W.-H. (2005). Myopia and associated pathological complications. *Ophthalmic and Physiological Optics*, 25(5):381–391.

Schall, J. D. (1995). Neural basis of saccade target selection. *Reviews in the Neurosciences*, 6(1):63–85.

Schober, H. and Hilz, R. (1965). Contrast sensitivity of the human eye for square-wave gratings. *JOSA*, 55(9):1086–1091.

Scholes, C., McGraw, P. V., Nyström, M., and Roach, N. W. (2015a). Fixational eye movements predict visual sensitivity. *Proceedings of the Royal Society B: Biological Sciences*, 282(1817):20151568.

Scholes, C., McGraw, P. V., Nyström, M., and Roach, N. W. (2015b). Fixational eye movements predict visual sensitivity. *Proceedings of the Royal Society B: Biological Sciences*, 282(1817):20151568.

Schütt, H., Harmeling, S., Macke, J., and Wichmann, F. (2015). Psignifit 4: Pain-free bayesian inference for psychometric functions. *Journal of vision*, 15(12):474–474.

Schütz, A. C., Braun, D. I., and Gegenfurtner, K. R. (2007). Contrast sensitivity during the initiation of smooth pursuit eye movements. *Vision research*, 47(21):2767–2777.

Schwob, N. and Palmowski-Wolfe, A. (2019). Objective measurement of visual acuity by optokinetic nystagmus suppression in children and adult patients. *Journal of American Association for Pediatric Ophthalmology and Strabismus*, 23(5):272–e1.

Seidemann, A. and Schaeffel, F. (2003). An evaluation of the lag of accommodation using photorefraction. *Vision research*, 43(4):419–430.

Shaikh, A. G. and Ghasia, F. F. (2017). Fixational saccades are more disconjugate in adults than in children. *PLoS One*, 12(4):e0175295.

Smith, G. and Atchison, D. A. (1997). *The eye and visual optical instruments*.

Smith III, E. L. (2011). The charles f. prentice award lecture 2010: a case for peripheral optical treatment strategies for myopia. *Optometry and Vision Science*, 88(9):1029.

Stein, N., Niehorster, D. C., Watson, T., Steinicke, F., Rifai, K., Wahl, S., and Lappe, M. (2021). A comparison of eye tracking latencies among several commercial head-mounted displays. *i-Perception*, 12(1):2041669520983338.

Steinmetz, J. D., Bourne, R. R., Briant, P. S., Flaxman, S. R., Taylor, H. R., Jonas, J. B., Abdoli, A. A., Abrha, W. A., Abualhasan, A., Abu-Gharbieh, E. G., et al. (2021). Causes of blindness and vision impairment in 2020 and trends over 30 years, and prevalence of avoidable blindness in relation to vision 2020: the right to sight: an analysis for the global burden of disease study. *The Lancet Global Health*, 9(2):e144–e160.

Stoimenova, B. D. (2007). The effect of myopia on contrast thresholds. *Investigative ophthalmology & visual science*, 48(5):2371–2374.

Strasburger, H., Rentschler, I., and Jüttner, M. (2011). Peripheral vision and pattern recognition: A review. *Journal of vision*, 11(5):13–13.

Swanson, W. H., Malinovsky, V. E., Dul, M. W., Malik, R., Torbit, J. K., Sutton, B. M., and Horner, D. G. (2014). Contrast sensitivity perimetry and clinical measures of glaucomatous damage. *Optometry and Vision Science*, 91(11):1302.

Taore, A., Lobo, G., Turnbull, P. R., and Dakin, S. C. (2022). Diagnosis of colour vision deficits using eye movements. *Scientific reports*, 12(1):1–14.

Tatiyosyan, S. A., Rifai, K., and Wahl, S. (2020). Standalone cooperation-free okn-based low vision contrast sensitivity estimation in vr-a pilot study. *Restorative neurology and neuroscience*, 38(2):119–129.

Taylor, C. P., Bennett, P. J., and Sekuler, A. B. (2014). Evidence for adjustable bandwidth orientation channels. *Frontiers in Psychology*, 5:578.

Thayaparan, K., Crossland, M. D., and Rubin, G. S. (2007). Clinical assessment of two new contrast sensitivity charts. *British Journal of Ophthalmology*, 91(6):749–752.

Turuwhenua, J., Yu, T.-Y., Mazharullah, Z., and Thompson, B. (2014). A method for detecting optokinetic nystagmus based on the optic flow of the limbus. *Vision Research*, 103:75–82.

Tzelepi, A., Laskaris, N., Amditis, A., and Kapoula, Z. (2010). Cortical activity preceding vertical saccades: a meg study. *Brain research*, 1321:105–116.

Valmaggia, C. and Gottlob, I. (2004). Role of the stimulus size in the generation of optokinetic nystagmus in normals and in patients with retinitis pigmentosa. *Klinische Monatsblätter für Augenheilkunde*, 221(05):390–394.

Valmaggia, C., Rütsche, A., Baumann, A., Pieh, C., Shavit, Y. B., Proudlock, F., and Gottlob, I. (2004). Age related change of optokinetic nystagmus in healthy subjects: a study from infancy to senescence. *British journal of ophthalmology*, 88(12):1577–1581.

Van den Berg, A. and Collewijn, H. (1988). Directional asymmetries of human optokinetic nystagmus. *Experimental Brain Research*, 70(3):597–604.

Vingrys, A. J. and Demirel, S. (1998). False-response monitoring during automated perimetry. *Optometry and Vision Science: Official Publication of the American Academy of Optometry*, 75(7):513–517.

Volkmann, F. C., Schick, A. M., and Riggs, L. A. (1968). Time course of visual inhibition during voluntary saccades. *JOSA*, 58(4):562–569.

Wai, K. M., Vingopoulos, F., Garg, I., Kasetty, M., Silverman, R. F., Katz, R., Laíns, I., Miller, J. W., Husain, D., Vavvas, D. G., et al. (2022). Contrast sensitivity function in patients with macular disease and good visual acuity. *British Journal of Ophthalmology*, 106(6):839–844.

Walker, R., Walker, D. G., Husain, M., and Kennard, C. (2000). Control of voluntary and reflexive saccades. *Experimental Brain Research*, 130(4):540–544.

Wallis, S. A., Baker, D. H., Meese, T. S., and Georgeson, M. A. (2013). The slope of the psychometric function and non-stationarity of thresholds in spatiotemporal contrast vision. *Vision research*, 76:1–10.

Watson, A. B. (2017). Quest+: A general multidimensional bayesian adaptive psychometric method. *Journal of Vision*, 17(3):10–10.

Weier, M., Stengel, M., Roth, T., Didyk, P., Eisemann, E., Eisemann, M., Grogorick, S., Hinkenjann, A., Kruijff, E., Magnor, M., et al. (2017). Perception-driven accelerated rendering. In *Computer Graphics Forum*, volume 36, pages 611–643. Wiley Online Library.

Wester, S. T., Rizzo, J. F., Balkwill, M. D., and Wall, C. (2007). Optokinetic nystagmus as a measure of visual function in severely visually impaired patients. *Investigative ophthalmology & visual science*, 48(10):4542–4548.

WHO (2022). Blindness and vision impairment. `https://www.who.int/news-room/fact-sheets/detail/blindness-and-visual-impairment`. Accessed: 2022-10-13.

Wichmann, F. A. and Hill, N. J. (2001). The psychometric function: I. fitting, sampling, and goodness of fit. *Perception & psychophysics*, 63(8):1293–1313.

Wilkin, D. and Brainard, J. (2012). Human biology.

Wismeijer, D. A. and Gegenfurtner, K. R. (2012). Orientation of noisy texture affects saccade direction during free viewing. *Vision Research*, 58:19–26.

Wojciechowski, R. (2011). Nature and nurture: the complex genetics of myopia and refractive error. *Clinical genetics*, 79(4):301–320.

Yablonski, M., Polat, U., Bonneh, Y. S., and Ben-Shachar, M. (2017). Microsaccades are sensitive to word structure: A novel approach to study language processing. *Scientific Reports*, 7(1):1–11.

Zemblys, R., Niehorster, D. C., Komogortsev, O., and Holmqvist, K. (2018). Using machine learning to detect events in eye-tracking data. *Behavior research methods*, 50(1):160–181.

Zheng, X., Xu, G., Wang, Y., Han, C., Du, C., Yan, W., Zhang, S., and Liang, R. (2019). Objective and quantitative assessment of visual acuity and contrast sensitivity based on steady-state motion visual evoked potentials using concentric-ring paradigm. *Documenta Ophthalmologica*, 139(2):123–136.

Zhou, W. and King, W. (1999). Monocular and binocular mechanisms in saccade generation. *Behavioral and Brain Sciences*, 22(4):704–705.

Zuber, B. and Stark, L. (1966). Saccadic suppression: elevation of visual threshold associated with saccadic eye movements. *Experimental neurology*, 16(1):65–79.

Zuber, B. L., Stark, L., and Cook, G. (1965). Microsaccades and the velocity-amplitude relationship for saccadic eye movements. *Science*, 150(3702):1459–1460.

9 Publications, conference contributions and talks related to this work

9.1 Peer reviewed publications

Neumann, A., Leube, A., Nabawi, N., Sauer, Y., **Essig, P.**, Breher, K., & Wahl, S. Short-Term Peripheral Contrast Reduction Affects Central Chromatic and Achromatic Contrast Sensitivity. MDPI Photonics, 9(3).

Essig, P., Müller, J., & Wahl, S. (2022). Parameters of Optokinetic Nystagmus Are Influenced by the Nature of a Visual Stimulus. MDPI Applied Sciences, 12(23).

9.2 Peer reviewed conference contributions

Essig P, Sauer Y., & Wahl S. (2021). OKN-onset is influenced by the contrast level of a visual stimulus. Investigative Ophthalmology & Visual Science, 62 (8), 3330-3330. ARVO, San Francisco (USA).

Essig P, Sauer Y., & Wahl S. (2021). The latency of reflexive saccades is influenced by contrast and correlates over the horizontal and vertical visual field plane. Journal of Vision, 22 (14), 3973-3973. VSS, St Pete Beach, Florida (USA).

10 Statement of own contribution

10.1 Publication 1 - Microsaccadic rate signatures correlate under monocularly and bin- ocularly stimulated conditions

Essig P., Leube A., Rifai K., & Wahl S. (2020). Microsaccadic rate signatures correlate under monocularly and binocularly stimulated conditions. Journal of Eye Movement Research, 13(5):3.

Contribution of the first author:
I developed the initial idea for the experiments and defined the methodology and performed the measurements on study participants. Furthermore I analyzed the data and wrote the initial version of the manuscript which I also improved based on my ideas and input from the other authors.

Contribution of the other authors:
Dr. Alexander Leube as a second author of the paper, conceived the study idea, supported the work with his experience in planning and performing experiments and along with Dr. Katharina Rifai was involved in the editing of the manuscript and data analysis. The last author, Prof. Dr. Siegfried Wahl, provided materials, supervised the study and helped to improve the manuscript.

10.2 Publication 2 - Contrast Sensitivity Testing in Healthy and Blurred Vision Conditions Using a Novel Optokinetic Nystagmus Live-Detection Method

Essig P., Sauer Y., & Wahl S. (2021).Contrast Sensitivity Testing in Healthy and Blurred Vision Conditions Using a Novel Optokinetic Nystagmus Live-Detection Method. Translational Vision Science & Technology, 10(12):12.

Contribution of the first author:
I developed the initial idea for the experiments and defined the methodology and performed the measurements on study participants. Furthermore I analyzed the data and wrote the initial version of the manuscript which I also improved based on my ideas and input from the other authors.

Contribution of the other authors:
The second author of the paper, Yannick Sauer helped to develop the initial idea for the experiment and also helped with programming of the visual test. The second author was also involved in providing comments prior submission. The fourth author of the paper, Prof. Dr. Siegfried Wahl provided materials, supervised the study and helped to improve the manuscript.

10.3 Publication 3 - Reflexive Saccades Used for Objective and Automated Measurements of Contrast Sensitivity in Selected Areas of Visual Field

Essig P., Sauer Y., & Wahl S. (2022). Reflexive Saccades Used for Objective and Automated Measurements of Contrast Sensitivity in Selected Areas of Visual Field . Translational Vision Science & Technology, 11(5):29.

Contribution of the first author:
I developed the initial idea for the experiments and defined the methodology and performed the measurements on study participants. Furthermore I analyzed the data and wrote the initial version of the manuscript which I also improved based on my ideas and input from the other authors.

Contribution of the other authors:
The second author of the paper, Yannick Sauer helped to develop the initial idea for the experiment and also helped with programming of the visual test. The second author was also involved in providing comments prior submission. The fourth author of the paper, Prof. Dr. Siegfried Wahl provided materials, supervised the study and helped to improve the manuscript.

11 Acknowledgements

This doctoral thesis was created with the kind support of many individuals to whom I would like to express my greatest acknowledgments. First of all, I would like to express my sincere gratitude to my advisors Prof. Dr. Siegfried Wahl and Prof. Dr. Frank Schaeffel for their continuous guidance during my doctoral studies and related research, their feedback, support, and motivation. Second, I would like to thank Dr. Alexander Leube for his guidance in the early stage of my doctoral studies, and for the constructive meetings and remarks he provided to me. Thank you all for this. Besides, I would also like to thank all my former and current colleagues in the Zeiss Vision Science Lab in Tübingen, for the great atmosphere to work in they have created. Thank you all for being always supportive, helpful, and open to a discussion that opened up new perspectives and solutions. I further thank all the volunteers for participating in the experiments I conducted during my doctoral studies. Finally and most importantly, I would like to express my deepest gratitude to my family and my friends for their constant support and encouragement throughout the last few years.